TAMPERE UNIVERSITY OF TECHNOLOGY

MIKKO HAKOMÄKI

ECG ARTEFACTS IN EEG MEASUREMENT

Master of Science Thesis

Examiner: Prof. Kari Mäkelä

Subject approved by the department council on 4th April, 2012

TIIVISTELMÄ

TAMPEREEN TEKNILLINEN YLIOPISTO
Sähkötekniikan koulutusohjelma
HAKOMÄKI, MIKKO: EKG ARTEFAKTAT EEG-MITTAUKSESSA
Diplomityö, 83 sivua, 7 liitesivua
Tammikuu 2013
Pääaine: Lääketieteellinen elektroniikka
Tarkastaja: Prof. Kari Mäkelä
Avainsanat: EEG, EKG, vektorikardiografia, artefakta, mallinnus

Fysiologisten signaalien rekisteröinti kliinisessä lääketieteessä on yhä tärkeämpää niin diagnostisten rekisteröintien kuin fysiologisten toimintojen monitoroinnissakin. Aivosähkökäyrä rekisteröinnit (EEG) ovat merkittävässä roolissa ja laajasti ja pitkään käytetty menetelmä aivojen toiminnan tutkimisessa. Sydänsähkökäyrä (EKG) on yksi suurimmista artefakteista EEG-mittauksessa, erityisesti neuromonitoroinnin aikana teho-osastolla ja leikkaussalissa, mutta myös unitutkimuksissa ja diagnostisissa monikanavarekisteröinneissä. Vaikka EKG:n häiritsevä merkitys tiedostetaan, ei EKG:n leviämisestä kaulan ja pään alueelle ole tehty kattavaa tutkimusta. Tämän diplomityön tarkoitus on tutkia EKG-signaalin leviämisestä kaulan ja pään alueelle, sekä löytää tekijöitä jotka vaikuttavat signaalin leviämiseen.

Diplomityö on jaettu kuuteen osaan. Johdannon jälkeen, kappaleessa kaksi, on kirjallisuuskatsaus sekä teoriaa EEG- ja EKG-mittauksen taustalla. Toinen kappale sisältää teoriaa myös mainittujen signaalien käsittelystä, sekä biosähköisten ilmiöiden matemaattisesta mallinnuksesta. Työn kolmas kappale käsittelee menetelmiä joita tutkimuksessa on käytetty. Kolmannessa kappaleessa, eli kokeellisessa osassa on rekisteröity EKG- ja EEG-signaaleja kolmelta testikohteelta sekä neljältä potilaalta. Tutkimukset sisältävät pään kääntöjä, sydämen lisälyöntejä, sydämen sähköisen aktiviteetin suunnan mittauksen sekä kaulan pituuden ja paksuuden mittauksen. Mainituista tutkimuksista analysoidaan eri tekijöiden vaikutusta sydämen sähköisen aktivaation leviämiseen. EKG:n sähkökenttien leviämistä kehossa myös mallinnetaan ihmiskehon realistisen matemaattisen mallin avulla. Tämän jälkeen EKG:n sähkökentät kaulalla, kasvoilla ja päälaella analysoidaan yksityiskohtaisesti käyttäen tuloksia mallinnuksesta ja mittauksista. Tulosten tarkastelu keskittyy kehon pinnalle, jättäen kehonsisäiset sähkökentät myöhempiin tutkimuksiin.

Tutkimuksen tuloksista käy ilmi, että EKG-signaalia voidaan rekisteröidä kaikkialta pään ja kaulan alueelta. Rekisteröidyn signaalin voimakkuus vaihtelee niin mittauspisteiden kuin henkilöidenkin välillä. Kaulan mitat, lisälyönnit sekä sydämen ja pään asennon havaitaan vaikuttavan rekisteröityyn signaaliin. Suurin potentiaalin muutos havaittiin, kun tutkittiin pään kääntöjä elektrodisijainneilla, joita käytetään anestesian syvyyden monitorointiin. Mainitusta syystä suositellaan kattavampaa tutkimusta anestesian syvyyden monitoroinnissa käytettävästä elektrodisijoittelusta sekä monitoroinnissa käytettävän signaalin sisällöstä. Tulokset antavat lisäksi ymmärtää, että vektorikardiografialla voitaisiin päätellä sydämen aiheuttaman sähkökentän voimakkaimman potentiaalialueen sijainti päälaella. Jos voimakkaimman potentiaalialueen sijainti tiedettäisiin, voitaisiin tätä tietoa käyttää kyseisen alueen välttämiseen, tai aluetta voitaisiin siirtää muualle kääntämällä potilaan päätä. Havaittiin, että sydämen sähköisen akselin suunta ja siten voimakkain potentiaalialue päässä on mahdollista määrittää myös suoraan EEG-elektrodeista, mikä mahdollistaa mittauksen tavallisessa EEG-tutkimuksessa ilman elektrodeja rintakehällä.

ABSTRACT

TAMPERE UNIVERSITY OF TECHNOLOGY
Master's Degree Programme in Electrical Engineering
HAKOMÄKI, MIKKO: ECG ARTEFACTS IN EEG MEASUREMENT
Master of Science Thesis, 83 pages, 7 Appendix pages
January 2013
Major: Biomedical electronics
Examiner: Prof. Kari Mäkelä
Keywords: EEG, ECG, artefact, VCG, model

Recording of physiological signals is increasingly important in clinical medicine both in diagnostic recordings and monitoring physiological functions, for instance during anesthesia. Electroencephalography (EEG) is a remarkable, widely and long time used method to get information about the functions of the brain. Electrocardiography (ECG) is one of the major artefacts in the EEG measurement, especially during neuromonitoring in intensive care unit and operating room, but also in sleep recordings and diagnostic multichannel recordings. Even though the interfering effect of ECG signal is known, extensive information about how and where the ECG spreads in the area of neck and head have not been studied. The aim of this thesis is to study the spreading of ECG signal in the area of neck and head, and the factors affecting to the spreading.

Thesis is divided into six parts. In chapter two, after the introduction, is literature review and theory behind EEG and ECG measurements. Second chapter includes also theory about the processing of mentioned signals, and mathematical modelling of bioelectrical phenomena. Third chapter of the thesis discusses the methods used in this thesis. In third chapter, which is the experimental part, ECG is recorded from three test subjects and four patients. To demonstrate the effect of different variables to the spreading of ECG signal, recordings include head turnings, extra systoles, measurement of the orientation of the heart and the measurement of length and thickness of the neck. A realistic mathematical model of the human body is used to calculate the distribution of ECG fields in the body. The electric fields of ECG on neck, face and scalp are analyzed in detail by using lead fields from the model and the results from the measurements. Main focus when inspecting the results is on the surface of the body. Inspection of electric fields inside the body is left for later studies.

Results of the study reveal that ECG signal can be recorded in every point around the head and neck. Magnitude of the recorded signal varies depending on the measuring points and test person. Results also show that size of the neck, extra systoles, orientation of the heart and orientation of the head affect to the recorded signal as well. Highest change in measured potential was found when the effects of turning the head of a person were measured by using the same EEG electrode positions which is used when monitoring the depth of anesthesia. For mentioned reason, more comprehensive study of the electrode locations and the signal structure used to monitor the depth of anesthesia is now suggested. Results also suggest that vectorcardiography (VCG) could be used to find out the location of strongest ECG signal. If the location of strongest signal would be known, the information could be used to avoid the area with highest interference, or to move the area by turning the head of the patient. It was also noticed that the direction of electric axis of the heart and thus the highest potential area around the head could be determined directly from the EEG electrodes, which would make it possible to do the measurement during a routine EEG measurement, without electrodes on the thorax.

PREFACE

Thesis was done in Seinäjoki Central Hospital, at the Department of Clinical Neurophysiology. Thesis had a research funding from Pirkanmaa Hospital District and from South Ostrobothnia Hospital District. I would like to thank Professor Arvi Yli-Hankala for the funding of this thesis. I wish to thank my supervisors MD Ville Jäntti and Professor Kari Mäkelä, who made it possible for me to do this work, and for their valuable comments and guidance through the work.

I would like to thank the personnel at the Department of Clinical Neurophysiology, especially MD Hannu Heikkilä for giving the opportunity to work at the department and PhD Eng Antti Kulkas for the huge amount of work he made with me during the year. MSc Naryan Puthanmadam Subramaniyam I would like to thank for the guidance with the modelling part of the work.

My family and friends I would like to thank for being there with me, and for the support they gave me during the studies. Especially I want to thank my brother Juha Hakomäki and my friend Mikko Matalamäki for the proof reading and comments.

Seinäjoki, 11th of December, 2012

Mikko Hakomäki

TABLE OF CONTENTS

ABBREVIATIONS

ACB	aortocoronary bypass
AV	atrioventricular
BIS	bispectral index
CT	computerized tomography
ECG	electrocardiography
EEG	electroencephalogram
EMG	electromyography
FDM	finite difference method
FIR	finite impulse response
ICU	intensive care unit
ME	monitoring electrodes
OR	operating room
QRS	period of heart cycle including Q-, R- and S-wave
SR	suppression ratio
VCG	vectorcardiography
3D	three dimensional

1 INTRODUCTION

Recording of physiological signals is increasingly important in clinical medicine both in diagnostic recordings and when monitoring physiological functions, for instance during anesthesia. Some of the recorded signals are based on transducers which produce electrical signals, but many electrical signals, such as electrocardiography (ECG) and electroencephalography (EEG), are generated by organs. The electrodes used to record physiological signals usually pick up the electric fields of more than one physiological source. In addition to electric fields of physiological sources, technical artefacts get recorded. Signals from other sources than the ones which are supposed to be monitored are considered as artefacts.

In EEG recordings, ECG is often an important artefact to notice. This is because the electric fields generated by the heart are strong, and they spread also to the head and can therefore affect EEG recordings measured from the scalp. Artefact generated by heart may cause difficulties in interpreting diagnostic multichannel EEG. The ECG artefacts may also cause difficulties in sleep recordings and neuromonitoring in intensive care unit (ICU) and operating room (OR). Several studies about ECG artefacts and spreading of ECG in the body have been done, but based on a literature review, none of these studies give extensive information about how and where the ECG spreads in the area of neck and head.

This thesis aims to study how and where the ECG signal spreads in the area of neck, face and scalp. Thesis also takes into account possible variables affecting to the spreading of the ECG signal. Knowing how and where the ECG signal spreads, it is possible to understand better the content of the EEG signal. The knowledge of the spreading of the ECG signal can also be utilized when developing new measurement equipment and processing tools in the future.

First part of the thesis consists of a literature review. The review starts from the anatomy and physiology of the heart and the brain, and covers the fundamentals about ECG and EEG measurements. The processing of the mentioned signals is also covered. The literature review also includes ECG artefacts in EEG recordings and modelling of electric fields generated by the heart. After literature review the methods used in the experimental part of the study are presented. The final parts of the thesis are results, discussion and conclusion. The results section presents the findings. In discussion section the findings are analyzed and their consequences are considered. Conclusion explains the whole thesis and its observations.

In the experimental part ECG is recorded from test subjects and patients. A realistic mathematical model of the human body is used to calculate the distribution of

ECG fields in the body. The electric fields of ECG on neck, face and scalp are analyzed in detail by using both lead fields from the model and the results from the measurements. Main focus when inspecting the results is on the surface of the body. If the modelling gives appropriate results, it will support the examinations of the inside of the body using the same model.

2 BACKGROUND

There exist plenty of artefacts related to physiological measurements, and ECG is one of them when considering EEG measurements. Artefacts are unwanted signals coming from some other source than the one which is wanted to measure. This chapter first shortly presents the anatomy and physiology of the brain and heart, the background of EEG, ECG and VCG measurements and gives a literature review to ECG artefacts. Later in this chapter background of the signal processing is presented in relation to mentioned signals. Last thing in this chapter is the theory behind the mathematical modelling of bioelectrical phenomena.

2.1 Brain and EEG

Brain consists mainly of glia cells and nerve cells, called neuron (Figure 2.1. A). Glia cells are supportive cells in the central nervous system, and do not conduct electrical impulses [26]. Neurons, unlike glia cells, conduct and produce electrical impulses.

Neurons consist of soma, dendrites and axons. Soma diameter is from couple of micrometers to hundreds of micrometers – this includes nucleus and other organelles. Dendrites are branches which receive the impulses which are coming to neuron. Axon is a branch which conducts the impulse from the neuron. Usually neuron includes only one axon, which branches out close to other cells and forms multiple expanded neural junctions. Axon can be even a meter long. Axon can connect neurons to each other or form a junction between a neuron and muscle cells. These junctions are not physical, but instead there exists so called synapse (Figure 2.1. B). Neuronal activity in the brain is based on the electrical changes in the neurons. The impulses are then conducted to axons, which move the electrical impulse from one cell to another through a synapse. When the electrical impulse reaches the synapse, ions are moved through a cell membrane with the help of ion pumps. As the ions change the membrane voltage, chemical agents are released from the synapse to synapse space. Agents connect to the receptors of the neighbouring cell, which leads to the moving of ions through the membrane of that cell, and the electrical impulse continues conducting. [23]

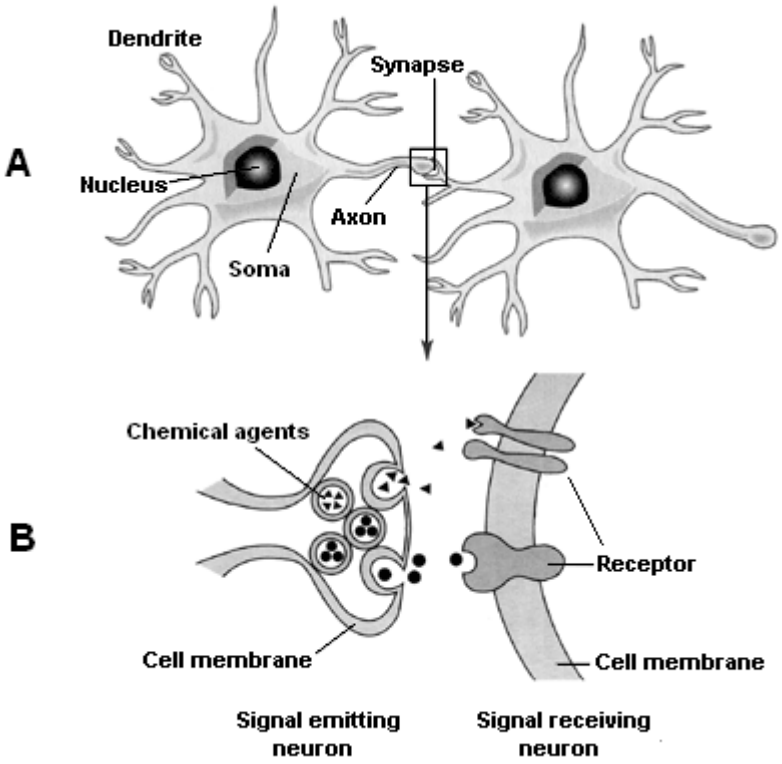

Figure 2.1. *Illustration of two neurons (A) and a synapse (B) connecting them. [18, modified]*

Electroencephalography (EEG) means the registration of synchronized membrane potential changes of a group of nerve cells with the electrodes usually from the scalp surface. It has been evaluated that synchronized activity on around 5 cm^2 sized area on the cortex can be detected from the surface of the scull with EEG. Electrical impulse proceeding in the axon itself can not be seen in EEG due to its short duration, which is around 1 millisecond. To be able to see summed internal and external currents of the cell related to synapse potentials in EEG measurements, the dendrites of the neurons have to be parallel to each other at the cortex. If dendrites are randomly organized, they just zero each other's potential changes. This kind of requirement of the dendrites directions is fulfilled in the big pyramid cells of the cortex. Most of the EEG phenomena are born from these apical dendrites of the cortex. [33]

Tissues outside the brain, especially cerebrospinal fluid and skull change the EEG signal significantly. Conductivity of the scull is around two times lower than brain tissue, and thus it attenuates EEG signal considerably. Different frequencies act differently as well, since lower frequencies can reach the surface of the scull without significant attenuating, while high frequencies' amplitude can decrease over 90%. In addition to frequency, the size of the active area affects to the attenuation, since the larger the area the less the signal is attenuated on its way to the scalp. [33] An example of recorded EEG signal can be seen in Figure 2.2. This example signal is recorded from the author at the department of Clinical Neurophysiology at Seinäjoki Central Hospital.

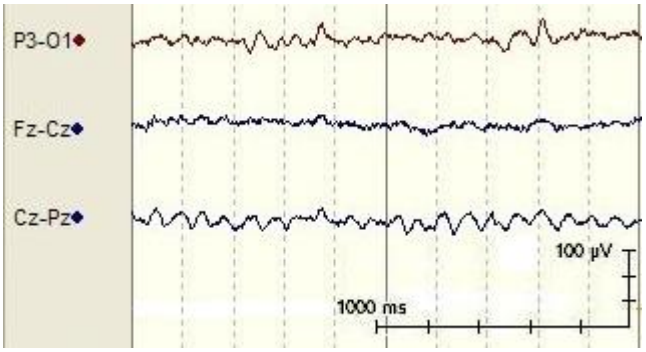

Figure 2.2. *An example EEG signal measured from three bipolar channels. In routine EEG measurement more channels are used. Image is captured from the NicoletOne EEG Reader Module Version 5.80.*

The most commonly used electrode placing systems in clinical use are so called 10-10 system and older 10-20 system (Figure 2.3.). In these systems the numbers 10 and 20 tells the relative distance in percentage between adjacent electrodes with respect to total distance in front-back or right-left distance of the scalp. [33]

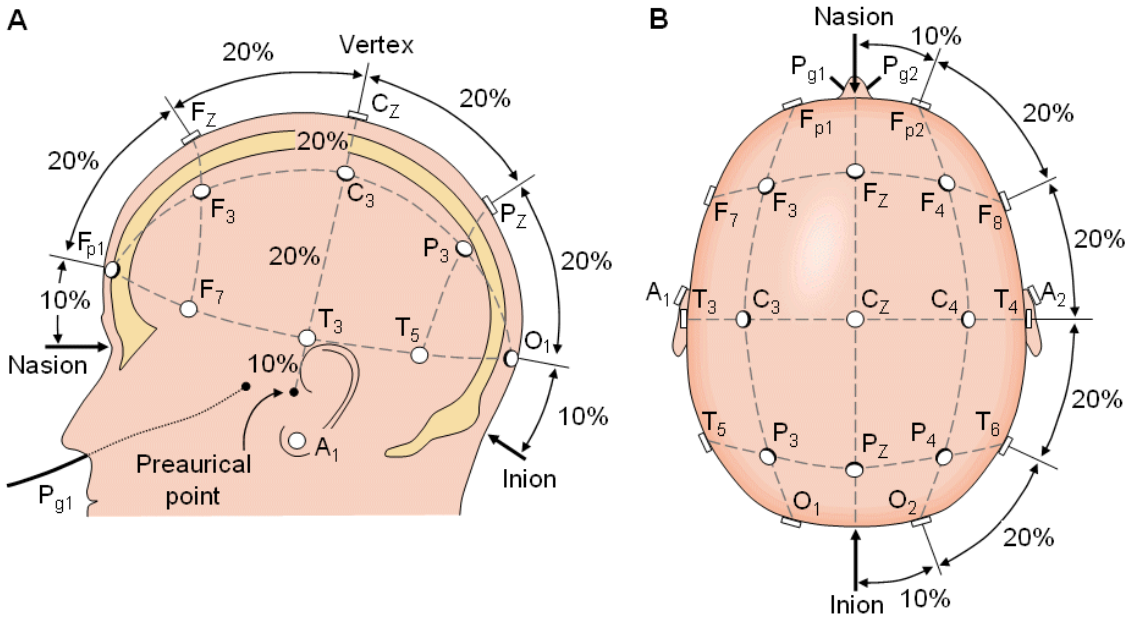

Figure 2.3. *International 10-20 electrode placing system illustrated from left (A) and above the head (B). A = ear lobe, C = central, P_g = nasopharyngeal, P = parietal, F = frontal, F_p = frontal polar, T = temporal and O = occipital. [25]*

Standardized electrode placing system makes it possible to compare the measurement results done to different persons or to one person at different times. [33] The system includes total of 19 electrodes on the scalp and one electrode on both ear lobes. In this study both the 10-20 system and a modified version of it with additional electrodes is used. This is explained more thoroughly on chapter 3.1.1.

Recording electrodes for EEG during anesthesia are placed in different manner than 10-10 or 10-20. During anesthesia the electrodes are placed on to the forehead of the patient and are used to calculate Bispectral Index (BIS). BIS is an artificial, processed value of measured EEG signal from the frontotemporal montage. BIS is a number between 0 and 100, where 0 means cortical electrical silence and 100 means normal cortical electrical activity. BIS is used to monitor the depth of anesthesia and is thus commonly used in intensive care unit (ICU) and operating room (OR). [2; 27]

2.2 Heart and ECG

Heart is a pump consisting of muscle and it weights 300-350 grams. Electrocardiography (ECG) is the most important and most used examination of the heart. ECG is the sum activity of action potentials of cardiac muscle cell. ECG method can be used to study and diagnose pulse frequency and pulse frequency variation, rhythm of the heart, conduction path of the electric stimulus and how heart is receiving nutrition and oxygen. In addition it can be used to evaluate damaged or scarred areas and the location and size of those areas and to evaluate hypertrophy of a cardiac muscle.

2.2.1 Anatomy and physiology

Cardiac muscle, also called as myocardium, is striated, which means that actins and myosins of it are organised to parallel filaments. Cardiac muscle cells are thicker (10-20 µm thick) than smooth muscle cells and they contain one nucleus. Cardiac muscle cells can branch out, but their heads are attached to each other, which is the way they form an important uniform net for depolarisation and contraction of a cardiac muscle. Wall of the heart is thickest in the left ventricle, which is pumping against the greatest resistant. The contraction of a cardiac muscle starts when there is an action potential on a cell membrane. Action potential leads to so called depolarisation where a brief opening of calcium ion channels occurs. In repolarisation calcium channels closes. Inside the cardiac muscle calcium concentration is very small, whereas in extracellular fluid the concentration is about 10 000 times higher. Difference in concentration affect so that calcium ions move into the cardiac muscle cell. Inward flowing calcium ions release calcium ions from the sarcoplasmic reticulum. Free calcium ions attach to actin and myosin proteins leading to sliding of these proteins compared to each other, which is called contraction of a muscle. After the contraction calcium ions are again attached to sarcoplasmic reticulum. [52, p. 290]

Heart has a specific cycle in its action. This cycle consists of contraction of atriums and ventricles in a specific order and way. Phases of a normal cardiac cycle are presented in Figure 2.4. The state when the blood is going from atriums to ventricles is called diastole, which is about 2/3 of the cycle in rest. In the beginning of diastole, right after the contraction of ventricles, atrioventricular (AV) valve opens and via the decreased pressure in ventricles, the blood which was gathered to atrium during the systole is now moving to ventricles. P-wave of the ECG-signal is caused by the

contraction of the atrium to move all the blood from atriums to ventricles, and the phase is called atrial systole, while ventricles are still on diastole. The electric heart stimulus which starts from the atrium is now at atrioventricular node (AV-node), and in the node it is being delayed a bit so that the blood is able to totally move to ventricles. On that time there can be seen a little pause in the ECG signal, between the points P and Q. At the beginning of systole, the pressure increases rapidly in ventricles caused by the fast spreading of electric stimulus from AV-node to ventricles, which makes ventricles contract. QRS complex can be detected. As the pressure increases in ventricles, the atrioventricular valves close, and when the pressure in ventricles is higher than in arteries, pulmonary and aortic valves (semilunar valves) open and the blood flows to pulmonary artery and aorta. At the end the muscle in ventricles relaxes and the pressure in ventricles decreases under the pressure of arteries, and the valves to arteries are closed again. [52, p. 291]

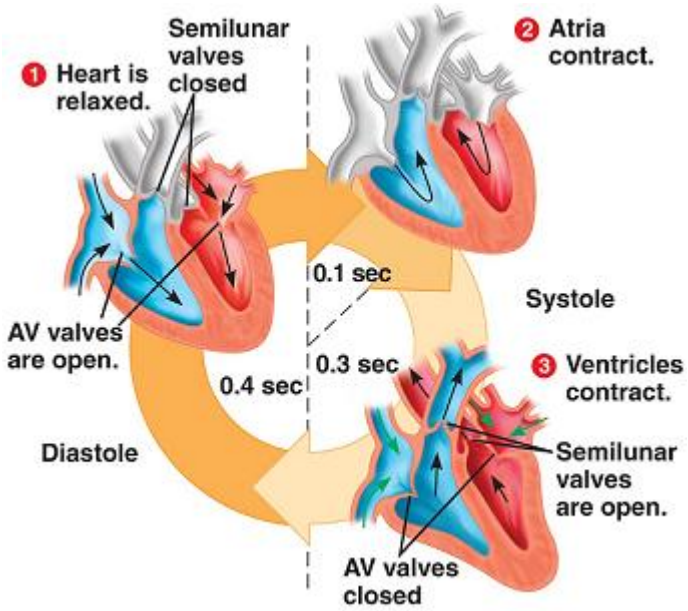

Figure 2.4. *Phases of a normal cardiac cycle with time approximation. [1]*

Heart rate is determined by many different functions of the body, but considering this thesis, it should be mentioned that respiration rate and volume affects to the heart rate [52, p. 292]. Moving of the lungs during the respiration may also change the direction and position of the heart a bit, which then affects to the orientation and strength of the detected ECG signal. [36]

Sometimes there are abnormalities during the normal heart cycle. One abnormality is an extra beat of the heart. There can be two kind of extra beats, one that is occurring in atriums, and one that occurs in ventricles. The further mentioned means the activation origin from the atrium or AV-node. Usually this affects so that the P-wave is abnormal and PQ-time is shorter than normally. The shape of the QRS complex itself remains about the same in atrium origin extra beat, but there exist a pause before next heart beat. Extra beat occurring in ventricles means the activation origin in

ventricles, from the place the activation in normal cycle should not origin. Ventricle origin extra beat is called extra systole. Extra systole can arise different ways and it produces abnormal QRS complex, which is due to slow conduction longer on its duration. Extra systoles can be once in a while seen on healthy persons as well. Extra systoles can be dangerous if they occur regularly and often, or if several extra systoles occur in a row. [52, p. 314]

2.2.2 ECG

Electrocardiography is a description of the function of the heart made by measuring bioelectrical activity of the heart. Cardiac muscle cell creates a current dipole around itself, with direction of the dipole being dependent of the phase of the potential activity of the cell (depolarisation and repolarisation) and the orientation of the cell in three-dimensional space. Magnitude of the registered current is dependent of the distance between the measuring point and the measured cardiac muscle cell. A vector quantity can be determined to present the moment of a current dipole (*m*), which has a unit of ampere meter. Parts of the heart that depolarize at the same time create their own vector component.

The sum of the current dipole moments of the cells is described with a heart vector (*H*), and it can be defined with an equation (Equation 1) presented below. In Equation 1, *V* is a volume and m is a moment of the dipole.

$$H = \int m \, dV \tag{1}$$

In one lead there are two or more electrodes, and the registering properties of it can be characterized with a vector quantity lead vector (*L*), which magnitude and direction is dependent on the location of the electrodes and the resistance of the medium between them. Unit of a lead vector is ohm/meter. Lead vector tells the direction in which the lead sees the heart in three dimensional space. Voltage measured from the lead A can be now calculated as a scalar product of two vectors, which is presented as an equation (Equation 2) below.

$$VA = LA \times H \times \cos\alpha \tag{2}$$

In Equation 2, α is the angle of the vectors. If it is assumed that $LA = 1$ and $H = 1$, the angle between the lead vector and the heart vector affects to magnitude of registered voltage as follows: if the angle between lead vector and heart vector is less than 90°, registered voltage is positive, if the angle is precisely 90°, registered voltage is zero, and if the angle is over 90°, registered voltage is negative. [52] Figure 2.5. illustrates three different leads, heart vector and the angle mentioned. Leads are in this case the limb leads I, II and III of Einthoven triangle, in where the measuring electrodes locate on both wrists and left foot.

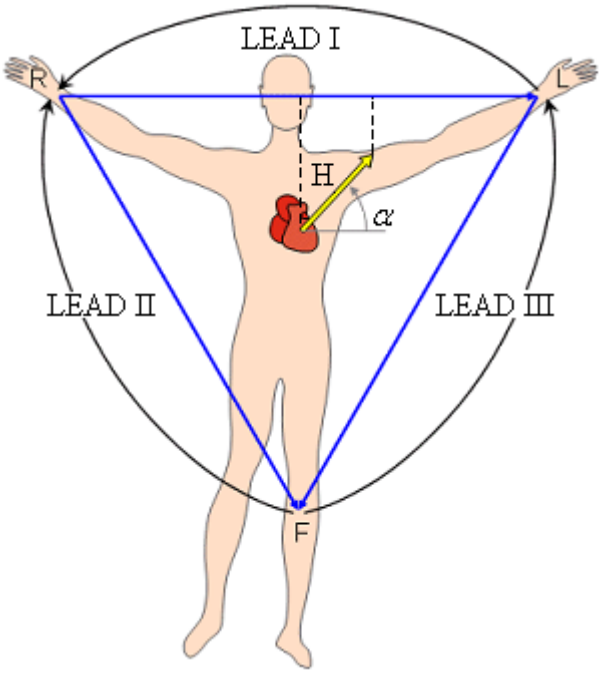

Figure 2.5. *Illustration of Einthoven limb leads, the heart vector H and the angle between heart vector H and lead LEAD I. [25, modified]*

The most used lead system for ECG measurement in clinical use is 12 lead system (Figure 2.6.). The most used way to present the ECG is to present it as a scalar presentation, which means that the voltages measured from different leads are presented as a function of time. [52]

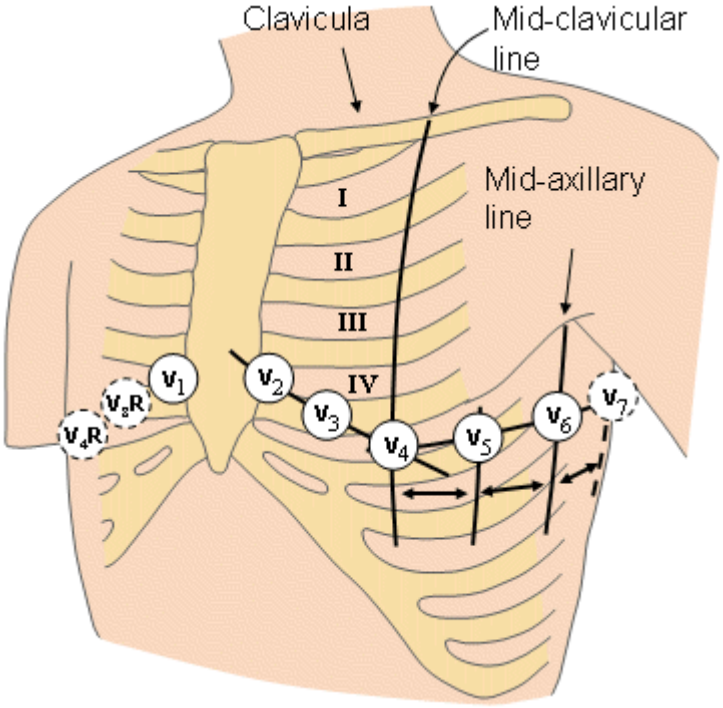

Figure 2.6. *Illustration of the electrode locations in 12-lead ECG method. In addition there are electrodes on both wrists and on left ankle.* V_{1-6} *are original electrodes of the method, while others seen in the figure are additional. Lines and clavicula mentioned in figure are used as coordinate points when placing the electrodes. [25]*

12-lead ECG system consists of nine electrodes, and 12 different leads can be derived from those. Leads are named as: *I, II, III,* aV_R, aV_L, aV_F and V_{1-6}. First six of mentioned leads are derived from the same three measurement points, which are both wrists and left ankle. Having this many leads, it is possible to calculate, and conclude already by seeing the signal, in which direction the heart vector is pointing at each time point. Different leads also make it possible to inspect different parts of the heart. [25]

2.2.3 Vectorcardiography

In vectorcardiography (VCG) the ECG electrodes are placed so that it is possible to register three leads, whose angles are as similar as possible with axes of orthogonal coordinate system. VCG is a way to present the ECG as a vector presentation, which means that voltage of one of the orthogonal leads is presented as a function of another orthogonal lead. By using VCG it is possible to get three plane projections of the changes in the direction and magnitude of a heart vector (Figure 2.7.). [52] The direction of each plane when observing human body is illustrated in Figure 2.8. There exists two main methods to measure VCG, Frank's method and in chapter 2.2.2. discussed 12-lead method. Either of these methods is suitable for localizing the heart vector or the current source itself creating the vector. The vector direction and strength are calculated. For localization of the vector, more channels and a model are needed.

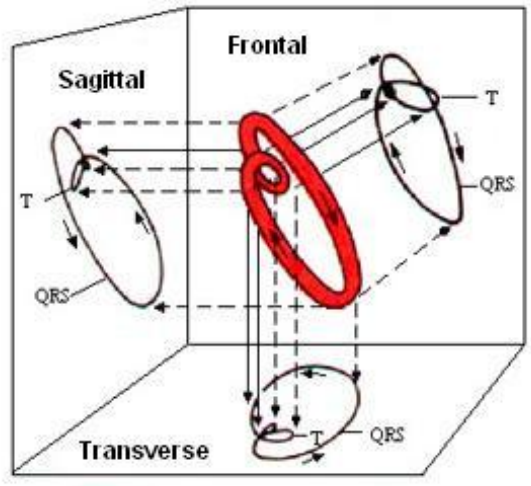

Figure 2.7. *Illustration of three different planes in VCG measurement. Red coloured object in the centre illustrates the location of the tip of the heart vector during the heart cycle. [54, modified]*

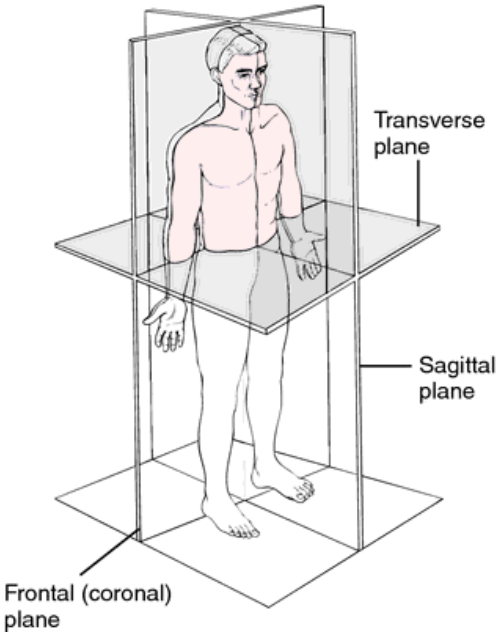

Figure 2.8. *Three different planes discussed in this thesis illustrated with a human body. [31]*

The most used VCG lead system is Frank's corrected lead system. [52] Frank's lead system includes seven electrodes in addition to reference electrode. Electrodes I, A, E, C and M are located at the same anatomic level. Level can be adjusted from the fifth interspace (between fifth and sixth rib), which is at the level of lower edge of the sternum. Lower edge of the sternum locates at the level of ventricles, which is the wanted level for electrodes. Electrodes M and E are placed on the back and front midlines of the body. Electrodes I and A are placed on both flanks exactly contrary to

each other. Electrode C is located on the midway between E and A. Electrode H is located in the neck about 1cm right from the vertebra C7. The exact place of electrode F is not that critical, but it should be located between the ankle and knee of the left leg. Electrode places are presented in the Figure 2.9. below. [13] Electrode on the left leg is not seen in the illustration.

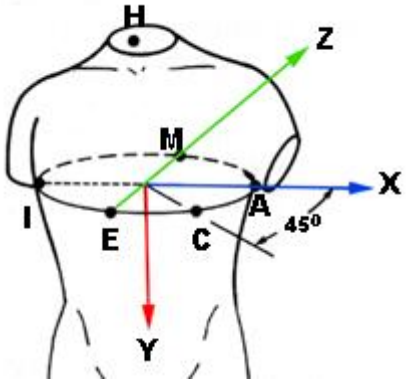

Figure 2.9. *Illustration of the electrode places in VCG measurement using Frank's method. One electrode not seen, locates in the left leg, above the ankle and below the knee. [12, modified]*

Magnitude of the measured signal on every axis in orthogonal coordinate system can be calculated from the registration of these seven electrodes by determining suitable coefficients to measured electrode voltages and by summing the voltage values on correct way. More detailed inspection of the calculation is left out from this thesis due to its length and less significance relevance to the issue itself examined. Equation for the calculation of magnitude in each axis in orthogonal coordinate system [13]:

$$\begin{aligned} V_X &= 0.610V_A + 0.171V_C - 0.781V_I \\ V_Y &= 0.655V_F + 0.345V_M - 1.000V_H \\ V_Z &= 0.133V_A + 0.736V_M - 0.264V_I - 0.374V_E - 0.231V_C \end{aligned} \qquad (3)$$

From the voltages V_X , V_Y and V_Z it is now possible to calculate the angle of the heart vector on each point in time using basic trigonometric functions. A normal vectorcardiography presentation of one heart beat is illustrated below in the Figure 2.10. The figure illustrates the duration of the heart vector to achieve six example points during heart cycle. Angles are presented next to axes, right side of the body marked with R, left side with L, abdomen with A and back with B. The loop of T-wave is marked separately with a character T. In VCG the direction of the heart vector can anyhow vary several tens of degrees between different persons [24; 52]. Duration and magnitude of the heart vector varies as well. Both magnitude and direction variation originates from the anatomical differences between different persons [36].

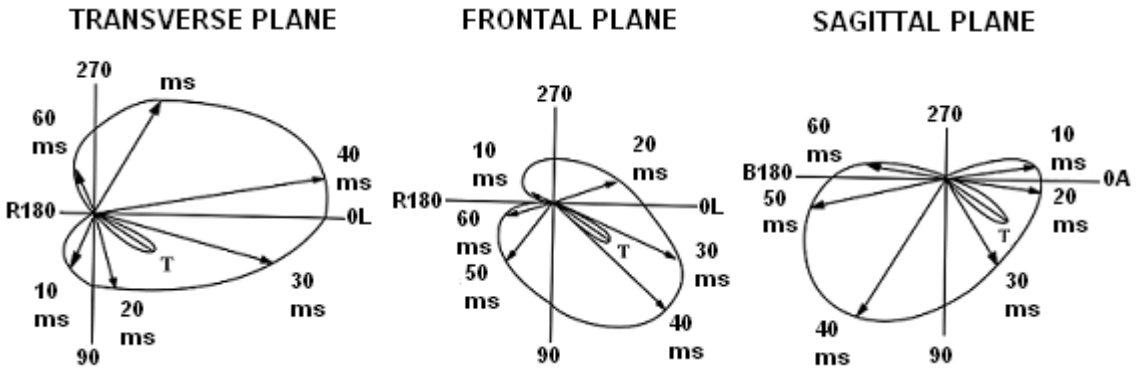

Figure 2.10. *Presentation of a normal vectorcardiographic QRS- and T-loop in three different planes. Some example duration and angle values are marked into the image. [12, modified]*

VCG presentation can be calculated from the 12-lead ECG measurement as well. Basic principal in VCG calculation from 12-lead measurement setup is to take projections of the lead vectors of the electrodes in all the orthogonal planes. Leads used in each plane are presented in Figure 2.11. Leads V_2 and aV_F are used to calculate the electric activity in sagittal plane. In frontal and transverse plane more electrodes can be used for the calculations: leads aV_R, aV_L, aV_F, I, II and III are used in frontal plane, while V_{1-6} are used in transverse plane. [25, Chapter 15]

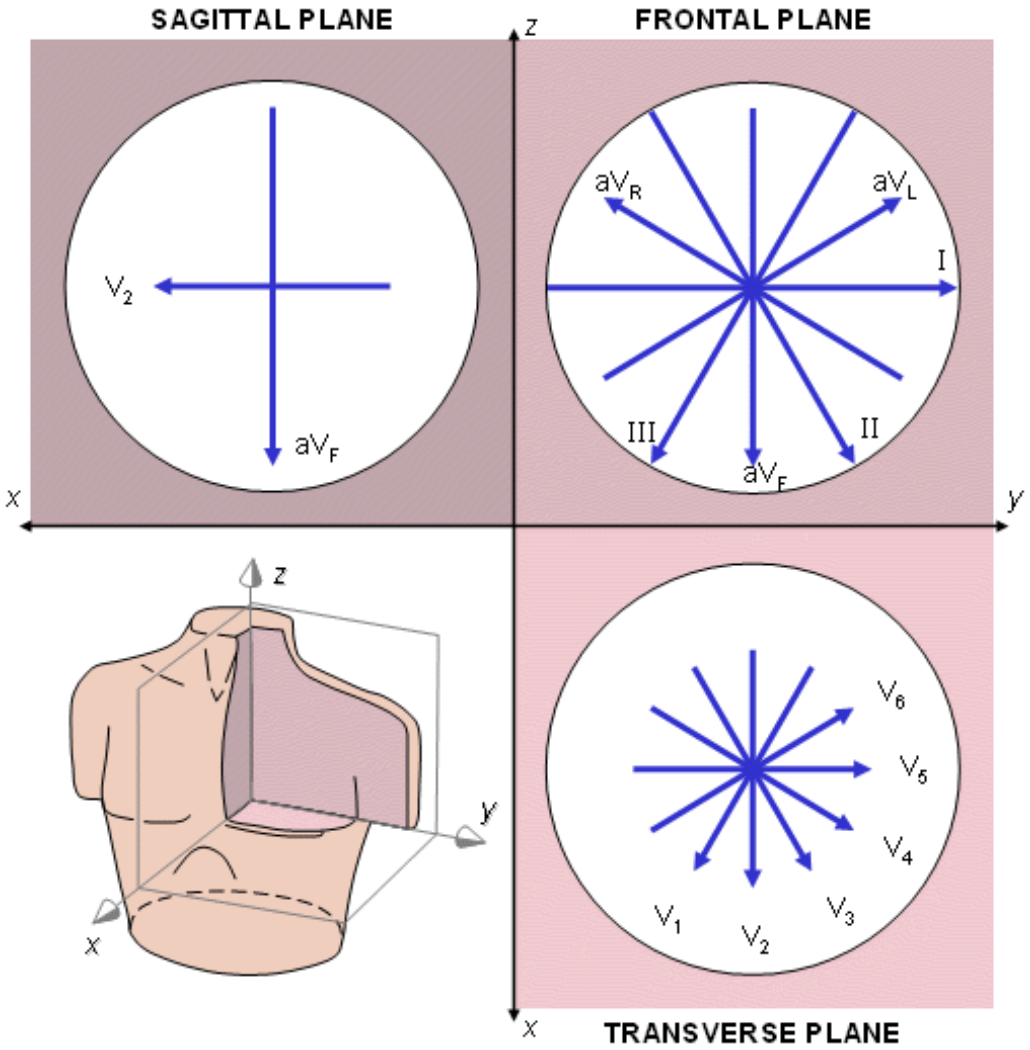

Figure 2.11. *Presentation of the leads in each plane used to calculate magnitude and orientation of a heart vector. [25, Chapter 15] Naming and direction of orthogonal axes differs from the ones used elsewhere in this thesis.*

In very basic situation the human body is thought as a homogeneous volume conductor. There exist also algorithms which do take into account aspects such that the volume conductor is not a spherical and homogeneous, and that the heart is not located centrally, which increases the accuracy of the angle calculation and makes the calculation more complex at the same time.

2.3 ECG artefacts

Thinking of identification of some signal originating from body functions, ECG signal is quite easy due to its regular rhythm and form. Nonetheless, the regularity and same shape is not self-evidence [43, look at 8]. In the situation where ECG signal is part of the EEG signal, the identification is more difficult. In the very basic situation the ECG signal is spread to the base of the scalp and it can be seen in ear electrodes. If ears are used as a reference, this can cause a problem, since in that situation the ECG signal is

seen in every EEG electrode. [8] Linked ears montage instead might reduce artefact. ECG artefact may be detected as a small spike every second, and it might resemble interictal spike or periodic lateralized or generalized periodic epileptiform discharges, depending on the measurement situation. [49, p. 248] Example of ECG artefact in EEG measurement is presented in Figure 2.12. EEG signal presented is from the data used in this thesis. ECG artefact can be seen as a spike in the EEG signal at the same time as the ECG signal has a spike. Artefact is seen in many of the EEG montages used in routine EEG measurement. Lowest signal in the figure is the ECG signal, and the fourth ECG complex is a ventricular extra systole. Extra systole is seen to produce different kind of artefact, peak being longer and not that sharp. Figure is taken with a normal program setup, which is used by doctors to analyze EEG recordings.

Figure 2.12. *Example data including easily seen ECG artefact in many of the EEG channels used in the EEG measurement. Fourth ECG signal is an extra systole. Lowest signal in the figure is the ECG signal.*

The physical dimensions of the test subject, might also affect to the ECG artefact. The body shape with babies [49, p. 248], and especially short neck can cause ECG signal to spread into parasaggital regions or even the midline, and the ECG signal can be detected on montages with bipolar electrodes placed closely to each other. [8] Shape of the body affects, because the dipole might be located closer to head, and have a better transmittance route to head [10, look at 49, p. 248]. Altering the head position may reduce the artefact. [49, p. 248] In addition to the length of the neck, affect of the orientation of the head and thickness of the neck is also studied in this paper. Respiration can cause some problems as well, since the motion of the body affects also to the orientation of the heart. Change in orientation might cause changes to the

amplitude of the ECG signal detected, or even make the whole QRS complex to disappear. Cardiac malfunctions affect to the functioning of the heart, which might be seen as a different kind of artefact compared to artefacts caused by orientation changes. Normal systolic pulse can also bring out artefacts, if electrode is placed on top of a small scalp artery [8; 10; 55, look at 49, p. 248]. In the mentioned case, the pulse wave causes varying of the impedance, which can cause different kind of artefacts depending of the movement of the electrode. Artefact caused by pulse wave is detected around 200-300 ms after the heart beat, since it takes some time for the pulse to travel from left ventricle to scalp. [8]

When diagnosing suspected electrocerebral silence, ECG artefact can be a serious problem [8; 28; 38]. ECG potentials sometimes resemble sharp-and-slow-waves or triphasic waves. In other instances ECG rhythm can be quasi-sinusoidal two or three times faster than the heart rate. [4, look at 8, p. 452] Sharp transients or theta or delta rhythms may be detected when cardiac arrhythmias or ventricular tachycardia occurs. ECG artefacts can be reduced, but usually not eliminated by disconnecting ECG monitors, repositioning the head of the patient and selecting montages less prone to ECG pickup. [49]

Depth of anesthesia can be monitored using different numerical values in addition to Bispectral Index. One of the subparameters incorporated in the BIS is the suppression ratio (SR), quantifying the percentage of suppression during burst suppression. EEG burst-suppression is an EEG pattern consisting of alternative periods of slow waves of high amplitude and periods of relatively low amplitude activity. [44] Several researchers have reported of ECG artefact related to BIS when monitoring the depth of anesthesia [15; 16; 28; 38]. Myles and Cairo [28] reported a case where they had an unexplained increase in BIS after cardiopulmonary bypass. During the surgery patient had BIS readings between 0-5 and suppression ratio of 100% indicating probable global cerebral injury. Later on patient had a sinus tachycardia and BIS reading increased to 38%, SR decreasing to 0%-2%. They also reported that the quality index of the signal was 90% - 100%, and no interference of external sources, pacemaker or muscle activity was detected. Raw EEG signal was unusual including slow regular wave synchronously with a pulse. This kind of pattern and BIS reading remained the last 40 minutes of the surgery. They repositioned the EEG electrodes, but even that did not affect to the value of BIS. Ischemic brain injury was confirmed later on. Even though ECG and EMG artefacts are normally filtered out by the BIS monitor, Myles and Cairo suspected that in their case the ECG or arterial pulsation was detected by the BIS monitor as an EEG signal, not as an artefact as it should be. [28] Puri and Nakra [38] observed same kind of findings as Myles and Cairo. They reported a case where all the tests of brain death were positive with a patient having ruptured intracranial aneurysm, in which an abnormal outward bulging vein in the brain has been ruptured causing internal bleeding [6; 38]. Despite the fact of existing brain death, they noted BIS values varying between 0 and 50 with suppression ratio varying between 100% and 25%. There was no significant electromyographic activity on the EMG strength indicator, and

by analysing the BIS monitor carefully they noticed that the monitor occasionally detected ECG signal as EEG signal. [38] Related to earlier case reports, Gaszynski [16; 38] had a same kind of abnormal BIS readings in his work with patients having severe brain injury. Gaszynski says that in some cases the changes in ECG can not be connected to BIS change [38], and suggests that the possible answer could be that brain really has some activity left, as the brain does not die completely in one moment. [16] In the paper of Gaszynski, like in most papers on BIS, the original EEG signal had not been recorded and analyzed, so this is merely guessing.

ECG might be detected in some or all channels especially if maximal sensitivities are used. ECG signal intruding to EEG measurements obscures the detection of low-voltage slow activity. This might be tried to be alleviated by using short time-constants on low-frequency filters, which leads to situation where aberrant ventricular contractions might resemble sharp waves [7, look at 8, p. 91]. Another problem that might occur with maximal sensitivities is ballistocardiographic artefact, which occurs when systolic pulse waves produce minute vibrations which are moved also to the bed and thereby to the attached electrodes as well. This kind of rhythmic low-voltage activity may resemble cerebral activity. Another clear artefact can be cardiac pacemaker, which occasionally produces high-voltage artefactual discharges. With patient who have cardiac pacemaker, an own channel should always be used for detecting ECG signal. [8, p. 91] Artefact to BIS readings caused, with high probability, by a pacer was reported 1999 by Gallagher, J. [15]. Gallagher reported case where an 81 year old man was in an aortocoronary bypass (ACB) surgery, in which an obstructed coronary artery is bypassed to prevent or cure lesion in the heart [31]. Weaning from the bypass was successful, but after that a junctional rhythm (abnormal AV-node originating heart rhythm [31]) was noted, and atrial pacing of the heart was started. Soon after that, an increase in BIS reading to value of 90 was noted. BIS value was unsuccessfully tried to be decreased using medicine. Recorded signal during the situation is presented below in Figure 2.13. The Figure 2.13. shows the increase of recorded BIS signal between time points of 16:55 and 17:15, and from 17:25 onwards.

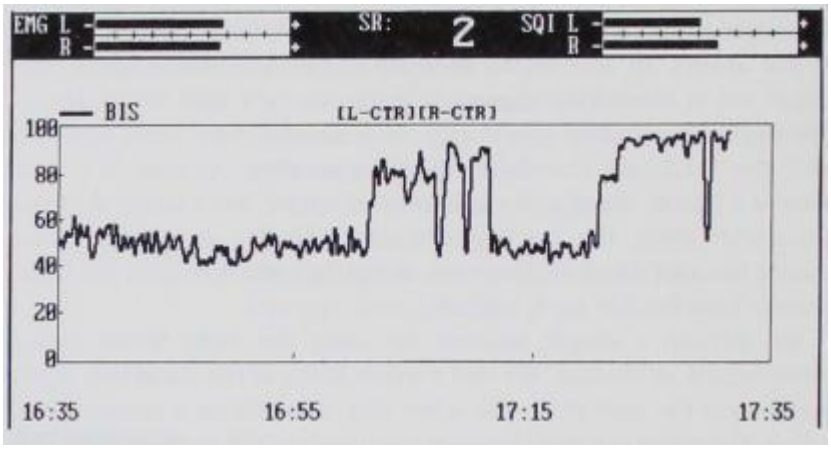

Figure 2.13. *Bispectral index trend display from the measurement done by Gallagher, J. D. Trend is showing sudden increases in the BIS value during the time between 16:55 and 17:15, and after 17:15 as well. [15]*

Gallagher expected the rise to be an artefact and stopped the pacing, followed by the decrease of BIS reading back to its earlier magnitude. Pacing was begun again few times, and every time BIS reading had a rise. Signal quality was said to be high and electromyographic intensities low and they suggest that the rise of the BIS reading was caused by the pacer. [15]

2.4 Processing of the EEG and ECG signal

Before analyzing the EEG signal, it is recommended to process the signal so that it includes as few irrelevant variables as possible. Processing also makes it easier to read the signal. Amplifiers have their own bandwidth where they function correctly and amplify all the recorded EEG signals as wanted. The minimum frequency limits for the correct constant functioning of the EEG amplifier are from 1Hz to 60Hz. In this frequency area the maximum acceptable fluctuation of the amplitude is 10%. Clinically the most important frequency bandwidth is from 1Hz to 30Hz. [33] For ECG measurement the appropriate low cut frequency is 0,5Hz [36; 37] and the usual high cut frequency is 100Hz. [37; 52]

In digital EEG devices the sampling frequency has to be over two times the high cut frequency to avoid aliasing of the signal. Filters attenuate the amplitude of the signals that are too high and low on their frequencies. At the same time filters distort the phase of the original signal, and thus change the shape and timing of the signal. This is the reason why EMG artefact originating from the muscles can not be just deleted away by moving the high cut frequency lower, but instead it should be tried to be diminished using other methods. Possible artefact originating from the electric main line is usually deleted by using a notch filter, which has a very narrow stop band. This kind of notch filter deletes the main line artefact almost totally, but takes away only a little portion of the actual signal, thus having only insignificant effect to the shape of the EEG signal itself. [33, p. 69]

2.5 Modelling

In addition to more conservative methods of measuring bioelectrical activity of the body, it is possible to mathematically compute bioelectrical phenomena inside the body. Functions and mechanisms of excitable membranes in living organs are closely related to bioelectrical activity. Modelling is computing of bioelectrical activity in virtual experimental setting, and it is a way to get better understanding of the functions and mechanisms behind the bioelectrical phenomena in human body. In the biophysical point of view the membrane excitation in cardiac cells and neurons can be treated as volume current source, and are thus similar. Results of the clinical observations of ECG and EEG arise from the volume conduction of currents within a body volume conductor. The difference in bioelectrical activity originating from different organ systems is primarily due to the different kind of physiological mechanisms behind the phenomena. Modelling is closely related to imaging methods, and from the method point of view modelling and imaging of bioelectrical activity can be treated within one theoretical framework. [5, Preface]

2.5.1 Forward problem

The forward problem of ECG means the calculation of the potentials on the surface of the body originating from the heart sources by using the theoretical equations of electromagnetism. To be able to calculate the potentials, the suitable representations of the heart sources and the body geometry are needed. There are two most often used methods to represent the heart sources; first more often used being a current dipole consisting of source and sink of equal magnitude with a very short distance between them. In the other method the body surface potentials are calculated using the actual potentials on the epicardial surface of the heart as the starting representation. [5, p. 43] In this work the former one is chosen, since it is easier to implement and the accuracy of the method is seen sufficient enough for the purpose.

Forward problem is in this case considered so that the potentials desired from the body surface are far enough to be able to represent the heart sources as a simple dipole model. When considering near field forward problems, the simple dipole representation might not be acceptable. The dipole source representing heart can be expressed as an equation

$$p = l\delta \tag{4}$$

In Equation 4 p is a vector with a direction of δ and a magnitude of $l\delta$. The direction is the direction of the line between the source and sink of the dipole. Dipole is now modelling the sum of all the ionic source currents that flow across the surface membrane of the individual heart cells into the extracellular space. As the simplest it can be represented with an Equation 5. In Equation 5 *J(r)* is the net source current density at a point characterized by the spatial vector *r*. *J* is the sum of all source current

densities J_S and the conduction current density σE, where σ is the conductivity and E is the electric field.

$$J(r) = J_S(r) + \sigma E(r) \tag{5}$$

The Figure 2.14. presents an illustration of the theoretical situation where there is a potential origin from the dipole p on the point situated at P in an infinite homogenous medium of conductivity σ. Potential at point P can be given by the Equation 6.

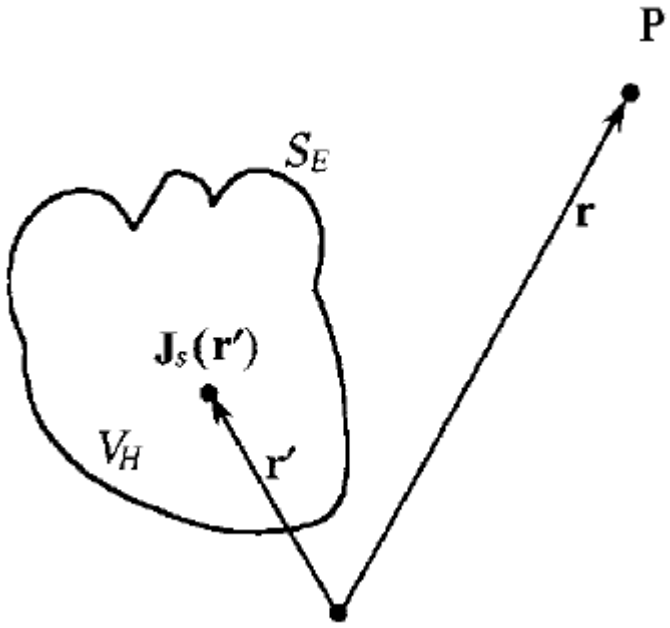

Figure 2.14. *A heart volume V_H, surrounding surface S_E in an infinite medium of uniform conductivity. The potential is detected at point P characterized by the position vector r. Variable r´ exists due to integration. [5, p. 45]*

$$\Phi(r) = \frac{1}{4\pi\sigma}\, p \cdot \nabla' \left(\frac{1}{|r - r'|} \right) \tag{6}$$

In Equation 6 r' is a variable of integration that traverses the source coordinates and r is a position vector. [5, p. 45] In practice the medium is not homogeneous, since there are many different tissues which have different conductivities. How to model a non-homogeneous medium is discussed in chapter 2.5.2.

2.5.2 Forward solution

Calculation of the body potentials from the heart source dipoles can be done by using one of two general approaches, called surface methods and volume methods. On surface methods only the interfaces are discretized, and thus the methods obtain the potentials

only on the interfaces. On the volume methods the medium volume is discretized three-dimensionally, and the potential can thus be obtained everywhere. [5, p. 53] In this thesis the later method is used, since more than just interfaces are wanted to be known.

In volume methods there are still several different methods that can be used. The method which is chosen is more accurately finite-difference method. Finite-difference method is chosen since it has a convenient coordinate system. The finite-difference method represents the medium volume by a three-dimensional array of regularly-spaced nodes that are connected to each other (Figure 2.15.). Between every node there is a resistor. Resistor value is chosen so that it reflects the resistance between the nodes. Between every node there exists an equation that calculates the potential between adjacent nodes. The equations are written by using a Kirchhoff's current law and the law of Ohm. [5, p. 58] In the modelling program used in this work, the finite-difference method is an approximation of Laplace's equation (Equation 7) and Poisson's equation (Equation 8):

$$-\nabla\sigma\nabla\Phi = 0 \tag{7}$$

$$-\nabla\sigma\nabla\Phi = I \tag{8}$$

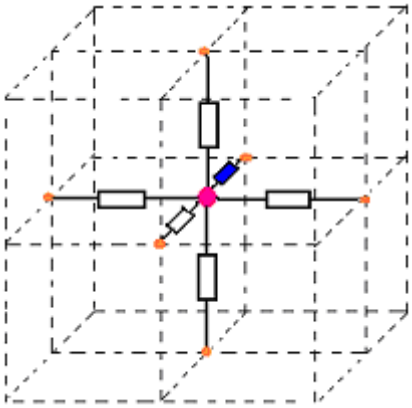

Figure 2.15. *Illustration of the node network used in finite-difference method. Eight voxels are connected to one node in the centre. Resistor values are defined as the connection in parallel of four edge resistors of neighbouring voxels [40, look at 29, modified].*

In Equations 7 and 8, ∇ is a Laplace operator, σ is a three-dimensional tensor of conductivity, Φ is the scalar potential and I is the impressed current source strength. The approximations are made in a rectangular grid of nodes, so that Laplace's equation is used at a source free node, and Poisson's equation when the node is a source node. [30] The solution is thus dependent of the resolution of the existing node information and the accuracy of the resistors represent of the medium resistances. Equations are solved by using iteration. The drawback of finite-difference method is the slow convergence. [5, p. 58]

2.5.3 Tissue conductivity values

Tissue conductivity values directly impact to the results derived from the model. Tissues have different conduction properties for electrical currents. When conductivity parameter differs in place to place, volume is called inhomogeneous. Conductivity is called anisotropic when conductivity differs in different directions. The basic equation of conductivity is presented below (Equation 9).

$$G = \sigma \frac{A}{l} \tag{9}$$

In Equation 9, σ is the electrical conductivity of the material, A is the cross-section area of the material and l is the length of the material. Equation 9 says that the larger the cross-section area and the shorter the conductive material is, the better conductivity. Relation between conductivity and resistivity is shown in the equation below. [53]

$$G = \frac{1}{R} \tag{10}$$

So conductivity and resistivity are inversely proportional measures. The conductivity values of human tissues are among other things dependent of the blood content and temperature, they are a function of the frequency and strength of the applied current and they show an inter-individual variability, and they are inhomogeneous and anisotropic [45; 46], [22, look at 5, p. 282]. Current density is linear with the applied electric field if the current densities are low, so in this case the law of Ohm is valid. The purpose to model different tissues with different conductivities is to get approximately the same potential distribution on the measured point as the real inhomogeneous tissues would give. [5, p. 282] On the study by Hyttinen et al. they got results which show increase of 10% on the body surface potential levels of the X, Y and Z dipoles, when the conductivities of all the tissues are increased by 10%. The effects were different depending of the tissues, while the increased conductivity in the tissues close to heart dipole sources, like blood and heart muscle increased the ECG potentials and the increase close to the surface decreased the ECG potentials. [19] If the purpose of the model is to localize the sources of the measured potentials, then only the ratio of the tissue conductivities is important, if the magnitudes of the measured potentials are important, then the absolute tissue conductivities should also be as correct as possible. [5, p. 282] Considering this study, realistic conductivities are used, since that is the usual way to construct the model, and only ratios of tissue conductivities would be more difficult to find. Conductivity, or in this case resistivity values that are used in this study are presented in Table 2.1., including 31 different tissues plus the value for air.

Table 2.1. *Table of segmented tissues and their resistivity values, which are used in modelling tasks of this thesis.*

Tissue	**Resistivity [Ohmcm]**	**Tissue**	**Resistivity [Ohmcm]**
Empty	75000	Lung inflated	1065
Marrow	2174	Intestine	10
Fatty tissue	2500	Kidney	391
Bones	6523	Liver	414
White substance	714	Glands	576
Grey substance	303	Spleen	5128
Skin	233	Stomach	600
Eye	196	Pancreas	576
Muscles skeleton	909	Gall bladder	576
Blood	150	Intestine contents	10
Liquor	65	Ventricle right	420
Neural tissue	625	Ventricle left	420
Lens	576	Atrium right	420
Optical nerve	725	Atrium left	420
Cartilages	576	Blood venous	150
Mucous membrane	576	Blood arterial	150

Resistivity values of different tissues have been collected from various references [3; 17; 19; 41; 42; 48; 57]. Most of the chosen values are the ones that are most used in the mentioned papers. But some of the values are chosen differently. This was done because values from different sources were not identical. The resistivity of the bones is a mean average of the two reference values [42; 57], which are thought to be the most correct ones. For optical nerve different resistivity values can be found for different directions [32], and the mean of those is chosen, since the model is constructed to be isotropic. For lung four different values were found, and the mean of those is chosen. For kidney and liver the value is taken as an average of two references, which are thought to be the most correct ones [17; 41]. For spleen only two references [17; 41] are found, and the chosen value is the mean of those. For stomach the chosen value is the mean of the three found references [17; 42], [48, look at 19]. Resistivity value for intestine contents is not found, though it is segmented as a separate tissue in the model data. Value for intestine contents is chosen to be the same as it is for intestine. For some other segmented tissues the resistivity value is not found from any paper, and those are chosen to be “other tissue” as it is said in two references. Other tissue is chose to have resistivity from the reference [41] that is thought to be most correct one. Tissues marked with a resistivity value of “other tissue” are lens, cartilages, mucous membrane, glands, pancreas and gall bladder. It has to be noted that common, so called correct resistivity values for the tissues do not exist at the moment. The difficulty of using values from many different references is that also the ratio between the tissue resistivity should be correct to get realistic results from the model.

3 METHODS

This chapter discusses the methods used in this thesis. Chapter discusses the experimental part of the thesis. In the experimental part the ECG is recorded from three test subjects and four patients. In the first subchapter is discussed the ECG measurements. Second subchapter discusses the current input measurement done to one of the test subjects. Third subchapter discusses the measurement related to monitoring of EEG derivation. Processing methods in measurements are discussed in the fourth subchapter. Models and simulations of the thesis are discussed in the fifth subchapter, while the sixth and the last subchapter discuss the visualization of the data.

3.1 ECG measurements

Main measurement setup includes a vectorcardiography (VCG) measurement together with electrode setup measuring surface potential in the area of neck, face and scalp. More accurate placing of the electrodes is discussed on next subchapter**.** The idea of the measurement is to measure the strength and orientation of electric activity of the heart, together with the registration of electric activity around the area of neck, face and scalp.

Measurement is done with various head orientations. The effect of the head orientation to the spreading of the electric activity of the heart over the neck and head is analyzed. Test is performed on three test subjects. A normal 12-lead ECG measurement is carried out separately to detect any abnormalities from the heart. 12-lead ECG is also used to calculate the magnitude and orientation of the heart vectors. Extra systoles are also studied with a separate measurement. In extra systole measurement the appearance of the potential distribution over the head area during an extra systole is studied. Results are then compared to normal heart beats. From the data of the extra systole study the potential change over the scalp during the whole cardiac cycle of a normal heart beat is also calculated. Measurements of the extra systoles and cardiac cycle of a normal heart beat are discussed in subchapter 3.1.5. Thickness and length of the neck of test subjects is examined as well to find any correlation with the length measures and the potential measured from the scalp.

3.1.1 Electrode setup

In addition to normal VCG electrodes, main measurement setup includes some of the basic 10-20 EEG measurement electrodes and electrodes around the neck and face. From the basic 10-20 EEG measurement electrodes, the electrodes in the axis from fore head to back of the head and from ear to ear are chosen. This kind of selection is made

because of the limitation of channels on the used amplifier, and to get recorded signal in two orthogonal directions over the head. In addition to these two directions, electrodes F3, F4, P3 and P4 on top of the head are chosen, leaving F7, F8, T5, T6, O1 and O2 out from the normal 10-20 EEG setup. Instead of leaving Fp1 and Fp2 out, O1 and O2 are left out, since the area of the fore head is thought to be more interesting considering EEG measurements during anesthesia. Reference electrode is located at the centre of electrodes C3, F3, Fz and Cz, and it is the reference to all the electrodes used. VCG electrodes are included to same reference, because the amplifier used does not support two different reference points. Another reference is mathematically calculated after the measurement is done. Calculation of a new reference is explained more accurately on subchapter 3.4.2. To get a more consistent recording of the spread of ECG signal from heart to head, few recording points are chosen from the upper body and face as well. All the channels used are listed in Table 3.1.

Table 3.1. *List of electrodes used in the custom measurement setup*

10-20 EEG electrodes	Additional electrodes	VCG electrodes
Fp1	Medial head of right clavicle	I
Fp2	Adam's apple	A
F5	Neck (on the level of Adam's apple)	E
Fz	Neck (on top of vertebra C7)	C
F4	Lower jaw (right back corner)	M
A1	Lower jaw (left back corner)	H
T3	Nose	F
C3	Chin	
Cz		
C4		
T4		
A2		
P3		
Pz		
P4		

Chosen points from the upper body and the face are medial head of right clavicle, Adam's apple, point on the neck on a same level with Adam's apple, C7 vertebra on the neck, back corner of lower jaw on both sides, tip of the nose and tip of the chin. Measuring of airflow was considered as well, because of the known effect of heavy respiration to the orientation of the heart. Measurements are performed during the normal respiration rhythm, and due to that the detection of airflow is left out from the final measurements.

3.1.2 Custom EEG cap and measurement equipments

Custom made EEG cap (Figure 3.1. A) is constructed to perform the wanted measurements. Cap is constructed of an original EEG cap from Electro-Cap International. Construction is done by customising attaching positions of electrodes.

Channels which are left out from the 10-20 EEG measurement electrodes are unconnected by cutting the wire from the electrode end, so that the wire is still attached to a connector of a cap. The wires which are cut are connected to longer wires having an electrode on the other end. Attaching longer wires makes it possible to connect otherwise unused cap channels to electrodes on some other locations. Attaching of the cap channels prevents also noise to exist via floating unused wires. Cap itself makes it easier and faster to attach EEG electrodes properly, and thus to perform the measurement correctly. Another way to proceed would be to left the cap out and manually find and attach all the electrodes to a proper location. In this particular case otherwise unused cap channels are attached to Adam's apple, point on the neck on a same level with Adam's apple, back corner of lower jaw on both sides of the head, and to VCG-measurement points M (back) and E (front). VCG-measurement points are explained on subchapter 2.2.3. Added wires and electrodes used on the wires are same kind as the ones in the cap. All the other additional wires and electrodes (Figure 3.1. B) which are used in the measurements are custom made as well. Conductor material of electrodes is tin. Using same materials on all the wires and electrodes minimizes the impedance variation originating from the equipments.

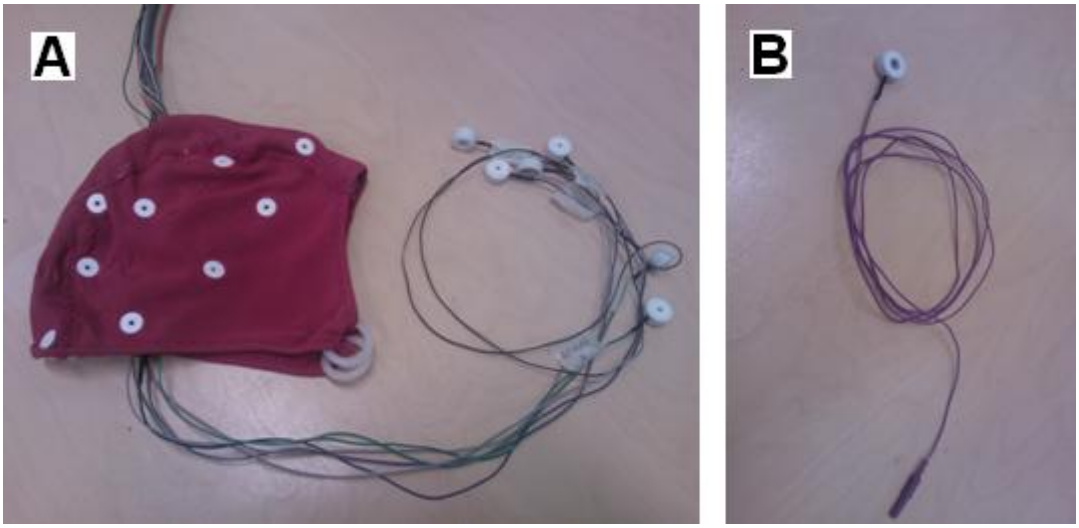

Figure 3.1. *Image of the custom made EEG measurement cap (A) and additional wire (B), which are both used in the measurements.*

NicoletOne EEG amplifier U32 is used in the measurements. Amplifier includes 32 recording channels. Impedance of the channels is automatically measured by the amplifier. Program used to run the system is NicoletOne EEG version 5.80. Special montage in the program is made to include the wanted channels with the wanted properties.

3.1.3 Measurement procedure

The measurement procedure starts with preparing the skin of a test subject in proper manner after which the electrodes are placed. Custom made electrodes are fixed on their place with tape. Conductive paste is used to guarantee desirable conductivity and impedance level. Chosen position for test subject is to lie on his back on a bed. Mentioned position is decided to avoid unnecessary movement, which could cause noise via the electrode movements and appearing muscle activity. Measurements are done with a bed that has a separately movable part where the head of a test subject is located (Figure 3.2.). This makes it possible to move only head so that it is in straight position with the rest of the body. With movable head part it is also possible to easily change the orientation of the head compared to the body.

Figure 3.2. *Image of the measurement setup. Separately movable part of the bed is seen under the head of the test subject. In the image the head of the test subject is lifted forward, while the body remains straight. Image is taken during the test measurements for the thesis, test subject being the author. Respiration sensor below the nose is left out from the final measurements. Amplifier used in the measurements is seen in the image next to test subject.*

At first the measurement is done so that test subject is lying on a bed, keeping his head in a normal position, eyes directed straight to the roof. During the measurement eyes are kept closed to avoid unnecessary artefacts origin from the eye movements.

Next the head is turned on a transverse plane to left and right, 45 degrees to both directions. Second plane for head turning is a sagittal plane, and the head is turned again 45 degrees to both directions, forward and backward. Recording time in each position is four to five minutes. In situations where the head is turned on some specific direction, head is supported with pillows if necessary to avoid tension in muscles around the neck. Angle of the turned head is always measured before starting the actual recording.

Various methods were considered for measuring the angle of the head. The difficulty in measurement is to get the angle of the head in all three direction at the same time, so that it is possible to know that head is only turned in one orientation at the time. It was noticed, that when the head is turned on a transverse plane, it easily turns in a frontal and especially in a sagittal plane as well. Same phenomenon can be noticed in other orientations as well. Another problem occurs when considering the point from which the head is turning. In a transverse plane the head is turned quite accurately around one axis, but the sagittal plane is more difficult. Human anatomy makes it impossible to turn the head in sagittal direction so that it would only move around one axis. In sagittal plane the cervical vertebras (vertebras existing in the neck) are moving along, and thus the whole neck is turned. Practically every cervical vertebra brings their own little axis to a turn, and thus the accurate calculation of the angle of the head in a sagittal plane is challenging. In a transverse plane the tissues of the neck are twisted during the head turn. Twisting of a neck is not affecting to the measured angle, since the axis compared to head is staying on a same place. On the other hand, twisting of the tissues is perhaps one variable that could affect to the spreading of the ECG signal over the head.

Since there are many variables affecting to the accuracy of the measured angle, and the knowing of the very accurate angle is not a main purpose of this research, the very accurate inspection of the angle is left out. Different ways to measure the angle were tested and those are explained next. One simple device to measure the angle of the head is a goniometer, which is a mechanical meter that can be used to measure angle between two axes (Figure 3.3 A). Goniometer is easy to use and small from the size. Accuracy of the goniometer is anyway quite poor when measuring the angle of the head. Goniometer is difficult to locate the same way every time, and it is difficult to measure the angle of the turned head without the effect coming from the cervical vertebras. Inclinometer is a measurement system to measure angle on respect to gravity. In Figure 3.3 B can be seen a mechanical inclinometer, which could be used for this purpose as well, but it has the same problems as goniometer. Inclinometer is difficult to use and repeating of the measurements the same way every time is difficult. One device that has been used at least in physiatrics to measure the movability of the head is called a cervical measurement system (CMS, Figure 3.3. C). Device makes it possible to measure the angle of the head in three directions by using two inclinometers to measure sagittal and frontal planes, and a compass to measure cervical rotation. [47, look at 34]. CMS, or a version from Kuntoväline Oy called CROM, is an accurate measurement system which takes into account all three directions at the same time and can be

attached to head so that it will not move during the measurement. CROM is not chosen for these measurements due to its high price. Self made angle gauge (Figure 3.3. D) is experimented as well but rejected due to its inaccuracy and bad usability for different orientation. Thickness of the neck affected to the measurement result as well with the self made gauge. Electronic orientation sensors were under inspections, but ready to use packages were noticed to be too expensive. Without ready to use package the method would have needed a lot of work to implement sensors for these purposes. Measurement system chosen, is a digital angle gauge (Wixey WR300, Figure 3.3. E). Due to the small size (5cm x 5cm x 3.3cm), digital angle gauge can be attached to head easily with a band.

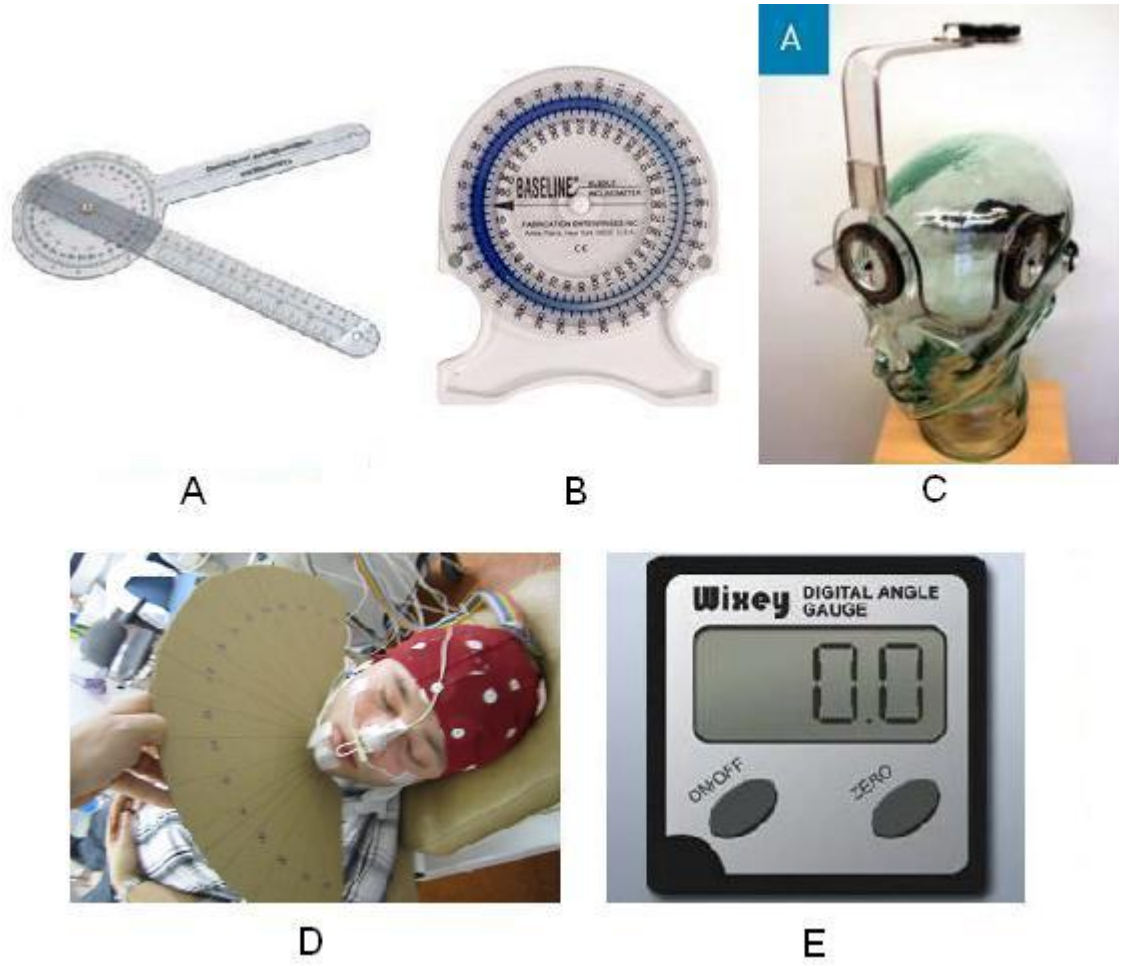

Figure 3.3. Head orientation measuring devices. ***A****: Goniometer [14]* ***B****: Inclinometer [14]* ***C****: Cervical measurement system [21]* ***D****: Self made angle gauge* ***E****: Digital angle gauge, Wixey WR300 [35]*

Attaching gauge to the head decreases the possibility of test subject to affect to the measured result, which then increases the accuracy of the measurement. Accuracy and repeatability of the Wixey WR300 is reported to be ±0.1 degrees [58], which is more than enough for the purpose. Wixey WR300 can also be reset to zero in any position. The movement of the head only in one direction is monitored with a laser pointer attached to the angle gauge. Laser pointer points on to the roof of the experiment

room. On the roof there is drew two perpendicular lines, from where it can be seen that the head is turned only on wanted direction in each turning orientation. If the laser pointer is pointing to the line, turning of the head is unidirectional. Before starting the recordings, test subject and the bed is located to the marked place so that the distance of the laser pointer from the surrounding walls is always the same, which is crucial for the monitoring of the head movements. Angle of the head can be red from the meter constantly, which makes it easy to observe the possible fluctuation of the angle.

Length and thickness of the neck of the test subject is measured as well. Measuring is done using a basic measuring tape. Length of the neck is measured between vertebra C7 and base of the skull along the neck surface. Thickness of the neck is measured right under the Adam's apple. All the used test subjects and patients are men, so the Adam’s apple is a suitable comparison point. The result of the measurement is approximated to the closest number with an accuracy of 5 millimetres.

3.1.4 12-lead ECG

To be sure that the hearts of three test subjects are working normally and do not have any anatomical or functional abnormalities, a normal 12-lead ECG test is recorded in a laboratory of Clinical Physiology at the Central hospital of Seinäjoki. Test is performed by the nurse trained for the purpose. Measurement is carried out test subject lying on his back on a normal hospital bed. Results are shown to a doctor for an evaluation. Device used for the purpose is MAC 5500 from GE Healthcare.

Since there is noticed some difficulties calculating the heart vector from the test subjects using Frank's method, the 12-lead ECG method is used for the purpose as well. The data got from the MAC 5500 is saved and processed in Matlab to produce VCG presentation and to calculate the angle of the heart vector in three directions. More accurate information of the processing is given in chapter 3.3. Angle of the heart is calculated for each of the planes separately. Exact algorithms in MAC 5500 for VCG lead calculations are not available.

3.1.5 Ventricular extra systole and normal cardiac cycle

Ventricular extra systole is an extra heart beat originating in the ventricles. Extra systoles, which differ of a normal heart beat signal from the shape and magnitude, complicates the possibility to remove ECG artefact totally from the EEG signal by using automatic detection algorithm. Examination of a potential distribution over the head during an extra systole is performed and it is compared to the potential distribution arisen from a normal heart beat. Measurement during extra systoles is performed for four patients having notable amount of extra systoles. One of these four data sets is from an earlier study done at the department, and for that reason the length measures from the neck do not exist. Measurement is performed by trained personnel during routine EEG examination at a department of Clinical Neurophysiology at Seinäjoki Central Hospital. Electrodes used are thus the normal 10-20 EEG electrodes, and the used cap is the

Electro-Cap International. VCG measurement and head turnings are left out. To be able to examine the ECG signal of extra systoles, it is a qualification that enough extra systoles appear during the 20 minutes EEG examination. Reason for earlier is explained later in subchapter 3.4.2. Two of the recorded data did have less than five extra systoles, and they are left out from more specific examinations. One data includes 10 extra systoles, and one 18 extra systoles, and those are selected for further examination. Mentioned two data sets are now on stated as Data 1 and Data 2. Data 1 is recorded in earlier study. Normal QRS complexes from these patients are also recorded during the same examination, and those are processed for the comparison. From the normal QRS complexes the potential distributions over the scalp are calculated during different phases of a cardiac cycle. In other measurements in this thesis normal cardiac cycles are recorded as well, but Data 1 is chosen for the cardiac cycle examination since the measurement is done with 19 electrodes. 19 electrodes give more information from the scalp. Data 1 also has high ECG potential values on the scalp, which makes it easy to visually present the function of the heart seen on the scalp.

3.2 Current input measurement

Current input measurement is performed only to test subject one. Using current input measurement it is possible to measure the effect of the known sources with a real subject. Input is performed with two Ag/AgCl electrodes placed on both sides on top of the clavicles, on the same line with ears. With test subject one the distance between electrodes is measured to be 23cm. Current between electrodes is illustrating the x-component of the heart vector, since the direction of the electric field between the electrodes can be thought to be about the same. X-component is the direction between the armpits. Measurement electrodes are the same that are mentioned in subchapter 3.1.1. Different input signal magnitudes and shapes are studied. Studied magnitudes are peak-to-peak input voltages of 0,7V, 1,4V, 2,8V and 5,6V. Input signal shapes tested are sinusoidal signal and square signal. Both positive and biphasic signal with frequency of 10Hz and symmetry of 50% are used. Since the idea is to compare the signal with the signal originating from the heart, it is desirable to use the signal of same order of magnitude. Peak-to-peak input voltage of 1,4 V generates about the same magnitude of potential over the scalp as the heart does and thus it is chosen to be used in measurement. Biphasic signal is noticed to work with the electrodes better than positive signal. Polarisation is observed in the measurement system when the input voltage is positive the entire time. Square signal gives a better respond to the measuring electrodes, and it is thus chosen to be the used signal shape. Recorded time in every position is now only around one minute, since the frequency is much higher than in ECG measurement.

Current input is performed using digital function generator TG1010A from Thurlby Thandar Instruments. Stimulation electrodes are attached on outputs of the generator. Trigger output of the generator is attached to the trigger input of the Nicolet

One EEG amplifier. Detecting trigger signal with amplifier makes it possible to save the measurement data with time points of triggering signals. Time points of the triggering signals are then used later, when data is processed. To be able to attach the trigger signal from signal generator to Nicolet One EEG amplifier, custom adapter is made.

3.3 Monitoring EEG derivation

Another measurement performed is the measurement of electric activity of heart using similar electrode locations as in anesthesia monitoring. Normally the anesthesia monitoring is done using the special tape electrode system and an own monitor outputting the measurement result. There exist a few different kinds of electrode systems, and the one called standard electrode system is presented in Figure 3.4.

Figure 3.4. *Example of electrode system used in anesthesia monitoring. [2, modified]*

In the study of this thesis, special monitor is not used and the electrode system is not the official electrode system. For mentioned reasons the measurement is called monitoring electrode (ME) measurement. The measurement is done for one test subject only, which is test subject one. The purpose of the measurement is to see how well the electric activity of heart is detected on the places of anesthesia monitoring electrodes, and how the detection of heart differs when the head is turned on different directions. In this thesis the electrodes are located on both sides of the head about 3cm backwards from the corner of the eye, before the hair line. Electrode on the left side of the head is marked as ME Left and the electrode on the right side is marked as ME Right. Reference electrode is located at the centre of the fore head. Ground electrode is in the middle between the reference and the electrode ME Left. Electrode places mimics the standard electrode setup presented in Figure 3.4. One electrode, not related to monitoring electrode locations, is located on thorax to detect ECG signal. Measurement is done for same head turnings mentioned in subchapter 3.1.3, each measurement lasting four to five minutes.

3.4 Processing methods in measurements

Processing of the measured data consists mainly of filtering and averaging, but also some manual combining or removing of the signals is done. Filters are chosen based on the cut off frequencies found from the literature. All filtering and signal processing is done using Matlab 7.10.

3.4.1 Filtering of the signals

Although the high cut frequency based on important frequency area is said to be 30Hz, clinically it is common to use higher high cut frequency when analyzing the EEG signal. All performed ECG measurements, including ME and extra systole measurements, are analyzed and presented with the high cut frequency of 70Hz, which is a common limit in clinical practice. [33; 36] Low cut frequency is set to be 1Hz. Transition bandwidth of the designed Finite Impulse Response (FIR) filter is set to be 0.5Hz. With the high cut frequency the transition bandwidth is 5Hz. Transition bandwidth is quite wide since the limiting of signal on that point is not that critical and very narrow transition bandwidth in filtering means more calculation time. Since the sampling frequency needs to be over two times the high cut frequency [33], for this study sampling frequency should thus be at least 140Hz. Sampling frequency is anyway set to be even higher, being 256Hz, which is a normal practice on the EEG recordings at the clinic. There is no need to limit the frequency bandwidth for the registration more, since the filtering can be added still when analyzing the results. [33] Another designed and used filter is a notch filter, which is used to delete the noise coming from the electric main line. Cut off frequencies of the notch filter are 49,6Hz and 50,4Hz. Stop band is 49,9 - 50,1 Hz. All the filtering is done after the recording to a raw signal using Direct-Form FIR filters. The code used to filter the signals is presented in Appendix A. Filtering is done separately to data from each electrode. Other filtering of this thesis is done with the same code, only including little variations on the frequencies. For current input measurements the high cut frequency is set to be higher, being 100Hz. The increase of high cut frequency in current input measurements is done because the stimulation is done with a higher frequency, and the cutting of the measured signal is not wanted. Duration of the changes in ECG signal and in current input signal is short. If all the little details would be wanted to be recorded, the sampling frequency should be around 2000Hz. 2000Hz would make it possible to detect events of 1ms in duration. Using that high sampling frequency is very demanding, since the size of the recorded data comes so large that the processing of it would take unacceptable long time, or the computer used should be very powerful. In the frequency range of 1000Hz or 2000Hz the capabilities of the recording electrodes and other materials used for recording comes to question as well. For the discussed reasons the recording frequency is set to be almost the same as normal clinical range, showing the same phenomena that are seen in normal clinical recordings, and more theoretical approach is left out.

The Matlab code used for magnitude and orientation calculations from VCG measurement is presented in Appendix B. It was later realized that the point of R-peak from the VCG measurement can be directly chosen by using the index value, which is always the same due to the method used to process the data. It might even be possible, that the code used in this thesis, gives in some case the wrong point for R-peak from the VCG measurement. In this case the correctness of the point is manually checked. Filtering of the VCG signals is done with the same code as the earlier mentioned

filtering, presented in Appendix A. In VCG measurement the sampling frequency is set to be the same as earlier mentioned, 256Hz. The usual high cut frequency for ECG measurement is 100Hz [37; 52]. In this case taking into consideration the usage and accuracy needed for the purpose, the high cut frequency can be much lower, even 40Hz is used. [37] High cut frequency is chosen to be the 70Hz, which is high enough for VCG measurement. Low cut frequency of the filtering is set to 0,5Hz. Transition bandwidths of low cut and high cut frequencies are 0,2Hz and 5Hz. The duration of a normal QRS complex is from 7ms to 10ms [52], and with the high cut frequency of 70Hz the data value is taken every 1,4ms, which is often enough to be able to calculate the magnitude and orientation of the heart vector during the heart cycle accurately.

3.4.2 Signal processing and calculations

To be able to see how well the ECG signal can be detected around the neck, face and scalp it is needed to remove the other signals from the recorded signal. Other signals referred are EEG signal and noise. The removal of the EEG signal and noise can be done by averaging the signal. Matlab code used to average signals is presented in Appendix A.

Averaging is done separately to data from each electrode. Averaging is done by first summing wanted signals, and then dividing it by the number of times summed. Since the EEG signal is random and not an episodic signal, it will come close to zero after averaging. ECG on the other hand is an episodic and quite symmetric signal, which will be enhanced by averaging. Since it is wanted to examine the ECG signal, first all the R-peaks of the QRS complexes are searched. R-peaks are searched from one of the channels measuring ECG on the thorax. Matlab code used to search R-peaks is presented in Appendix A. Chosen R-peaks are plotted to manually check that all the chosen peaks really are R-peaks. After this the averaging of the signal from the electrodes located on neck, face and scalp is done on the very same time as the found R-peaks exist. Averaging is done by using a time window chosen to be 128 samples before the R-peak, and 127 samples after the R-peak. With a sampling frequency of 256Hz, the used time window is one second. Averaging is done to every electrode on every head position. Length of the averaged data is chosen to be 170 seconds. Data includes around 200 QRS complexes. Amount of QRS complexes depends of the heart rate of the test subject. If the one second time window will exceed the data matrix in the beginning or in the end, the exceeding time window is left out. All the recorded data is manually checked for artefact peaks which would distort the averaging. During the measurement reference is the reference of the cap. Afterwards an average reference is calculated to be able to clearly visualize the differences over the head. Average reference is taken from the electrodes F3, Fz, F4, T3, C3, Cz, C4, T4, P3, Pz and P4, being thus symmetric over the head area. The average reference includes more electrodes on a frontal direction than on a sagittal direction. In ME measurement reference is the electrode in the middle of forehead, named Cz. Matlab code used to calculate the new reference is presented in Program 3.1. Calculation is done separately to data from each of the electrodes.

Concerning the measurement of extra systoles, the systoles are manually looked up from the recorded data, and connected in Matlab to be one single signal including only the found extra systoles. Normal QRS complexes used as comparison are processed from 170 seconds part of the signal in Data 1. Because of larger amount of noise, 240 seconds long part is used in Data 2. Extra systoles are manually removed from the data of normal QRS complexes. In the extra systole measurement and normal cardiac cycle study the calculated reference is the average reference of all the 19 scalp electrodes. Otherwise the processing and calculations are done the same way as in the earlier explained ECG measurement.

```
% Changing the reference of a data to be the electrode Cz

cz_data_electrode = data_electrode - data_cz;

% Average of the 11 chosen electrodes

average11 = ( cz_data_c3+cz_data_c4+cz_data_cz+cz_data_f3...
+cz_data_f4+cz_data_fz...
+cz_data_p3+cz_data_p4+cz_data_pz+cz_data_t3...
+cz_data_t4 ) / 11;

% Changing the reference of a data to be the average reference

average11_data_electrode = cz_data_electrode - average11;
```

Program 3.1. *Matlab code used to calculate a new reference for a data. In this case the new reference set, is first Cz and then the average reference of mentioned 11 electrodes.*

In the current input measurement the used time window is different compared to the measurements without current input, since the frequency of the input current is different compared to the frequency of the heart rate. When frequency is 10Hz, one phase of the input signal is 100ms. To be able to inspect the signal properly, a bit longer time window is chosen, it being 164ms. Used reference is the same as it is in the ECG measurements. The length of the processed signal is around 30 seconds, and includes around 300 stimulus signals. In ME measurement the heart is again the source of wanted signal, and thus the frequency of the signal is the same as it is in the other ECG measurements. Length of the processed signal is 170s. The actual processed and calculated data is from the montages ME Left - Reference and ME Right - Reference.

VCG calculations from the Frank's lead system are done from the part of the measurement where the head is oriented straight. To decrease the effect of an individual QRS complex and to get a mean value of VCG instead, the average of the QRS complexes is taken. Data includes around 200 QRS complexes. Time window used on the point of one QRS complex is 128 samples both before and after the R-peak. Time window is thus one second. If the time window will exceed the data matrix in the beginning or in the end, the exceeding time window is left out. Matlab code presented in

Appendix A is used for VCG data as well. Baseline of the signal from every electrode on Frank's lead system is checked manually, and corrected if needed. After averaging Equation 3 is used to calculate the voltage magnitudes on directions X, Y and Z in the orthogonal coordinate system. Now the VCG presentations can be illustrated during the whole heart cycle. Matlab code to calculate the magnitude and orientation of a heart vector is presented in Appendix B. Orientation of the heart vector on the maximum point of the R-peak is calculated in the following way. First the maximum point of the heart vector is searched. Magnitudes in that time point in the directions of X, Y and Z are taken. The angles are now calculated from the magnitudes of X, Y and Z using tangent of the trigonometric functions. To be able to present the angles on the way they are usually presented in VCG presentations, it is needed to add 90 degrees on a sagittal plane and take an inverse of the angle in the transverse plane. Equations are presented below.

$$\text{Angle in frontal plane} = \arctan(Y / X) \tag{11}$$

$$\text{Angle in sagittal plane} = \arctan(\text{Z/Y}) + 90^{o} \tag{12}$$

$$\text{Angle in transverse plane} = -\arctan(\text{Z/X}) \tag{13}$$

VCG presentation and angle calculation from the 12-lead ECG system is done from the X, Y and Z leads, which are produced by the device. Device gives the measured values five times smaller than the real values are, so all the results are multiplied by five. Results in sagittal direction are given as inversed by the device. To get a normal presentation form, and thus more easily comparable results, the Y- and Z-leads are inversed. Magnitude and orientation of a heart vector during R-peak is calculated with the code presented in the later part of Appendix B. Calculated magnitudes are used in modelling.

3.5 Models and simulations

Modelling part of the work includes creation of the model itself, and simulation using the created model. Creation consists of assembling the correct data matrix, determining the resistivity values in the matrix, and creating a file that can be used in modelling program. To simulate the function of the heart, also the heart and the electrodes must be included to the model. Data that is used to construct the model is from The Visible Human Project, which is a project of U.S. National Library of Medicine. The Visible Human Project aims to create a complete, anatomically detailed, three-dimensional representations of the normal male and female human bodies. The data used for modelling is the data of a male and it is a three-dimensional matrix at one millimetre intervals created from the images taken with transverse computed tomography (CT), magnetic resonance imaging (MRI) and cryosection. [56]

In the Department of Biomedical Engineering, Tampere University of Technology, there are two data matrixes from The Visible Human Project already made

for this kind of purpose. One data matrix is from neck to the head without hands down from the shoulders, and another is from abdomen to the neck. Both of these matrixes are segmented including 31 different tissues and air. The tissues which are used in this thesis are given in the background section of the thesis. Since the mentioned data matrixes are overlapping each other, the other one is cut so that they can be combined to one data matrix including correct data of the human body between head and abdomen. The combining is done using Matlab 7.10. The program used for the modelling is Bioelectric Field Software (BFS). BFS is a software which is made in a project at Tampere University of Technology to create a program for bioelectric field computing using finite difference method. BFS converts the characters in the data matrix to ascii codes, and do not accept all the numbers. For mentioned reason some of the characters representing tissue codes are changed. Change does not affect to the resistivity values of the tissues. After the data matrix is made appropriate for further use, it is converted to Original file format (from now on referred as 'orig-file'), which is then used by BFS. File conversion is done in Matlab with a script from the Department of Biomedical Engineering, Tampere University of Technology. Resistivity values of different tissues are entered to the orig-file. In addition to the resistivity values mentioned in the background, another model is done using resistivity value of blood for the whole heart, including the heart muscle. Tissues with different resistivity values near the dipole affects a lot to the current field arising. By giving the same resistivity value for the whole heart, it is tried to minimize the effect on arising current field. [20]

The model is created from the information of the orig-file by using BFS. Now a complete net of nodes between different voxels of the data is made and sources can be adjusted to the model. Heart is chosen to be modelled as a dipole, but instead of using one, three dipoles are used. Each dipole is oriented to a direction of one axis in orthogonal coordinate system. The usage of three dipoles makes it possible to create a potential vector, which is pointing to a desired direction. In this case the potential vector is the heart vector, and the desired direction and magnitude are the direction and magnitude of an R-peak. Direction and magnitude of R-peak is calculated from each test subject using 12-lead VCG. Although VCG was studied using both Frank's method and the 12-lead system, the modelling is done by using the resulting vector magnitudes from 12-lead method. Dipoles are first each modelled separately with a same current strength. Electric fields in the model are calculated separately with each dipole. Generated voltages are then multiplied with calculated magnitudes from VCG measurement of each test subject. Multiplication is done the way that voltages generated by X-directional dipole, are multiplied with the X-directional vector magnitude of VCG calculation. Voltages generated by Y-directional dipole are multiplied with the Y-directional vector magnitude of VCG calculation. The same is done for Z-direction. After multiplication, all the voltages are summed. This will result to a situation where each electrode point has only one voltage value. Voltage value is the sum of the voltages of all the three dipoles. Using the calculated magnitude values of same test subject for each of the directions in multiplication, the resulting vector simulates the

electric activity of the heart of that specific person. With this kind of vector it is possible to simulate a situation which is more like in a real life, and compare the results between the simulation and the measurement. Source (+) side of the dipoles is set to be 1A and sink (-) side -1A. Location of the dipoles is an estimate, and did not include any calculations. The point for the dipoles is chosen to be at the point of AV-node, between the ventricles and atriums. The point is looked up by the eye from the data matrix, using Matlab to visualize the anatomy. Chosen point is thus not very accurate. The accuracy is anyway thought to be good enough, since the dipole representation is anyway a simplification from the real life situation. In real life the electric activity of the heart is not detected in one exact point but on a larger area around the heart. More accurate realization could be achieved by including several dipoles, or to by locating the dipoles into the ventricle, where the R-peak is for the most part producing.

To be able to compare the results between simulations and measurements, the electrode locations are needed. Electrode locations are taken from the EEGLAB v10, which is widely used interactive Matlab toolbox for processing continuous and event-related EEG and other electrophysiological data [11]. EEGLAB has its own head model, and it has the electrode locations suitable for that specific head. For the purpose of this thesis, the locations has to be fitted to the head of the male person in Visible Human Project. Fitting is done by scaling the dimensions of the used head with the coordinate system taken from the EEGLAB. After the scaling is done, the new values are used in BFS to find the nearest skin-air surface points of those coordinates. To make the simulation more realistic, the points found are manually moved a bit so that the electrode points are tilted a bit backward over the scalp. EEG measurement cap is also a bit tilted on the head of the test subject. After the moving of electrodes, the electrodes O1, O2, T3, T4, Fp1 and Fp2 are not anymore on the same level, like they are not in real life measurement either. Electrode locations are the determined points over the scalp. The method used is not the most accurate one, since all the phases bring some error within. Electrodes used in the simulation are point electrodes, while another option could be to create disc electrodes. Disc electrodes simulate real life electrodes better, but they also need some more work to be implemented into the model. Point electrodes are thought to be accurate enough for the purpose.

3.6 Visualization of the data

All the data gathered from the measurements and simulations can be inspected in numeral way, but the visualization usually makes it easier to inspect the situation. In this thesis most of the data is visualized in 3D form using EEGLAB v10. For the visualization the visualization data matrix suitable to EEGLAB was made in Matlab. Data matrix makes it easier to place the desired data to a suitable form for EEGLAB. EEGLAB has electrode location files as its own, but modified electrode location file is made since the order of the electrodes in saved data from the model differs from the ones that EEGLAB uses. The same order of electrodes in electrode location file and in

saved model data makes it a lot easier to put own data to the file inspected. The coordinates of the electrodes which EEGLAB uses are from the sphere coordinate system that is projected on the surface of the scalp of the 3D head model in the EEGLAB [11]. Projection and the usage of the head model which is not the head of the test subject creates some difference between the coordinates used for calculation and the real ones. The usage of the sphere coordinates also creates some difference since the program assumes that the Fp1, Fp2, T3, T4, O1 and O2 are all at the same level. In practice all the electrodes are tilted a bit backwards, so that O1 and O2 are a bit lower than T3 and T4, and Fp1 and Fp2 are a bit higher than T3 and T4. The non-sphere shape of the head affects via the projection as well. The difference on electrode places between real situation and the visualization is anyway seen as not that significant, since the overall situation is more important. The amount of the electrodes used is low, so the resolution of the measurement is low as well. All the data, except ME and extra systole measurement with normal cardiac cycle study is inspected using average reference, including electrodes F3, F4, C3, C4, T3, T4, P3, P4, Pz, Cz and Fz.

4 RESULTS

Findings from all the measurements and simulations are presented in this chapter. Results are in most of the cases presented visually, but the main observations are also discussed. Chapter is divided into five subchapters. First subchapter presents the findings from VCG measurements. Second subchapter presents the findings from ECG measurements. Findings from current input measurement are presented in third subchapter, while the results from the monitoring electrode measurements are presented in fourth subchapter. Last chapter presents the findings from the modelling, and the comparison between the models and measurements.

4.1 Vectorcardiography

Results of the vectorcardiography measurements are presented in this chapter. Measurement was carried out for three test subjects. Results from the VCG measurement done with Frank's lead system are presented in Figures 4.1., 4.2. and 4.3. The Figures 4.4., 4.5. and 4.6. present the results from the 12-lead ECG system. Results differ so much from each other that they are presented on different scales. Different scales make it easier to do more accurate inspections of the VCG loops themselves.

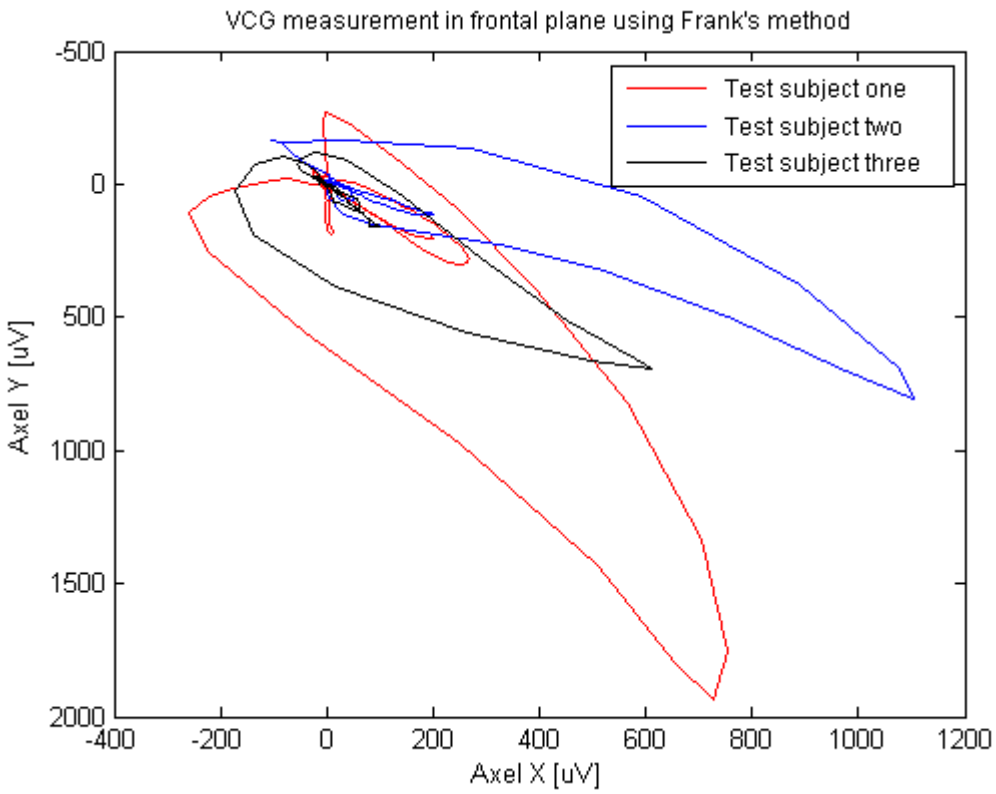

Figure 4.1. *VCG presentation of three test subjects presented in frontal plane. Presented data is from the measurement done with a frank lead system.*

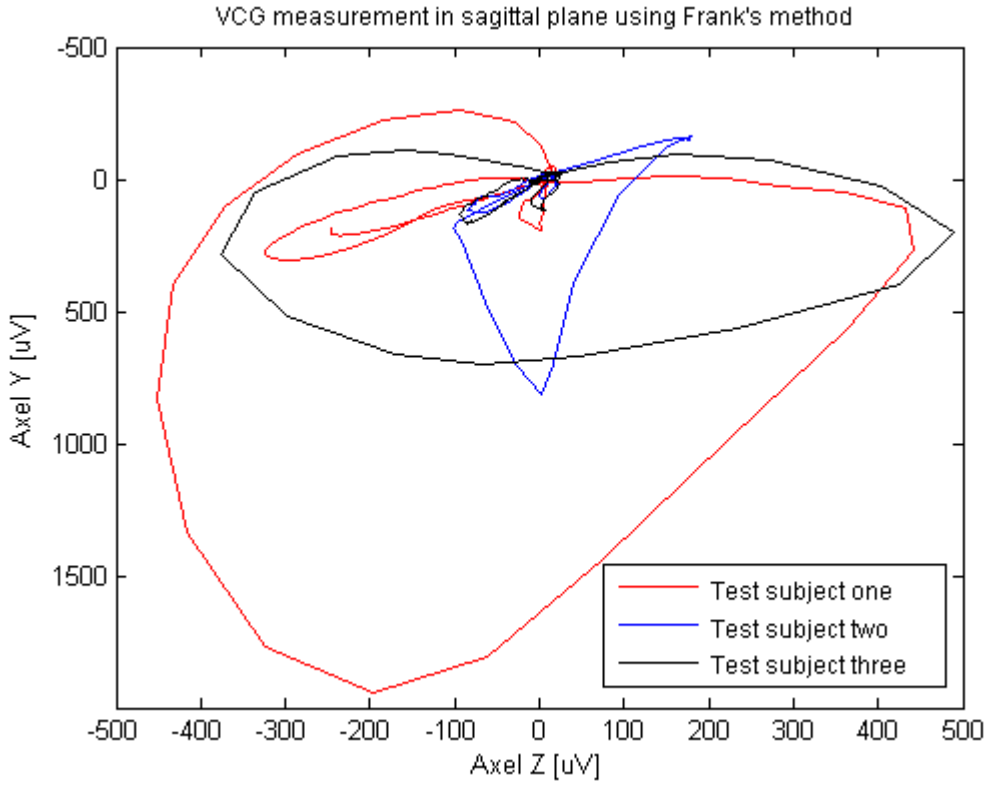

Figure 4.2. *VCG presentation of three test subjects presented in sagittal plane. Presented data is from the measurement done with a frank lead system.*

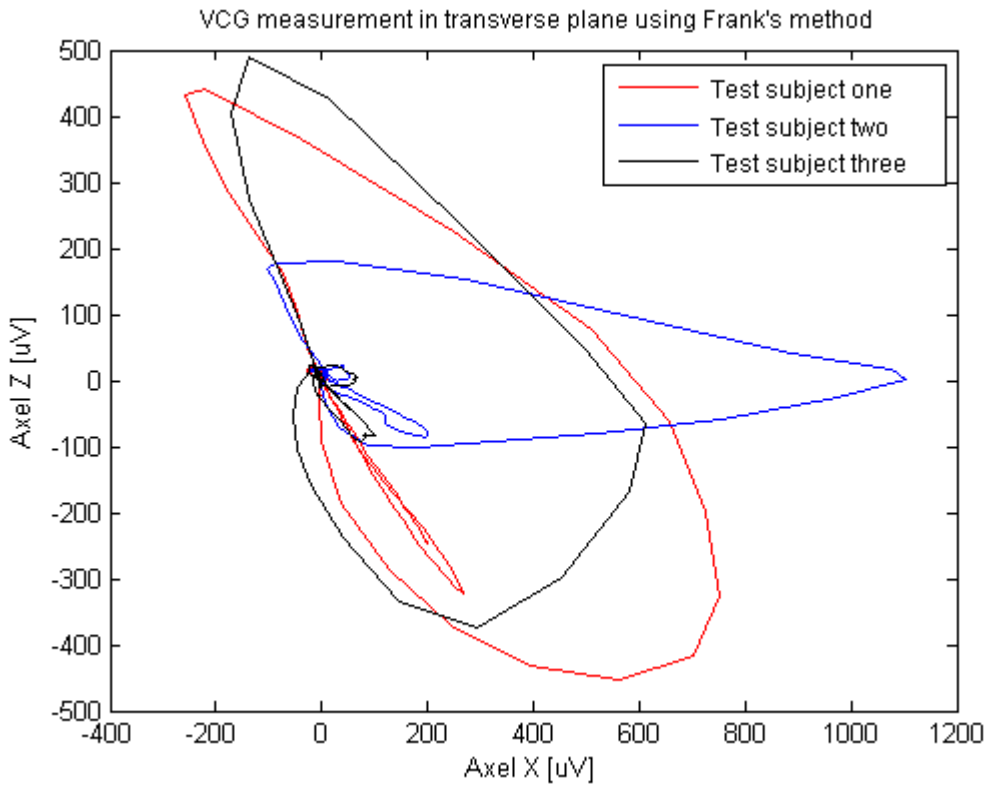

Figure 4.3. *VCG presentation of three test subjects presented in transverse plane. Presented data is from the measurement done with a frank lead system.*

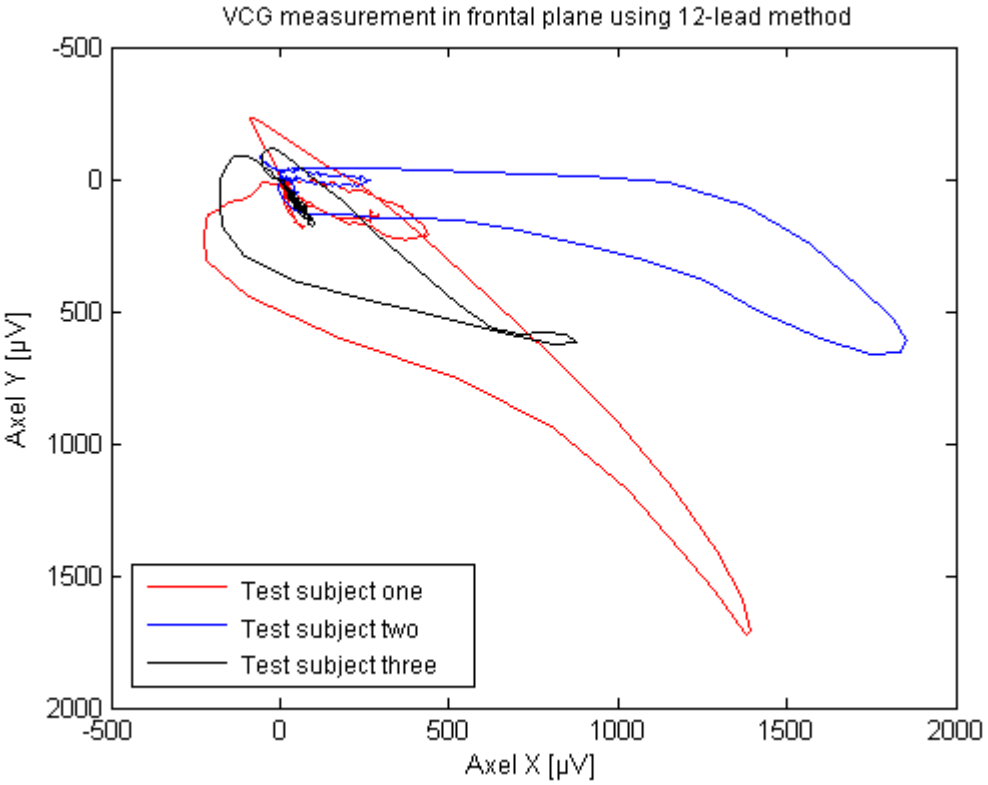

Figure 4.4. *VCG presentation of three test subjects presented in frontal plane. Presented data is from the measurement done with a 12-lead ECG system.*

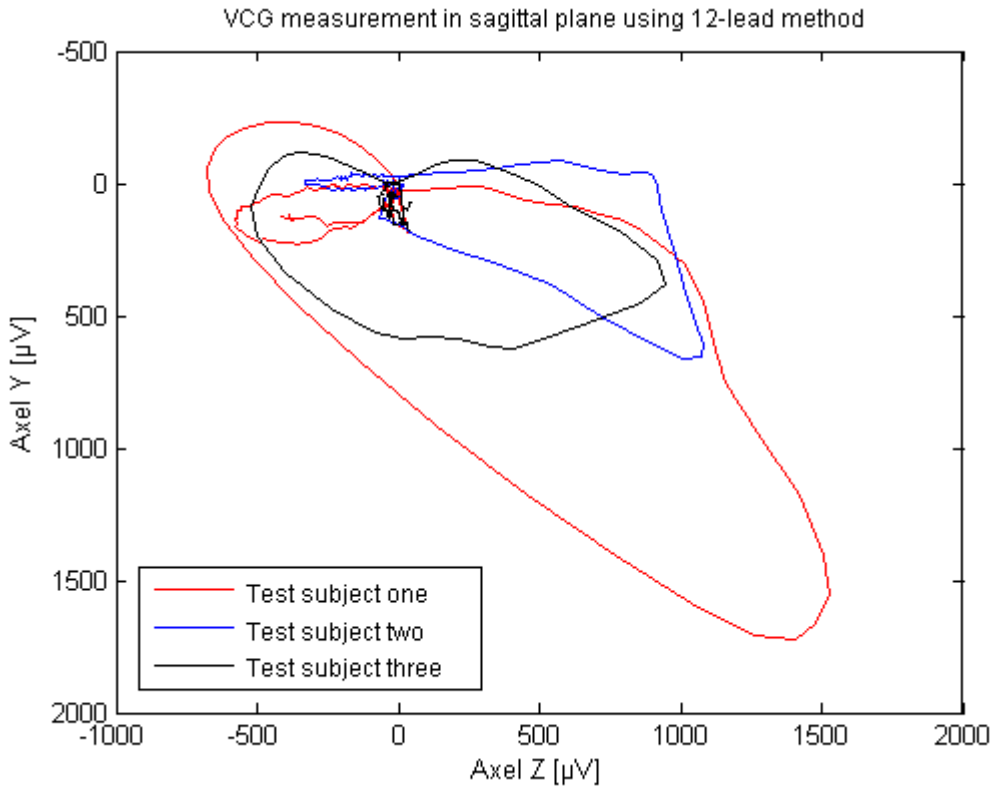

Figure 4.5. *VCG presentation of three test subjects presented in sagittal plane. Presented data is from the measurement done with a 12-lead ECG system.*

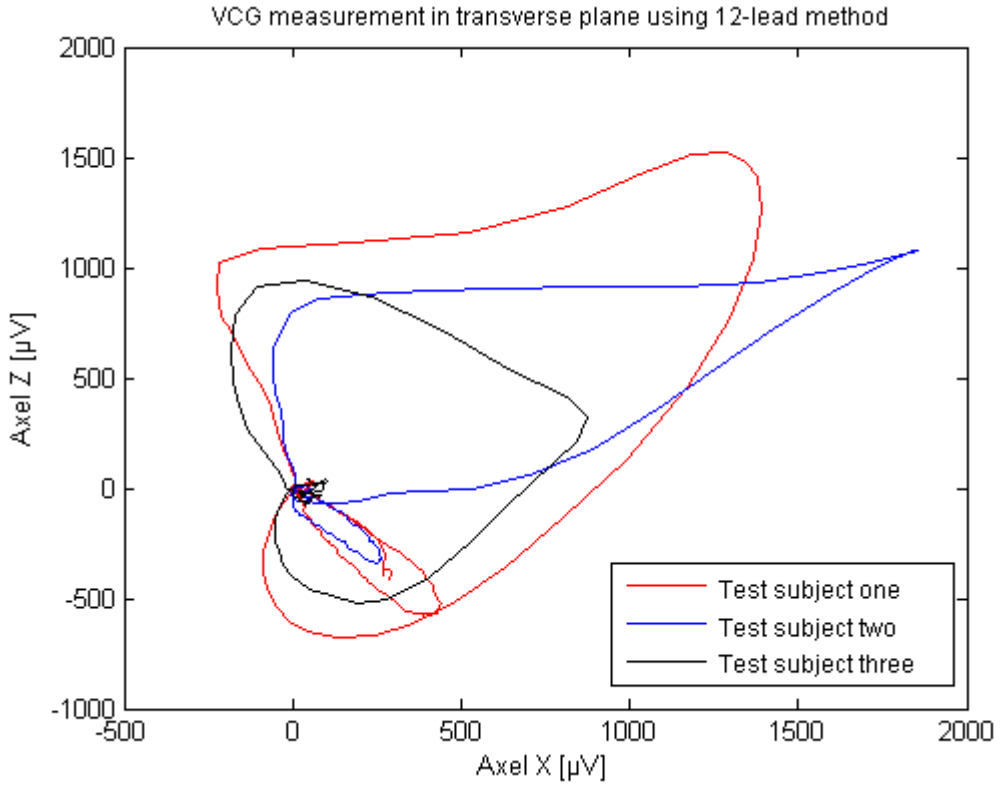

Figure 4.6. *VCG presentation of three test subjects presented in transverse plane. Presented data is from the measurement done with a 12-lead ECG system.*

The magnitude of the electric activity of the heart can be noticed to be very different between the measurement methods. While the magnitude in the direction of Y-lead can be seen to be quite similar on both methods, the Z- and X-leads differs in this. Especially the values of Z-lead differ a lot. On the time of R-peak the magnitude of Z-lead is from 3µV to -197µV between the test subjects on Frank's method, and from 410µV to 1410µV on 12-lead ECG method. When inspecting the shapes of the vectorcardiography measurements, one should be careful, since shapes can vary a lot between persons. If the shapes are anyway compared to ones presented in literature, the shapes of 12-lead measurement resemble the ones presented in literature [52, p. 310]. When inspecting the shapes from the measurement done using Frank's method, it is noticed that the shape in transverse plane is different from the one in the 12-lead measurement. The shape of transverse plane got using the Frank's method is found from the literature as well [13]. Since the results from the Frank's method are scaled differently between different leads, the shape of the presented results does not represent the real situation. The shape of VCG measurement on test subject two is noticed to clearly differ from the shapes of test subjects one and three. Magnitudes taken from the VCG loops on the time of R-peak are presented in Table 4.1. Angle of the electric activity on each plane is presented in Table 4.2.

Table 4.1. *Magnitudes of the lead voltages on the time of R-peak. Voltages are measured using both Frank's lead system and 12-lead ECG system. Magnitudes are presented from the three test subjects.*

	Test subject one		Test subject two		Test subject three	
Lead	Frank [µV]	12-lead [µV]	Frank [µV]	12-lead [µV]	Frank [µV]	12-lead [µV]
X	727	1380	1103	1750	612	815
Y	1934	1725	809	665	696	625
Z	-197	1410	3	1010	-66	410

Table 4.2. *Angle of the heart vector on the time of R-peak. Angles are measured using both Frank's lead system and 12-lead ECG system. Angles are presented from the three test subjects on three different planes.*

	Test subject one		Test subject two		Test subject three	
	Frank	12-lead	Frank	12-lead	Frank	12-lead
Frontal plane:	69.4°	51.3°	36.3°	20.8°	48.7°	37.5°
Sagittal plane:	84.2°	129.3°	90.2°	146.6°	84.6°	123.3°
Transverse plane:	15.2°	-45.6°	-0.1°	-30°	6.1°	-26.7°

First notice from the resulting values of lead magnitudes in Table 4.1. is that on Frank's method the magnitude of Z-lead is significantly lower than on the others. It is found from literature that on average the magnitude of Z-lead is not less than 90% of the magnitude of Y-lead [9]. Now the Z-lead is calculated to be 10% of Y-leads magnitude on its highest, and remarkably low on all the test subjects. Other notice is that on test subject three the values between X and Y lead are quite similar. Using Frank's method, the magnitude of Y-lead on test subject three is seen to be higher, while with 12-lead

method the magnitude of X-lead is higher; the difference is anyway not that huge on either case. Highest magnitude is found from test subject one, when Y-lead is measured using Frank's method. When considering the results from 12-lead measurement, the Y-lead has the highest magnitude on test subject one, while on test subject two and three the highest magnitude is in the X-lead.

The angles presented in Table 4.2. are compared with heart vectors during R-peak presented in the literature [52, p. 310]. From comparison it is noticed that all the measured values are in normal range, except the angle in frontal plane on test subject one, when Frank's method has been used. Normal angle value is said to be 10-65 degrees in frontal plane. Since the calculated value is 69.9 degrees, it is out of normal range. Mentioned values are just the most common ones, and it is not ruled out that heart could not be oriented differently. More detailed inspection of the angles reveal that the heart vector of test subject two is oriented more horizontally than the heart vector of test subject one and three. Heart vector of test subject two is turned only 20.8 degrees downward in frontal plane. The heart vector of test subject one is oriented downward the most. Heart vector of test subject one is turned 51.3 degrees in frontal plane. Heart vector of test subject one is turned the most in transverse plane as well, being turned -45.6 degrees to the back side of the body. Direction of a heart vector is thus seen to vary a lot between persons, which is expected.

Error to VCG measurements proceeded with Frank's method might come from the placing of the electrodes, since the measurement is performed by a person not familiar with the practice of the method. Electrode M is located on the back of the test subject, who is lying on a bed over the electrode M, pushing it against the bed. Electrode M can thus be giving wrong kind of signal compared to other VCG electrodes. Impedances are measured in the beginning and end of the study. Occasional variation is seen, but in most of the cases all the impedances were below five kOhm. Five kOhm is thought to be a limit of a proper impedance. Impedances might have been varied during the study. Electrode M is used in calculations to calculate the magnitude of Z-lead. Values of Z-lead are similar with all the test subjects, when compared to X- and Y-lead. For this reason, it is thought that the error coming from the impedances is not that significant. Reference locating in the head was thought to be a possible error source, since it is not a common reference point on Frank's method. Reference point was tested to be in another location, but the measured values were still similar. Although all the noise sources were tried to separate from the measurement equipments, occasionally the noise level seen in the signal was quite high. Especially in VCG measurements the wires of the measurement setup located quite far from each other. Distance between wires is thought to bring more noise than if the wires would be for example wrapped around each other. In 12-lead measurement the personnel was experienced and thus decreased the possibility to locate the electrodes wrong. As a method, 12-lead system is thought to be less accurate than Frank's method. In this case exact algorithms and accuracy of the MAC 5500 device is not known, which is the reason that the amount of possible error is hard to evaluate. The possible error is noticed

to be highest in the case of Z lead, due to the fact that fewer electrodes are possible to use for the measurement of Z-directional potential.

4.2 ECG measurements

Results from the measurements that are made for three test subjects without any stimulation, and the results from the measurement of extra systoles and cardiac cycle are presented in this chapter. First is presented the results from the measurements on the scalp, then the second subchapter presents the results of the head turnings. Third subchapter presents the results from the extra systole and cardiac cycle study, while the last subchapter takes into account the results from the area of face and neck. Results show the appearance of the electric activity of the heart in the signal recorded from test subjects. Time point inspected is the time of R-peak of the QRS complex, recorded from the thorax. Exceptions are the cardiac cycle presentation and the histogram presentations of the difference in the potential of electrodes between different head orientations. Cardiac cycle results are presented from various different time points. Histograms inspect the time point in where the ECG originating signal is recorded strongest. That specific time point varies between the electrodes. Average reference mentioned in chapter 3.6 is used. Major part of the results is presented with 13 electrodes on the scalp, since no more were used in those measurements. Some measurements are done by using more electrodes on the scalp, and could still be presented using only those same 13 electrodes. Mentioned way would make the results convergent and directly comparable. Results of the measurements done with 19 electrodes on the scalp are though presented with 19 electrodes. This is done for the reason that during the study it was noticed that the missing electrodes are significant when concerning the electric activity recorded over the scalp. For the mentioned reason all the presentations of the results are not convergent with each other.

4.2.1 Measurements on the scalp

At first an example of a raw signal is shown. Signal is from Data 1 from the heart cycle study. Next to it is presented a processed signal from the same data. Signals are presented in Figure 4.7. The left image of the Figure 4.7. is a processed signal from the time points of all the QRS complexes, while the right image is a raw signal from time point of one QRS complex. Observed electrode is P4. Used reference is the average reference of all the 19 electrodes in the measurement cap. Presented case is one of the best succeeded processing. In some cases the level of noise is about the same as the level of ECG signal. Strength of the ECG signal varies between persons and electrode locations, and thus the ratio of the noise and ECG signal level is also dependent of the strength of the ECG signal. Figure 4.8 presents the potentials over the head measured from the EEG electrodes, without electrodes on the face or neck. Results are presented as a potential distribution over the scalp, using 3D head model. Colour bar in the image illustrates how the potential distribution between negative and positive potential is

presented. It should be noted that due to the missing electrodes on the face, the potential distribution shown in the three dimensional image is not true under the level of ears. Potentials are taken during the R-peak of QRS complex and the results are shown from all three test subjects. Reference is the average reference mentioned in chapter 3.6.

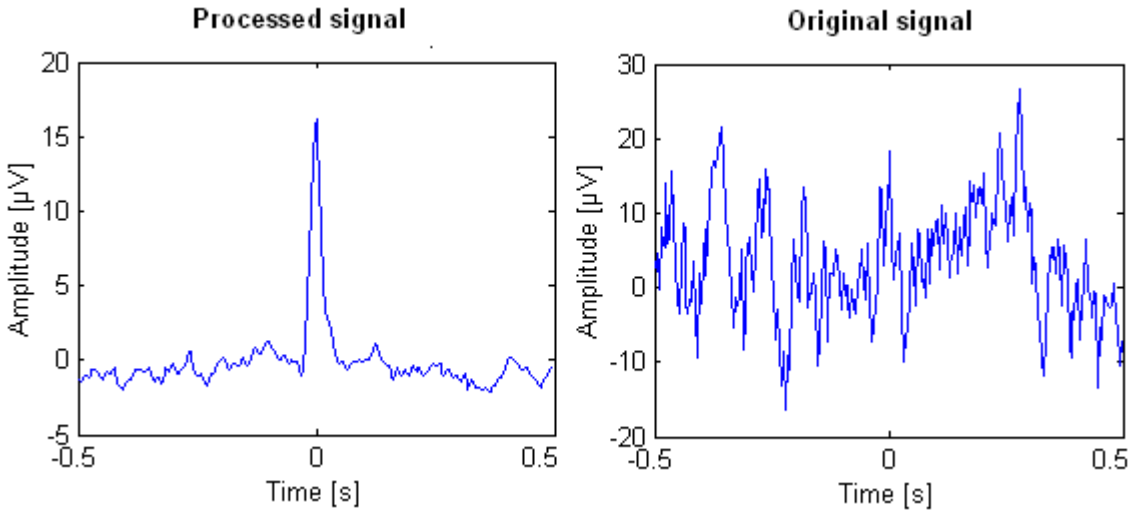

Figure 4.7. *Comparison of original signal and processed signal. Raw data is from the time point of one QRS complex, while processed signal takes into account time points of all the QRS complexes in the data.*

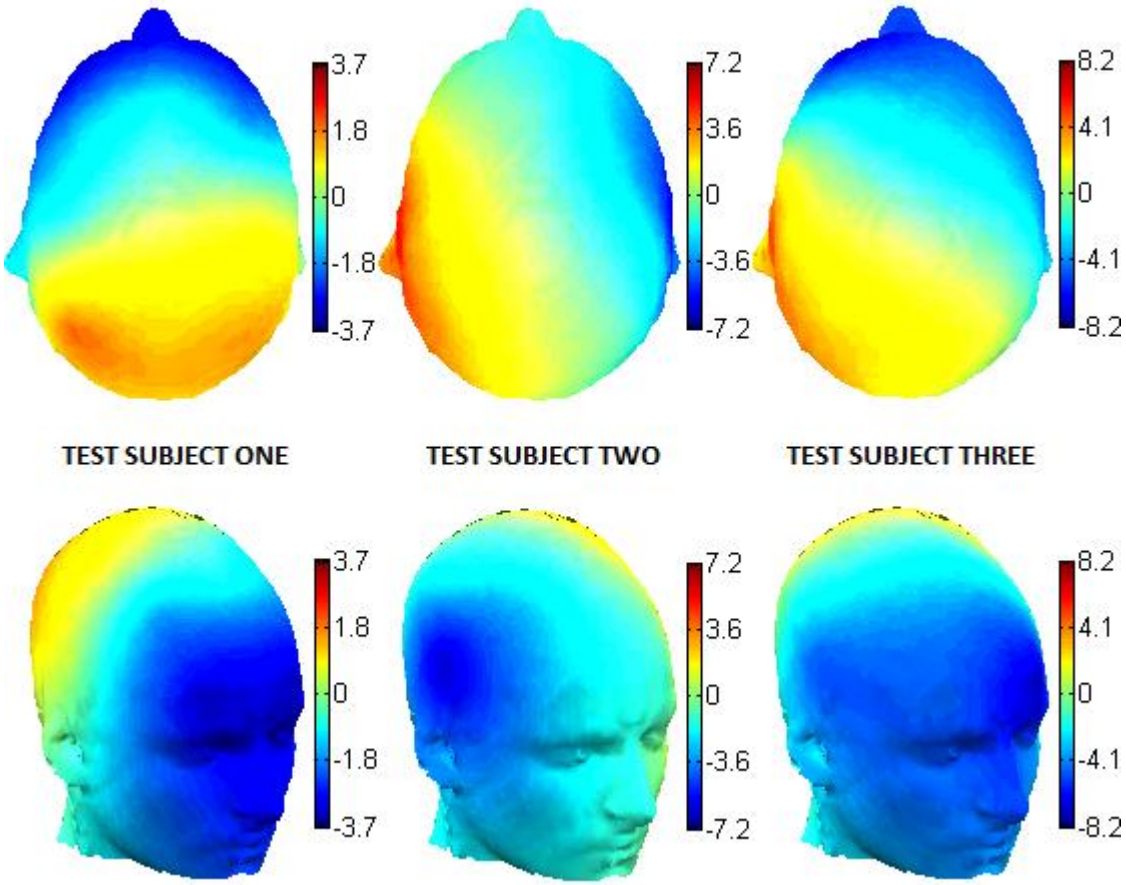

Figure 4.8. *Average potential distribution over the scalp from three test subjects at the time of R-peak. Results are shown on two different angles. Only the potential from 13 chosen scalp electrodes are taken into account. Presented potential values are microvolts.*

Figure 4.7. shows how clearly the R-peak of QRS complex is seen after processing the data. Variations between electrodes are though found, and the amplitude of the ECG signal on this particular case was one of the highest. From the results shown in Figure 4.8. can be seen that the potential distribution produced by the heart can vary a lot between individuals. On test subject one the positive potential can be detected on the back of the head, locating a bit more on the right side. The highest positive value is recorded on a scalp surface, slightly behind the right ear. The negative region of the potential distribution can be seen on an opposite side of the head. Most negative point locates near the left eye. Potential distribution produces a line of zero potential passing through the scalp from behind the left ear to in front of the right ear. On test subject two the potential distribution is totally different compared to test subject one. Positive potential area is found from the left side of the head, and the highest positive value is seen on a scalp surface behind the left ear. Negative area locates on the right side of the head, and the highest negative value is in front of the right ear. The zero potential line is now passing through the head roughly on a normal direction compared to the situation on test subject one. Zero potential line goes from the right side of the back of the head

to the forehead over the left eye. Third test subject, which is seen on the right in the Figure 4.8.**,** can be seen to produce a potential distribution which is something between test subject one and test subject two. On third test subject the positive potential area locates on the left side of the back of the head, and the negative area locates on the right side of the forehead. If the electrodes O1 and O2 would have been taken into account, the positive potential would probably locate more on the back of the head. Zero potential line is similar with test subject one, although it is now passing through the head from behind the right ear to in front of the left ear.

The direction of change in the potential distribution is different on test subject two compared to test subject one and test subject three. On test subject two the potential distribution goes from positive to negative more or less in a frontal direction, which means from left side of the head to the right side of the head. With test subject one and test subject three the distribution goes from positive to negative through the scalp in a sagittal direction, which means from the back of the head to the forehead. The same observation can be noticed if the exact potential values of the electrodes over the head are explored.

Interesting notice is that on test subjects one and three ECG signal is observed to have same magnitude first in negative and then in positive potential, or the other way around. Observation is done on some of the electrodes along the line between the ears. Same phenomenon is observed in 12-lead ECG, which is presented in the Figure 4.9. together with a measured signal from the scalp in the study of this thesis. Presented 12-lead ECG signal is taken from the literature [51, p. 421]. Presented electrodes are V4 from 12-lead measurement and C4 from EEG electrodes.

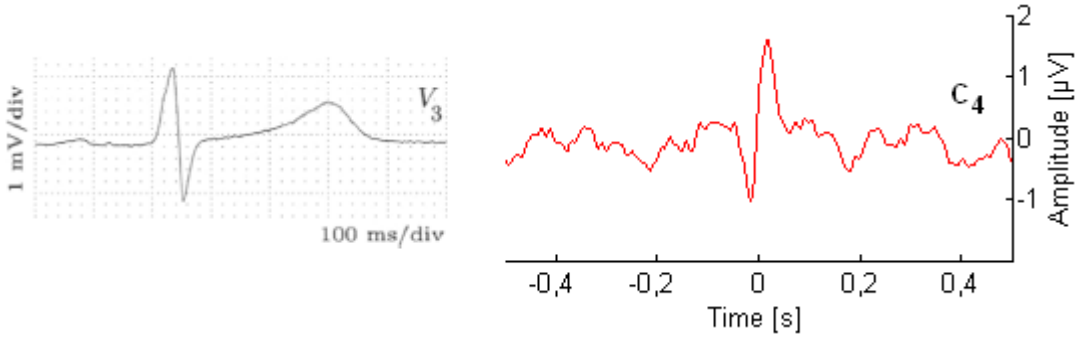

Figure 4.9. *Presentation of two ECG signals. Signal on the left is from the literature* [51, p. 421]*, and the recording electrode is V3 of 12-lead measurement. Signal on the right is from the measurements of this thesis, and the recording electrode is EEG electrode C4.*

Figure 4.9. shows that the heart produces same kind of phenomenon in the electrodes placed on thorax as it produces to electrodes placed on scalp. In these kinds of cases the potential value chosen in the study was the higher absolute value of the peaks. Phenomenon is thought to origin from the fact that to some electrode montages the heart vector is oriented as a normal during the R-peak. In mentioned situation the

measured potential is zero, but before and after that exact time point the potential increases. Increase will be either to more negative or more positive value, depending of the direction in where the heart vector is moving at that point. In electrode C3, which is located opposite side of the head as the C4, the phenomenon is seen the way that before the zero point the potential is positive, and after it is negative. The fact that the phenomenon was not seen on test subject two is thought to be caused because of more horizontal direction of the heart vector in frontal plane during the R-peak. Horizontally directed heart vector does not act as a normal to any EEG electrode montage with the used reference. Results suggest that the direction of the heart vector can be determined from the EEG electrode montages as well.

4.2.2 Head turnings

The effect of the direction of the potential distribution can be seen clearly when studying the results from the head turnings. Figure 4.10. presents the results of the head turnings from the measurement done to test subject two. Results are presented as a potential distribution over the scalp using 3D head model. View point is set over the head. Colour bar in the image illustrates how the potential distribution between negative and positive potentials is presented. Two head positions are left out, since the backward and forward turning of the head does not change the direction of the potential distribution notable compared to straight position. Reference is the average reference mentioned in chapter 3.6.

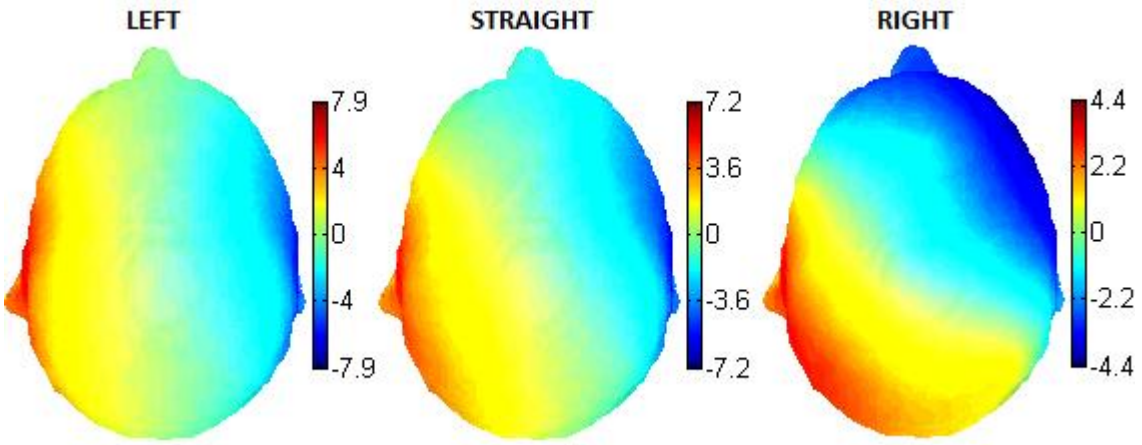

Figure 4.10. *Average potential distribution over the scalp on three different head position at the time of R-peak. Potential distributions are calculated from the measurements done to test subject two. Presented potential values are microvolts.*

From the results shown in Figure 4.10. can be seen that turning the head affects to the potentials measured over the scalp. When the head is turned to the left, the area of positive potential is directly on the left side of the head, while negative area is on the right side of the head. Zero potential line goes directly in a sagittal direction. When the head is turned to the right, the area of positive potential is found farther back, than it is

in straight position. Negative area on the other hand locates more on the front side of the head. Turning the head to the right brings higher potential values closer to the top of the head. It can be seen that turning the head do not change the electric field itself, but the direction of the potential distribution over the scalp varies between different head positions. At the same time the locations of the electrodes change compared to the potential distribution. On test subject one and three the turning of the head backward changes the potential distribution as well. On test subject one the electrode potentials seem to increase and bring higher potential values at the centre of the head. On test subject two happens the opposite, and potentials are mostly decreased when the head is turned backward. In forward position there seems to be only a little difference or no difference at all when looking at the results visually.

Figures 4.11, 4.12 and 4.13 present the potential difference on EEG electrodes between different head positions from all the three test subjects. Difference is in percentages and the baseline is set to be the values measured when the head is in a straight position. Inspected potential values are now the highest ECG signal values recorded in each electrode. Measured values are separated on the figures using different colours for each of the head positions. Measurement done when head is turned backward is marked with a red colour, forward with a green colour, right with a white colour and left with a blue colour. The results from electrode Cz are left out from all of the figures since the differences are minor compared to others. On test subject one electrodes C3, C4, Pz and Fz are left out from the figure due to the very low voltage values, which make the reading of the results difficult. In most of the electrodes the baseline is easily recognized, but with electrode P3 the signals between different head positions are manually shifted on to the same line. Shifting of the signals makes it possible to compare the measured values between each others. On test subject two the electrode F3 has a lot of noise during the measurement in where the head is turned backward and right. On test subject three the electrodes C3 and P3 are noisy during the backward and forward measurement. Backward result from C3 is left out from the presentation. Reference is the average reference mentioned in chapter 3.6.

Figure 4.11. shows that on electrodes Fp1, F3, P4 and T4 the potential increases when the head is turned to the right. On F3 and T4 the potential is decreasing when the head is turned to the left. On Fp1 the potential is the same when the head is turned left. On P4 potential is increased a bit when the head is turned left, but still less than when the head is turned to right. Potential increases on electrodes T3, P3, F4 and Fp2 when the head is turned left and decreases on electrodes P3 and Fp2 when the head is turned right. On electrodes T3 and F4 the potential increases as well when turning the head right, but less than when turned to left. Mentioned changes are expected after seen the results in Figure 4.10**,** and the potential distribution of test subject one in Figure 4.8. If any electrode moves farther from the zero potential line when the head is turned, it is expected that the absolute potential value increases. Results presented with numbers thus confirm the observation. Highest increase in potential values seems to be when the head is in the backward position. Backward position gives the highest potential

difference on all the electrodes, except on P3 and T4. Electrodes P3 and T4 locate on the zero potential line, which might affect to the potential change in backward position. Highest potential change is measured on electrode P4, being 69% higher when the head is turned backward than it is when the head is positioned straight. Changes are smallest on a forward position.

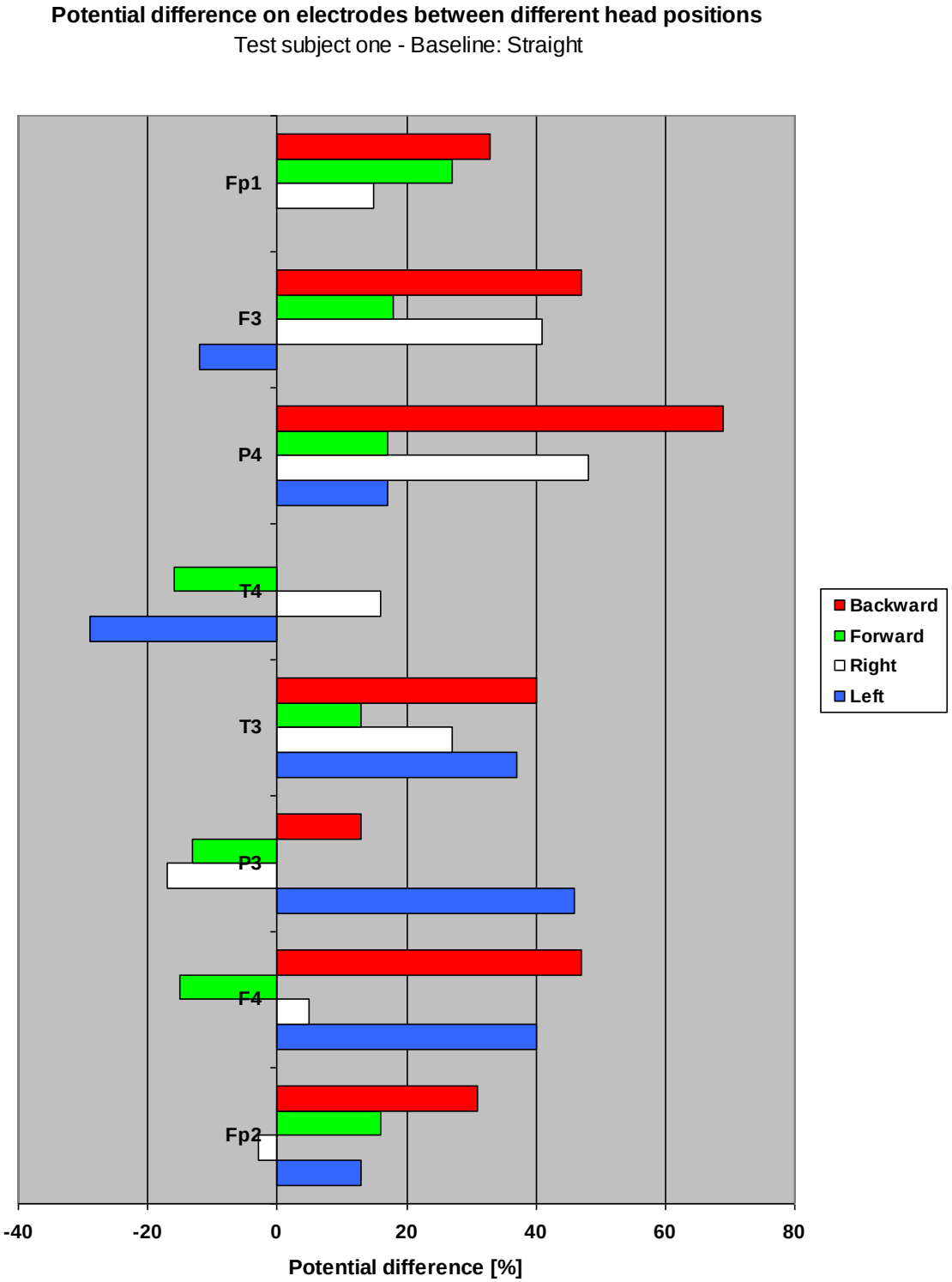

Figure 4.11. *Presentation of the potential differences on electrodes between different head positions. Highest ECG signal value in each electrode is inspected. Presented results are from test subject one.*

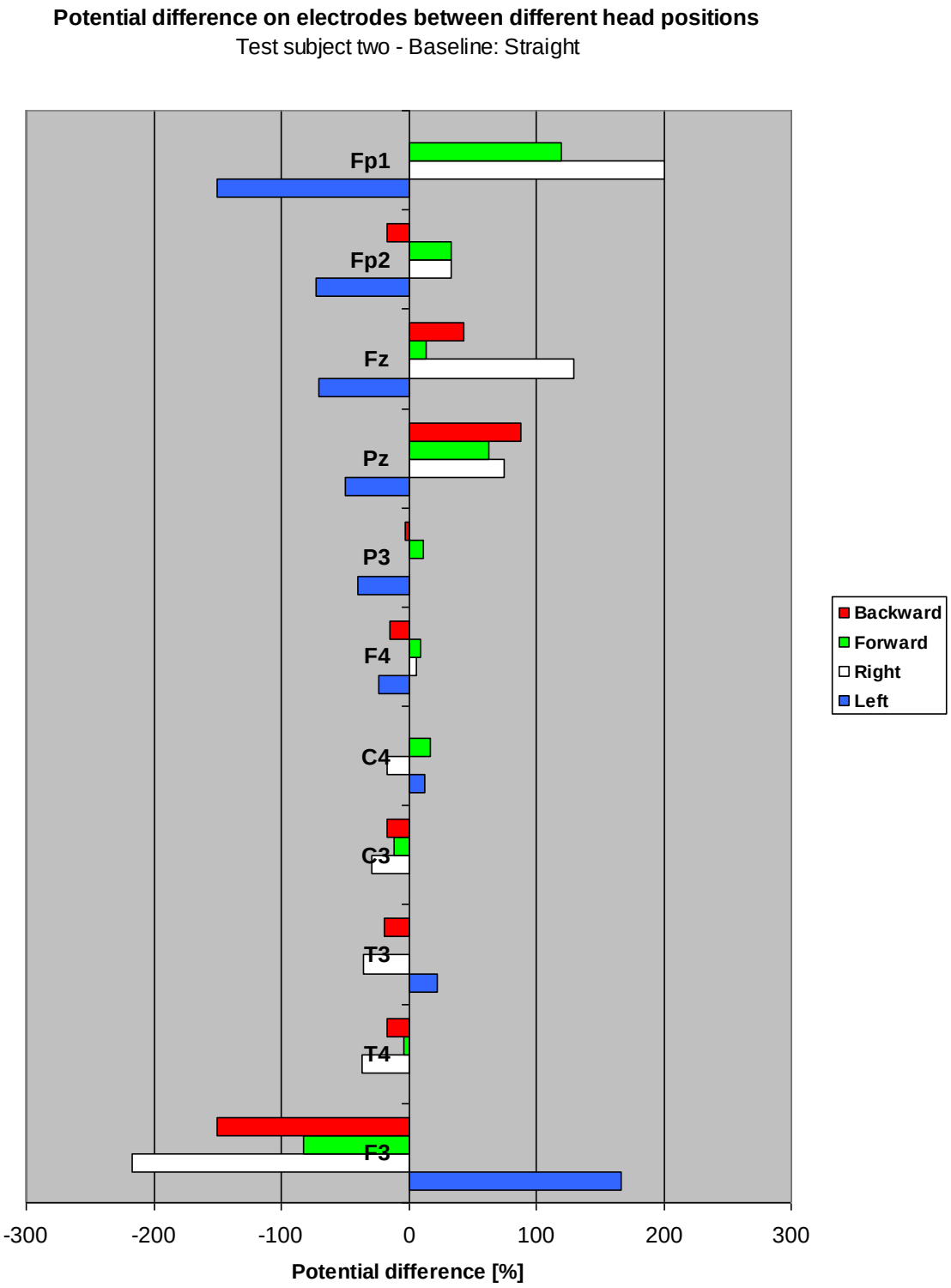

Figure 4.12. *Presentation of the potential differences on electrodes between different head positions. Highest ECG signal value in each electrode is inspected. Presented results are from test subject two.*

On test subject two the potentials changes on electrodes are different of those that test subject one has. On test subject two the change on electrodes Fp1, Fp2, Fz, Pz, P3 and F4 is decreasing potential while turning the head to the left, and increasing potential when turning to the right. The opposite effect is seen on electrodes C4, C3, T3,

T4 and F3 in which the potential is decreasing when turning the head to the right and increasing while turning to the left. P4 is left out from the Figure 4.12. due to the high potential change. Difference in P4 is 200% in the case where head is turned to the left, -420% when turned to the right, -200% when turned to backward direction and -20% when turned to forward direction. It should be noted that the potential on straight position is almost zero on the electrode P4, so the huge percents do not necessarily need high potential values. It can be seen from the results shown in Figure 4.12. that when the electrode is turned closer to the zero potential line shown in Figure 4.8., the lower value will be measured. Largest potential differences appear on electrodes F3 and Fp1. Difference is -217% on electrode F3 when turning the head to the right and 167% when turning the head to the left. On electrode Fp1 the difference is 200% when turning the head to the right and -150% when turning to the left. The resulting signal from F3 is quite noisy and hard to evaluate on the situation when the head is turned to the right. Changes on difference head positions are higher on test subject two than on test subject one. While on test subject two the difference of the potential is over 50% in 15 different situations, on test subject one the crossing of 50% difference happens only once. Reason for the difference could be the direction of the potential distribution and the effect of that to the amount of potential change on each electrode during the head turning. Length and thickness of the neck might also affect to the amount of potential change. Changes on backward and forward positions follow the changes of the right turned position. Exceptions are electrode C4 during the forward position and Fp2, P3 and F4 during the backward position. In most of the cases the potential difference in backward and forward position is though smaller compared to the situation in where the head is turned to the right.

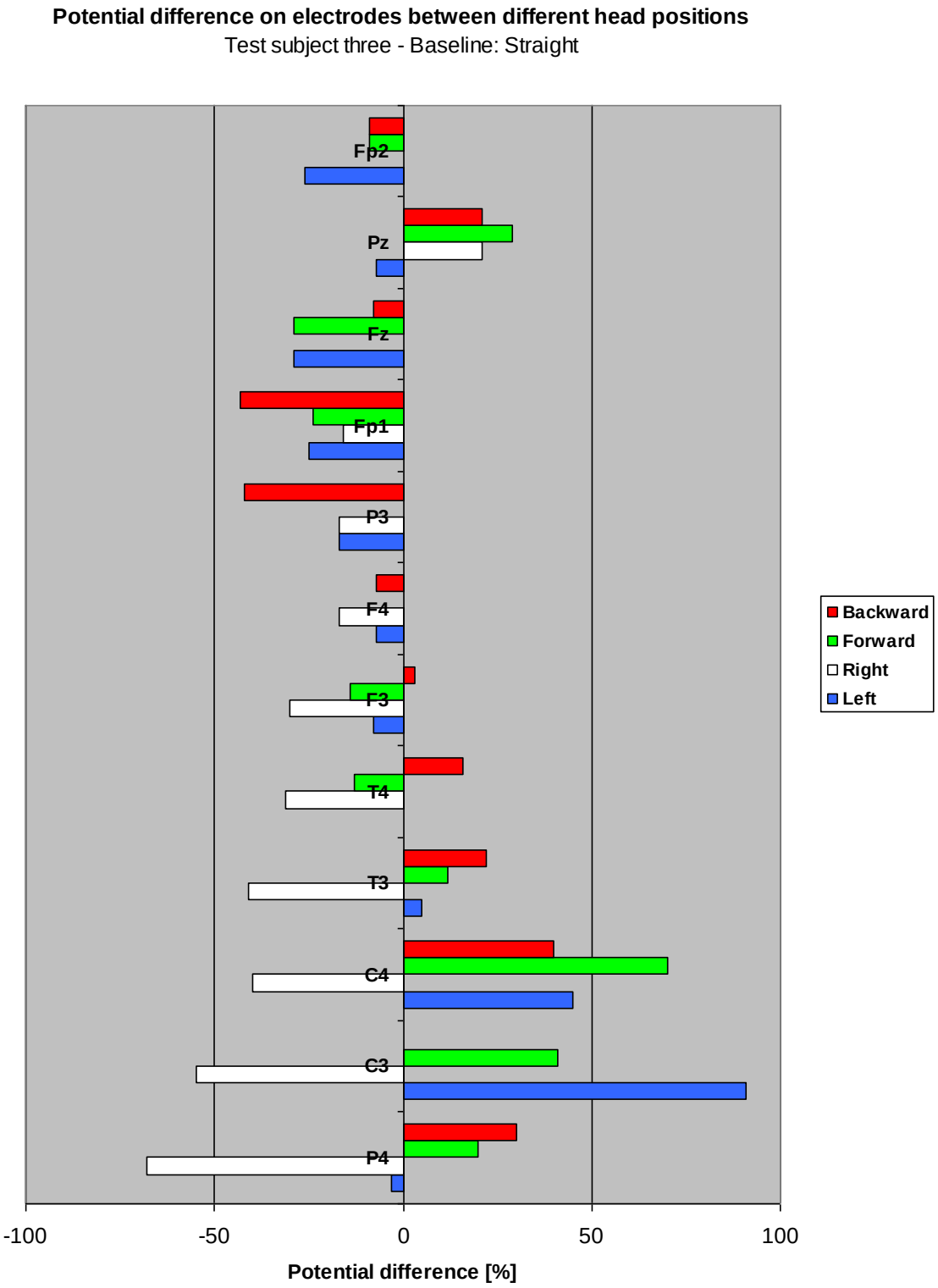

Figure 4.13. *Presentation of the potential differences on electrodes between different head positions. Highest ECG signal value in each electrode is inspected. Presented results are from test subject three.*

On test subject three the differences are slightly different compared to test subject one and two. On test subject one and two about half of the electrodes react the same way to the turning of the head to the right, and another half when turning the head

to the left. On test subject three electrodes are not divided so equally. It can be seen from the results shown in Figure 4.13., that the turning of the head to the left decreases the potential value on electrodes Fp2, Pz, Fz, Fp1, P3, F4, F3 and P4, while the value is same or increased on electrodes T4, T3, C4 and C3. Turning the head to the right decreases potential value on all the electrodes, except electrodes Fz, Pz and Fp2 in which the value is the same or increased. Changes of the forward and backward positions seem to roughly follow the changes of the left turned position. Exceptions are few electrodes in which the potential change is towards the opposite potential. Largest potential change occurs on electrode C3, when the head is turned to the left. In that case potential is increased as much as 91%. Otherwise the potential changes are not that high as they are on test subject two. Crossing the limit of 50% change can now be found only on four different situations. Test subject three was not able to turn the head the desired amount, especially to forward and backward direction. Turning angle was 30 degrees when turning the head to the backward direction, while it was 34 degrees when turning the head to the forward direction. Left and right turnings were three and four degrees less than the wanted 45 degrees. Differing turning angles might be the reason for the differences in the results.

4.2.3 Ventricular extra systole and normal cardiac cycle

Figure 4.14. presents the results from the extra systole study, including both the Data 1 and the Data 2. There are shown the data from the extra systoles and from the normal heart beats on the same person. In this case there are 19 electrodes of the 10-20 electrode system affecting to the visualized result, and it is thus not directly comparable to the results presented earlier. Electrodes A1 and A2 are left out from the 10-20 system in the visualization, due to the fact that the potential values measured from the ears are much higher than the potential values measured from the scalp. High potential difference would affect so that the potential distribution visualized would not give so much information of the scalp area. Average reference includes the same 19 electrodes, differing thus from the reference used in other results presented earlier. Results are presented as a potential distribution over the scalp, using 3D head model. View point is set over the head. Colour bar in the image illustrates how the potential distribution is presented between negative and positive potentials.

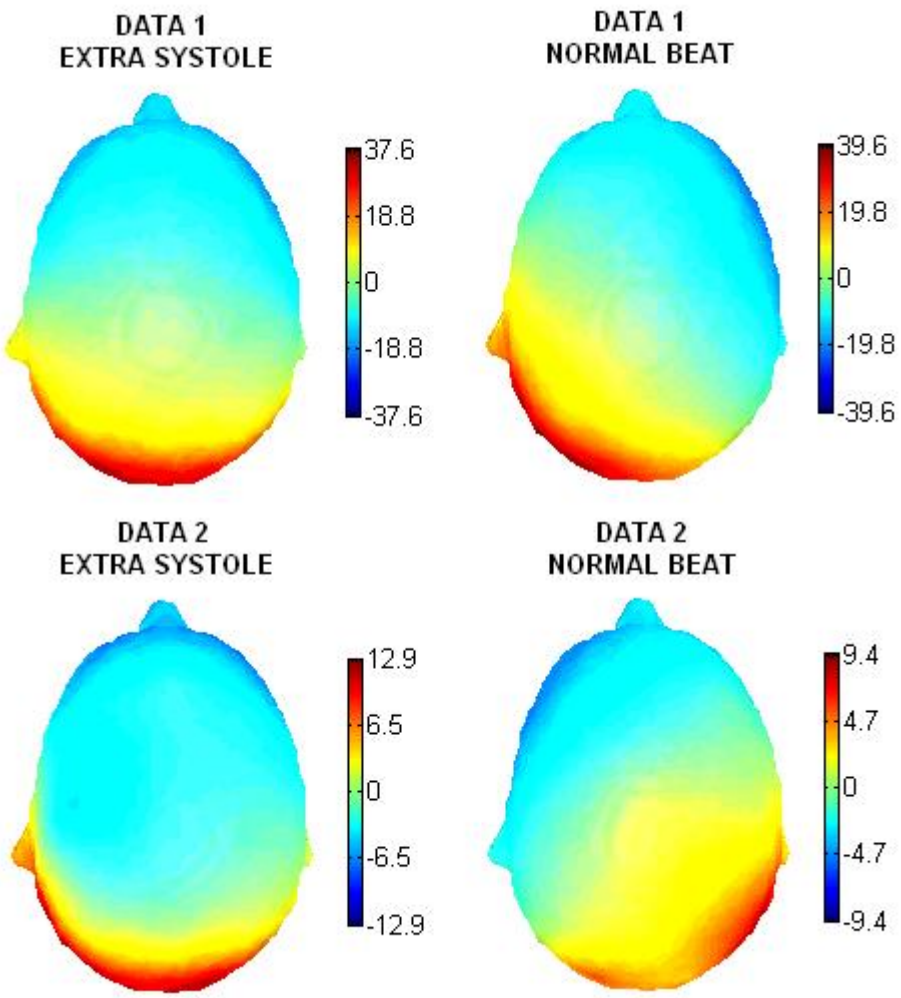

Figure 4.14. *On the left is presented the average potential distribution over the scalp during extra systoles from two different test subjects. On the right is presented the average potential distribution of a normal heart beat from the same two test subjects. Time point inspected in both cases is the time of R-peak. Presented potential values are microvolts.*

Figure 4.14. presents that at least in these two cases the potential distributions over the head area are different from each other, when comparing extra systole and normal heart beat on the same. With Data 1 both the extra and the normal heart beat produces positive potential side to the back of the head and negative to the forehead. Distribution produced by the normal heart beat is anyhow oriented slightly differently. On the case of normal heart beats, maximum positive area is nearer the left ear than the right ear, and negative area is nearer the right ear than the left ear. Maximum positive and negative potential areas produced by the extra systoles are almost directly on the line between back of the head and forehead. Positive area locates on the back of the head, while negative area locates on the fore head. Same kind of difference is seen with Data 2, although the direction of the orientation change is the opposite. With a normal heart beat, the maximum positive potential goes nearer the right ear, and maximum

negative potential goes nearer the left ear. Maximum positive and negative potential areas produced by the extra systoles are almost directly on the line between back of the head and forehead in Data 2 as well. The exact potential values on Data 1 are about the same in both normal and extra systole measurement, while in Data 2 the exact potential values are in most of the electrodes a bit higher during the measurement of extra systoles.

Normal heart beats of Data 1 are also used to calculate the potential distribution of a normal cardiac cycle seen over the scalp. All the 19 electrodes of the 10-20 electrode system are used in the visualization. Electrodes A1 and A2 are left out. Reference used is the reference of the EEG cap. Potential distribution over the head during a normal cardiac cycle, including P-, Q-, R-, S- and T-wave, is presented in Figure 4.15. Two points between Q and R, and between R and S, are chosen to illustrate how the potential distribution changes between these two phases of a cardiac cycle. Results are presented using 3D head model. View point is set over the head. Colour bar in the image illustrates how the potential distribution is presented between negative and positive potentials. It should be noted that the potential values are different in each phase of the cardiac cycle. R-peak of the cardiac cycle is set to be the zero time, and the timing of other phases is calculated compared to it.

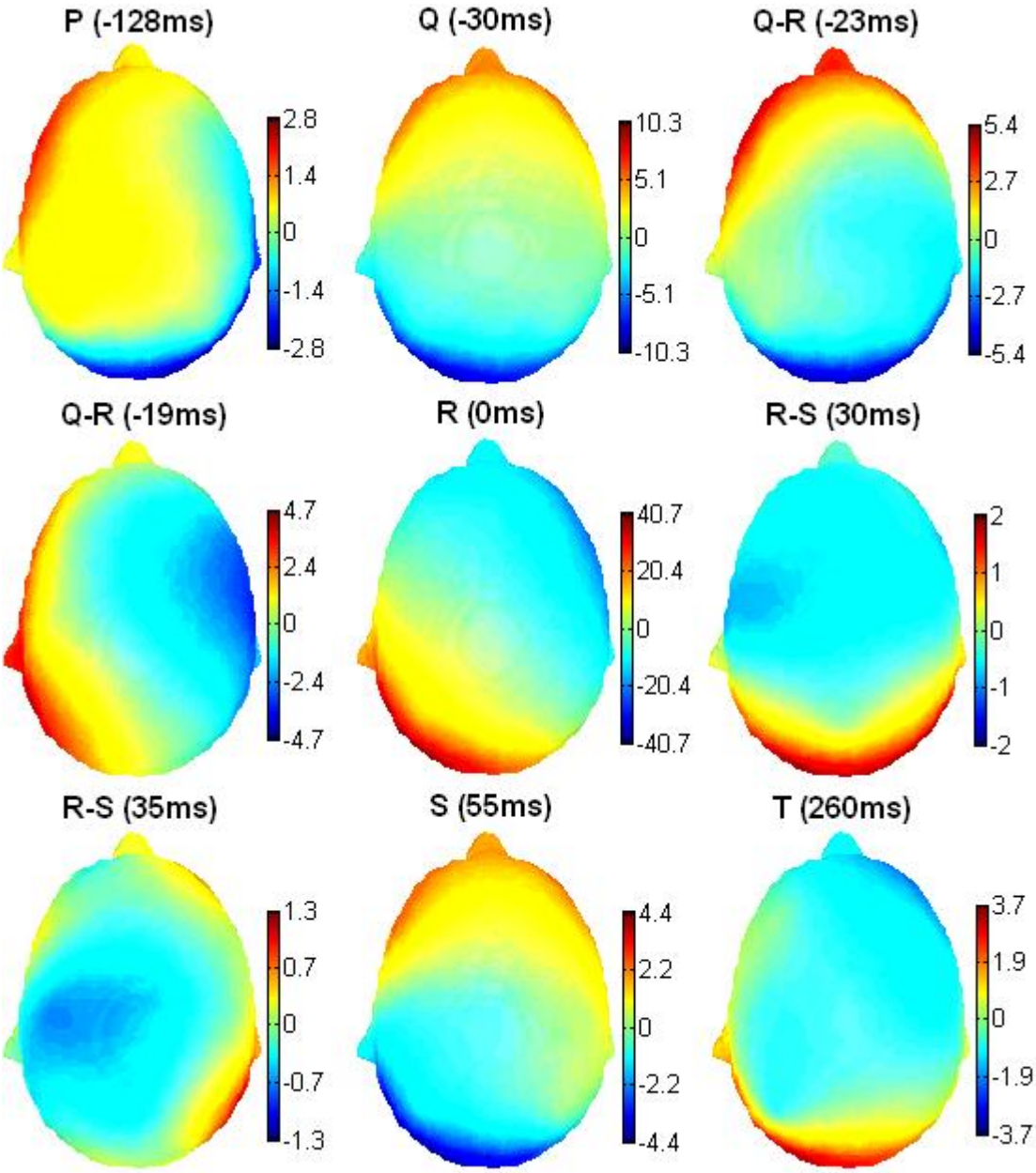

Figure 4.15. *Presentation of heart origin average potential distribution over the scalp during different phases of a normal cardiac cycle. R-peak of the cardiac cycle is set to be the zero time, and the timing of other phases is calculated compared to it. Presented potential values are microvolts.*

Figure 4.15. shows that the potential distribution over the scalp during normal cardiac cycle varies a lot. Potential distribution is seen to go around the scalp between the phases Q and S. Ventricles are active between the phases Q and S. Same kind of phenomenon can be seen in the results of VCG measurement. On the time of P-wave the highest potential values are found between the ear and the eye on the left side of the head. Q-wave is seen to generate a positive potential area on to the forehead. After Q-wave the distribution starts the turn so that the positive potential area moves nearer the left ear and after that towards the back of the head. On the time of R-peak the positive potential has reached the location on the back of the head. Positive potential area is now

situated a bit more on the left side of the head. After R-peak the positive potential area begins to move towards the left ear and towards the fore head after that. On the time of S-wave, the positive potential area has reached the fore head. When T-wave is recorded, positive potential is again on the back of the head. Total duration of a heart cycle in Data 1 is 388ms. Calculated duration is the time between the peaks of P- and T-wave. Duration is noted to be quite short, since the normal duration between P- and T-wave is informed to be as much as 480ms in its shortest. A lot of variation between persons is anyway informed to be found, and the heart rate of a person affects to the resulting duration as well. [52, p. 313] Presented result is only from one person, and can not be generalized. On some other person potential distribution might be seen differently. The basic function of the heart is though the same with every person, and thus the turning of the potential distribution will exist on every person during the heart cycle. The location of potential values on the scalp can be thought to differ between persons, like it is seen to happen when studying the appearance of the R-peak.

4.2.4 Results from the neck and face

Earlier presented results in this chapter are only from the upper part of the head. Next presented results take into account electrodes from the face and neck. Figure 4.16. presents the results from the ECG measurement, so that in addition to 13 scalp EEG electrodes mentioned in Table 3.1., there are taken into account the electrodes on chin, nose, ears and on both sides on lower back of the jaw. Results show the overall picture of the potential distribution over the head during the R-peak. Results are presented as a potential distribution over the head surface, using 3D head model. View point is set in front of the face. Colour bar in the image illustrates how the potential distribution is presented between negative and positive potentials. Reference is the average reference mentioned in chapter 3.6.

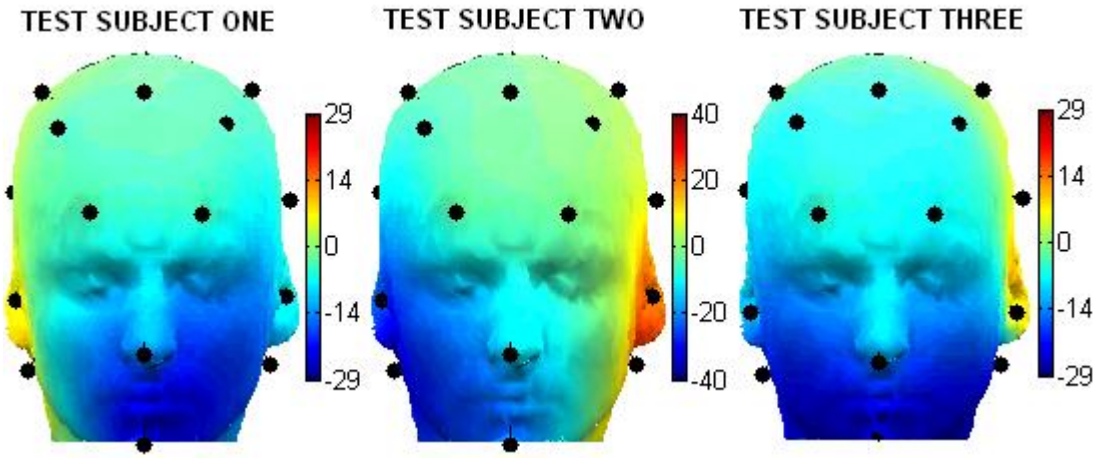

Figure 4.16. *Average potential distribution origin from the heart presented over the head surface on three test subjects at the time of R-peak. Used electrode locations are presented on the figure with black dots. Presented potential values are microvolts.*

Figure 4.16 shows that the measured potentials on the face and ears are higher than those, which are measured from the upper part of the head. Potential distributions are found to be similar between Figures 4.16. and 4.8. Test subject one has positive potential on the right side of the head, and the opposite side of the head is negative. Test subject two has very clear partitions between positive and negative area. Left side of the head is positive, and right side is negative. Test subject three has the positive values on the left side of the head, like it is in the Figure 4.8. Although the attachment of face electrodes was done carefully, electrodes detached or had poor connectivity on some occasions. Occasional detaching and poor connectivity brings some error to the results, even after the averaging over a longer period of time. In the visualization with test subject three the electrodes on the ears, on lower jaw and on chin are placed differently than those of test subjects one and two. The difference on placing being so minor, it is thought not to result any significant differences to the visualization.

Potentials measured from the electrodes on the face and scalp differs significantly compared to the electrodes on the neck and clavicle. It is thus thought that the visualization of all the electrode potentials together does not give any remarkable information from the head. If the exact potential values of the four electrodes on neck and clavicle are examined, it can be seen that in two out of three test subjects the potential on the right side clavicle is two to four times higher than the potentials on Adam's apple, on the neck at the same level with Adam's and on the neck on top of the vertebra C7. With test subject three the potential on clavicle is the same order of magnitude than on the other mentioned electrodes below the head. A bit lower potential is thought to be caused by a poor connection on the mentioned electrode, or due to misplaced electrode. Attaching of the electrode over the clavicle was noticed to be difficult. The potential measured from the neck at the same level with Adam's apple is the smallest of the mentioned four electrode locations on all the three test subjects. Difference between the two closely placed electrodes over C7 and the one on the neck on the level of Adam's apple might be caused by the fact that there is much more fat tissue under the electrode on the level of Adam's apple. Fat acts as an extra insulator causing lower potentials measured. Between the electrodes on Adam's apple and the electrode over the C7 there is variety of some percents of which one measures higher potentials on which situation. On mentioned two electrodes there is not seen any systematic difference on the potential between different head positions and test subjects. From these results could be drawn a conclusion that the electric activity of the heart is spreading evenly to the head pad the front and back side of the neck. The potentials between the left and right side of the neck was not examined in this paper.

4.2.5 Affect of physical dimensions to the potential magnitude

Affect of physical dimensions of the neck to the magnitude of the measured potential is studied. Neck measures are presented in Table 4.3. Table 4.3. presents also the calculated average potentials. Electrodes used for the average potential calculation are Fp1, Fp2, F3, F4, Fz, C3, T3, C4, T4, Cz, P3, P4 and Pz. Electrodes are the same

electrodes that were taken into account in earlier presentations. Exceptions are presentations of Data 1 and Data 2, which were calculated using 19 electrodes. Reference is the average reference mentioned in chapter 3.6. Since Data 1 is from the earlier study, the information of exact length and thickness values are not known. Test subject in Data 1 is though known to have very short and very thick neck.

Table 4.3. *Length and thickness of the neck of the test subjects, and average potential of the electrodes Fp1, Fp2, F3, F4, Fz, C3, T3, C4, T4, Cz, P3, P4 and Pz. Reference is the average reference mentioned in chapter 3.6.*

Test subject	Length [cm]	Thickness [cm]	Average potential [µV]
Test subject one	13.0	36.0	2.1
Test subject two	14.0	41,5	2.4
Test subject three	9.0	45.0	3.8
Data 1 - Normal beat	NaN	NaN	9.7
Data 2 - Normal beat	12.0	38.0	3.4

Table 4.3. shows that test subjects have quite different neck measures. Test subject one has the narrowest and second longest neck, while test subject three has the shortest and thickest neck. Lowest average potential is measured from test subject one, and highest from the test subject in Data1. From the measured neck length and thickness values, the highest potential value is on test subject three. Study seems to result that the shorter and thicker the neck, the higher potential value measured. Mentioned kind of phenomenon is expected when thinking the basic law of electricity, which is presented as an Equation 10. The information known about test subject in Data 1 supports the conclusion. Conclusion is not faultless, since the material tested is not large enough. If test subject one and two are compared, it can be noticed that though the length of the neck is shorter on test subject one, the potential is lower. Thickness of the neck on test subject one is smaller than on test subject two, which might affect more than the length and thus result in such potential values. Observation suggests that first of all the potential can not be estimated just by one of the measures, but both of them are needed. Secondly, it would seem that the difference in thickness of the neck affects more to the measured potential, than the length. The variation between the neck lengths and neck thicknesses on human are anyway not studied in this paper, so the relative difference on thickness between subject one and two might be higher than what the difference in length is. The amount of different tissues on the neck most probably affects to the measured potential on the scalp as well. Some people might have the neck of same thickness, but the other has great amount of muscles, while the other has mostly fat. The resistivity of the fat is more than twice the resistivity of the muscle, which will affect to the conduction of the current origin from the heart. Effect would exist especially if the conduction happens more on the outer side of the neck, in where the fat and muscle would mostly locate.

4.2.6 Error sources

When measuring such a low potential values as EEG, there are several error sources affecting to the resulting signal. These error sources are on all of the measurements done in this thesis. The electric mains line noise is one error source. Error coming from the main line is erased using notch filter, but at the same time the data on the very same frequency is deleted. Although the measurements are done at the department of Clinical Neurophysiology, the rooms are not originally designed for accurate measurements, like EEG. Noise coming from the environment might thus be quite significant. Measurement cap has custom wires which are not attached to each other. That is why the wires probably gather a bit more noise than the ones which are originally present in the cap. Since measurements are done to humans, there is always some movement present. Especially with test subject three, there was quite a lot of movement during the measurement. Although the measured signal was manually checked for spikes which are clearly not related to real measurement, there might be left some erroneous data. All the erroneous data could not be deleted, since there is always some noise from the movements or bodily functions present. Muscles create their own error to the signal. Although the impedances were checked before and after the measurement, the possibility that impedances were different during the measurement is always present. Electrode impedances change easily especially during the head turnings, since the head moves the wires. The accuracy of head turnings, as mentioned in the methods, is not on a very accurate level. Digital meter guarantees that the measured value from the meter is always taken with a same digital accuracy. There is a lot of moving parts in the measurement setup for angle measurement, and thus the accuracy is not that good. In the measurements where the neck length and thickness were measured, measuring tape was used for the measuring. Use of measuring tape causes poor accuracy. Length and thickness measurements are performed by different persons, which bring more variation to the results. Attaching the cap to the head is done by trained personnel, but there is always some variation on the location of the cap. Different location will then affect to the location of the electrodes over the scalp. Electrode places on the area of neck and face might differ as well, since the test subject is always different, and different person is attaching the electrodes.

Since the analyzed data is averaged, some variation might exist in practice. In practice, every heart beat might differ a bit from each other. In some cases the potential values on the points of R-peak are manually looked up and read from the processed data. Manual method might bring error, if the results are misread.

4.3 Current input measurement

In this paragraph is shown the result of the current input measurement done to test subject one. Result from the current input measurement is presented as visualized 3D head model, which is shown in Figure 4.17. Result shows the appearance of the input

current in the signal recorded from the test subject. Only the EEG electrodes located on the upper head are taken into account. Electrodes on the face and neck are left out from the visualization. In chapter 3.6 mentioned average reference is used.

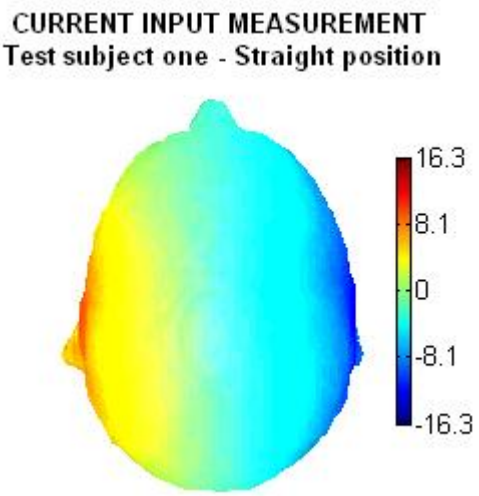

Figure 4.17. *Average potential distribution over the scalp on current input measurement. Measurement is done to test subject one. Presented potential values are microvolts.*

Figure 4.17. shows that the change in potential distribution over the scalp goes from negative right side of the head to the positive left side of the head. Green coloured zero potential line locates a bit more on the left side of the scalp. Head turnings to the left and right have similar effects to the potential distribution as the head turnings in ECG measurements do, and they are not visualized in this context. Turning head backward and forward do not change the potential distribution remarkable compared to straight position, and those results are not presented visually. Turning the head backward affects to the exact potential values measured, so that all the electrodes measure higher potential value during the turning. Forward turning do not change the exact potential values remarkable. When preparing the measurement, it was noticed to be difficult to place the stimulating electrodes symmetrically. Asymmetric placing easily produces error in symmetry of the potential distribution measured. So in addition to error sources mentioned in subchapter 4.2.6., there is at least this probable error source challenging this particular measurement.

4.4 Monitoring EEG derivation

The results from ME measurement are presented in Figure 4.18. Figure 4.18 shows the heart origin potential difference on the electrodes between difference head positions. The electrodes observed are ME Left and ME Right, both compared to reference electrode. Difference is in percentages and the baseline is set to be the values measured when the head is in straight position. Measured values between different head positions are separated in the Figure 4.18. using different colours. Measurement done when head

is turned backward is marked with a red colour, forward with a green colour, right with a white colour and left with a blue colour.

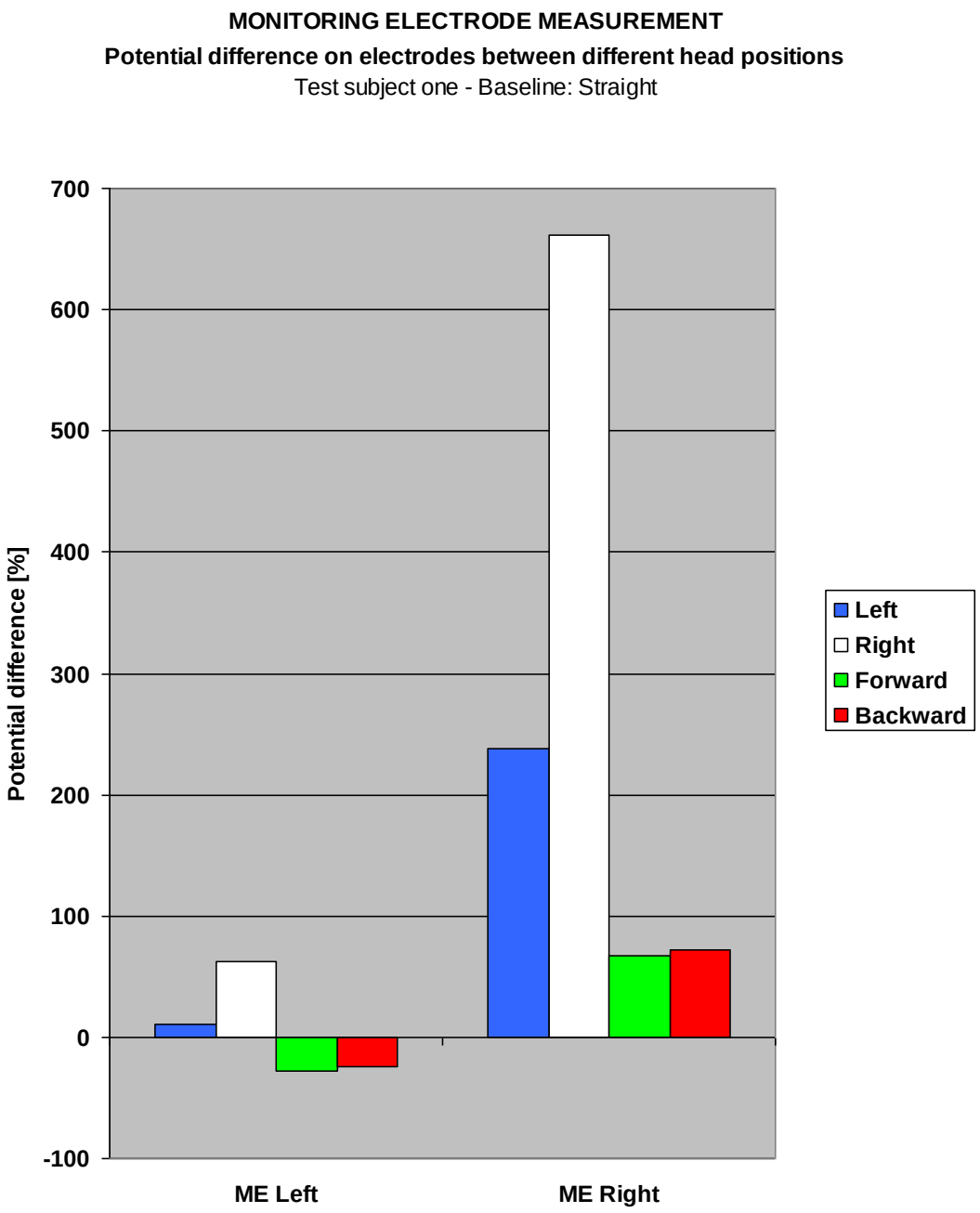

***Figure 4.18**. Presentation of the potential differences on electrodes ME Left and ME Right between different head positions. Measurement is done to test subject one.*

Figure 4.18. shows that the potentials measured from the ME electrodes vary between different head positions. Differences are much higher on electrode ME Right than those on electrode ME Left. Observation might be explained by the fact that the ground electrode locates closer to the electrode ME Left. It can also be seen that on

electrode ME Left the potential decreases when turning the head forward or backward, while potential increases when the head is turned to the left or to the right. On electrode ME Right the potential increases on all the directions the head is turned. In addition, the potential difference is higher on ME Right, than on ME Left, in every direction. Potential difference is highest on both electrodes when the head is turned to the right. Highest change on electrode ME Right is 662%. On electrode ME Left the highest change is significantly lower, being 63%. While the potential differences are higher on electrode ME Right, the absolute values measured are higher on electrode ME Left. Exception is when the head is turned to the right, and the value on electrode ME Right is higher than the value on ME Left. Mentioned phenomenon might be originated from the situation that the potential distribution over the head surface is formed so that electrode ME Left is on the area of higher values, either positive or negative, and electrode ME Right is near the area where the potentials are smaller and might change between negative or positive, if the head is turned. From the exact values can be anyway seen that the situation is not that in this particular case. All the values of ME Left are negative, and all the values of ME Right are positive. Now the electrode ME Left is just located on a more constant potential area, while the electrode ME Right is located on the area where the potential varies a lot. These changes are of course only from one test subject, but it is notable that significant changes can appear. The ground attached to the bed, on where the measurement was done, detached during the last measurement. In the last measurement the head was turned backward. Mentioned incident might bring some noise to the measurement, although there was none seen by the eye.

4.5 Models and their comparison to measurements

This chapter presents the results from the modelling done in this thesis. Two models were created, one that has own resistivity values for each of the tissues segmented, and one that models the whole heart as blood. Figure 4.19. presents the results of the simulations where the model including all the tissue resistivities is used, and dipoles are created with the information got from each test subject in the VCG measurement. Figure 4.20. presents the results including the electrodes on face, and the 13 EEG electrodes mentioned in Table 3.1. Figure 4.19. and Figure 4.21. visualizes the results using only the 13 EEG electrodes mentioned in Table 3.1. Figure 4.21. presents the results simulated with a model where the whole heart is modelled as a blood. Results are visualized with 3D head model and presented as a potential distribution over the scalp. View point is set over the head in Figures 4.19. and 4.21., and in front of the face in Figure 4.20. Colour bar in the images illustrates how the potential distribution is presented between negative and positive potentials. Reference is the average reference mentioned in chapter 3.6.

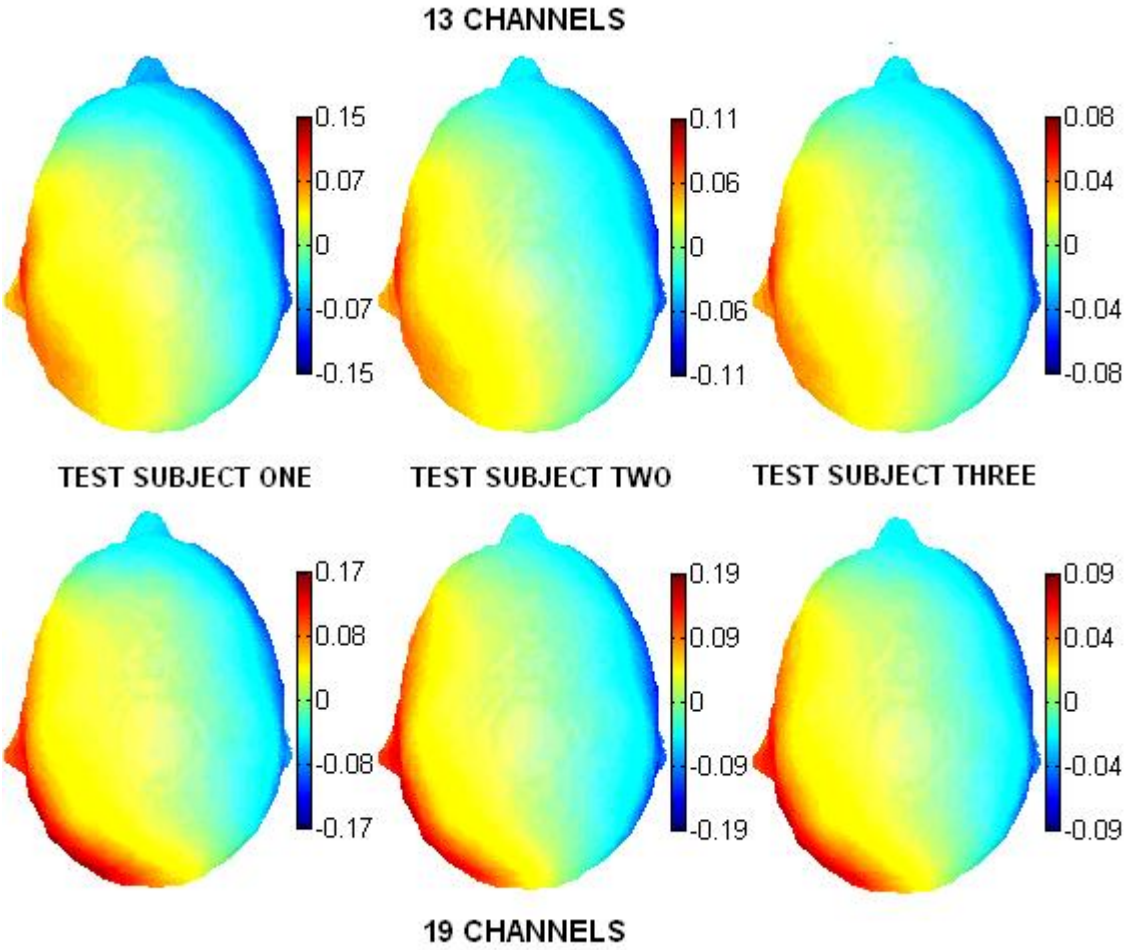

Figure 4.19. *Potential distribution over the scalp from the simulations done with a model where all the tissues have their own resistivity value. Simulation is done with the dipole information from three different test subjects. Simulations are done with two electrode number, 13 and 19.*

Figure 4.19. shows that the simulations done with the information of different test subjects result almost same kind of potential distributions. It can be seen that the results of the simulations on test subject one shows the area of maximum positive potential to locate around the left ear, a bit more nearer the back of the head than on the case of test subjects two and three. The presentation with 13 electrodes locates the maximum positive area nearer the left ear, and the centre of the back of the head is already lower potential area, coloured with yellow. With 19 electrodes the maximum potential area is seen to continue to the centre of the back of the head, and on test subject one over it to the right side as well. Maximum negative potential area locates between the right eye and the point behind the right ear. When observing the situation with 13 electrodes, the negative area continues a bit farer on forehead on test subject one than with test subject two and three. With 19 electrodes the negative area is less on the forehead, and on test subject two it is seen to continue a bit closer of the back of the head than it does on test subject one and three. The area of positive potential has a minor difference when using 19 electrodes. The area of positive potential continues a bit closer to the top of the head and the right side of the head. All the simulations shows the

same phenomenon: when 19 electrodes are taken into account, the positive potential area seems to move closer to the top of the head, and negative area on the other hand seems to drop lower on the head. The difference is though not that significant.

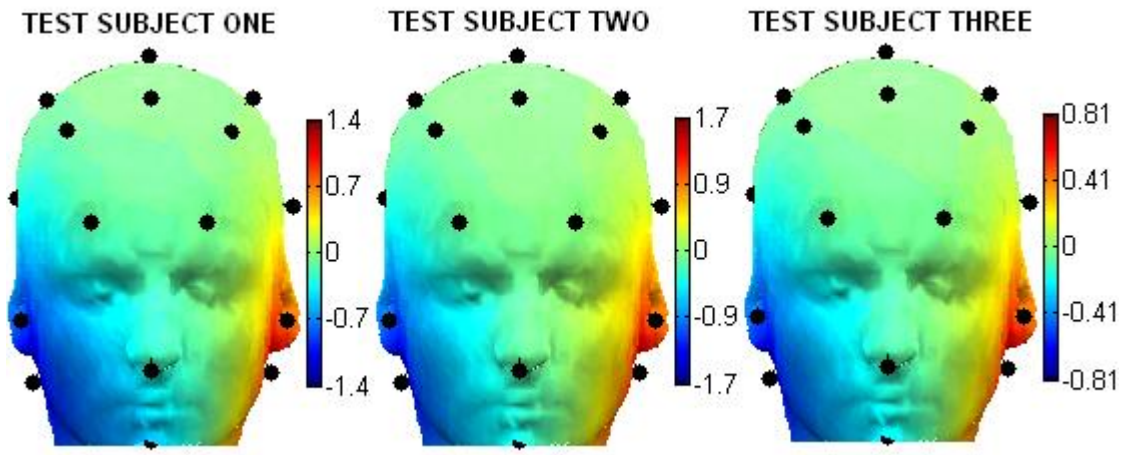

Figure 4.20. *Potential distribution over the head surface from the simulations done with a model where the all the tissues have their own resistivity value. Simulation is done with the dipole information from three different test subjects. Visualization includes 19 electrodes, which are presented on the figure with black dots.*

Figure 4.20. shows that the potential distribution on the area of face do not change almost at all between the simulations that are done with the information from the three test subjects. Minor difference on the simulation done with the information from test subject one can be seen, when it is compared to two others. On the simulation with the information from test subject one, the negative area continues further from the right cheek, over the chin and the nose, and the same way the positive area is farer from the nose and chin on the left side of the face.

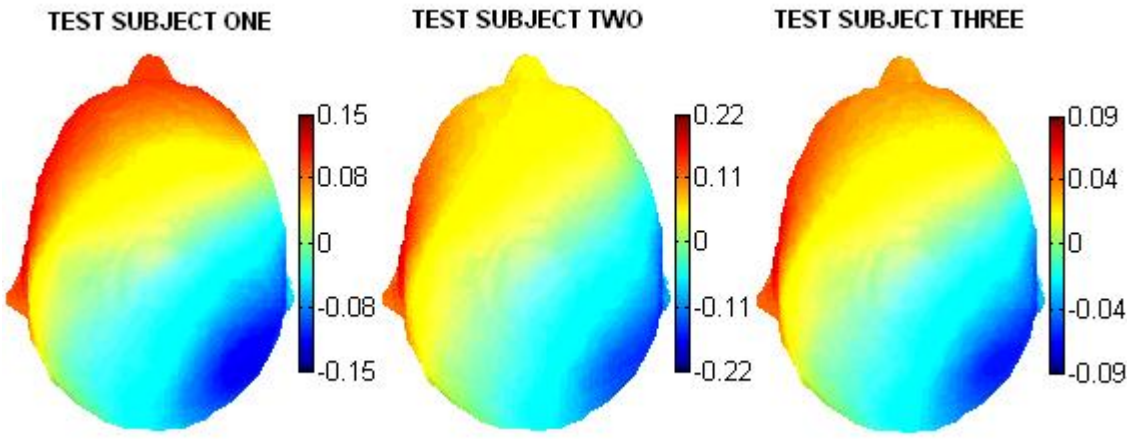

Figure 4.21. *Potential distribution over the scalp from the simulations done with a model where the whole heart is modelled as blood. Simulation is done with the dipole information from three different test subjects. Mentioned 13 electrodes are used for the calculation of potential distribution.*

Figure 4.21. shows that when the model where the whole heart is modelled as blood is used, the positive potential area locates mostly on the fore head. With the information of test subject one, the positive potential area is quite equally distributed over the fore head. The most negative area is located on the right side of the back of the head, continuing over the right ear. With the information from test subject two, the simulation shows the positive potential area to locate on the area between the left eye and the left ear, being emphasized near the ear. Most negative area is located on the same spot that it is located when using the information of test subject one - the area is just smaller in the case of test subject two. With the information from test subject three, the simulation shows about the same results as it did with the information from test subject one. Both maximum potential areas are just a bit farer from the top of the head.

To make it easier to compare the results between measurements and modelling, Figure 4.22. presents the results of both of those done with 13 electrodes. Only the results from the simulation done with all the resistivity values are in the figure. Results from the simulation done with the model where whole heart is modelled as blood are more clearly differing of two earlier mentioned, and are discussed verbally in the later part of the chapter.

Figure 4.22. shows that there are significant differences between the results from the measurements and the results from the simulations. In all the simulations the positive maximum potential area locates on the left side of the head. In the measurements the positive maximum potential locates on the right side of the head on test subject one, and partly with test subject three as well. Same can be noticed with the maximum negative potential area on test subject one, while it is more on the left side of the head in the measurements and more on the right side of the head in the simulation. There is significant difference on the location of maximum negative potential area on test subject three as well. Comparing the simulation and the measurement of test subject two, it can be seen that the results are quite the same. Both the maximum negative and the maximum positive area are just a bit closer to the top of the head in the results from the measurement. When the results from the face electrodes are compared between the simulations and the measurements, the same kind of notice is done in the case of test subject two. Results from the simulation and the measurement are almost the same with test subject two. In the measurement the negative area on the face though continues a bit higher over the temple and a bit farer over the nose and chin. When observing the simulations and measurements concerning test subjects one and three, differences are clearly seen. While the measurements show that the face is almost totally negative potential area on both of the test subjects, the simulations are almost the same as they are in the case of test subject two.

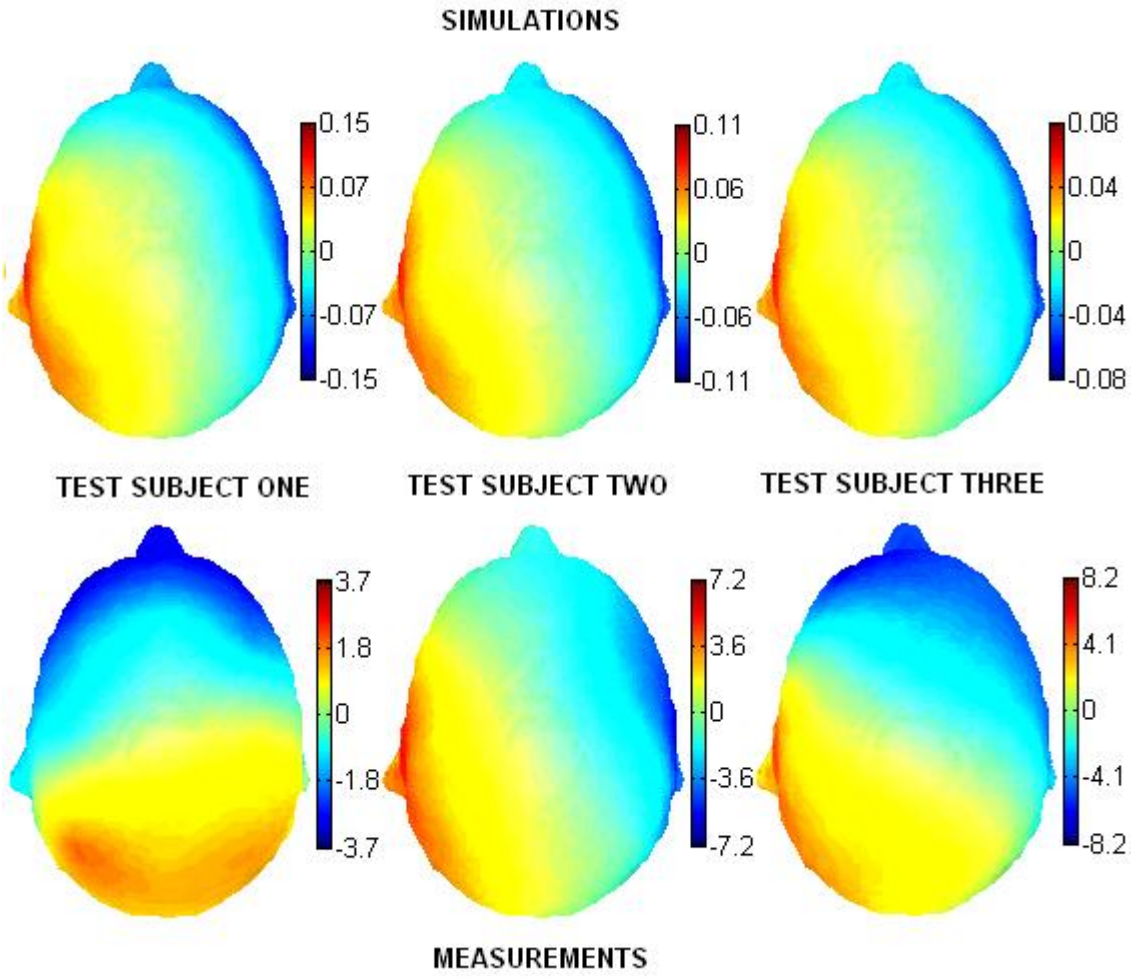

Figure 4.22. *Combined image of the results from simulations and measurements done to same three test subjects. Simulation results are the results from the model with all the resistivity values. Both results are presented with the electrode number of 13.*

When observing the actual values from the electrodes used in the simulations, it is noticed that the potential values in the x-directional dipole simulation are much higher than those of y- and z-directional dipole simulation. Calculations reveal potential values from x-directional simulation to be 1.9 times higher than y-directional by the median of all the electrodes. Ratio between x- and z-direction is even higher, median being 5.0. Combining the dipole magnitudes from the VCG measurements done with 12-lead method, and the potential magnitudes from the simulations, it is noticed that the z-directional dipole affects to the resulting potential distribution much less than x- and y-directional dipoles. Basically the results are thus composed mostly by the potentials of the dipoles in x- and y-directions. Since x-directional dipole produces much higher potential values than the y-directional, the main potential values affecting to the results are the potentials originating from the x-directional dipole. On test subject one the magnitude of y-directional component in VCG measurement is 1725, while the magnitude of x-directional component is 1380. Situation on test subject one strengthens the affect of the y-directional dipole potentials enough, to see the difference in the

potential distribution as well. When the potential distribution of each dipole is observed separately, it is noticed that the y-directional dipole produces the maximum positive potential area on the left side of the back of the head. Maximum positive potential area generated by the x-directional dipole locates on the left side of the head as well. In addition it is known that the affect of Z-dipole to the results is a minor. When mentioned observations are combined, it is realized that the situation in where the results on the simulation and real life measurement would be the same on the case of test subject one, can not exist with the model and information used in this study. This is because test subject one has the highest potential value on the right side of the head in the measurement, but in the simulation the highest potential value would not locate on the same area even if the z-directional dipole would affect more. The highest positive potential area generated by z-directional dipole locates quite equally around the back of the head.

From the simulations done with a model where the whole heart is modelled as blood, the results differ a lot from the results of the measurements and other simulations done with a different model. When the potential distribution of each dipole is observed separately, it is noticed that the potential distributions of y-directional dipole and z-directional dipole are oriented differently compared to those in the other simulation. Y-directional dipole originates a maximum positive potential area to the fore head and near the right ear, while in the other simulation the maximum positive potential area of y-directional dipole is on the back of the head. Z-directional dipole now originates a maximum positive potential area, which is located on the left side of the head. X-directional dipole originates a maximum positive potential area on the left side of the head in this situation as well, but it is placed a bit more on the front side of the head. It is thus seen that the nearby tissues and their different resistivities change the potentials originating from the dipoles a lot. In this case the potentials originating from the heart modelled as blood result totally different kind of potential distribution as the heart in practice does.

Since modelling is a mathematical way to present bioelectrical activity in virtual experimental setting, the variables of the calculations determine the results. If there is an error in variable, the result of the simulation done with a model is erroneous. In this case the tissue resistivities are perhaps the most affecting variable in the calculations. Resistivities of the human tissues are not a commonly known fact, and thus the chosen resistivity values in this study are as well a collection from several studies trying to determine those. Many of those might be wrong, and some tissues in human body are not modelled at all. One tissue which affects a lot to the potentials measured from the scalp, is the bone. It is not just the resistivity value that matters, but also how the tissue is modelled. In the models of this thesis, all the bone tissues are modelled with one resistivity value, which most certainly brings some error to the resulting simulation. Error coming from the bone tissue is even more remarkable, because the study is concentrated to the area of head. Bone of the skull locates between the measurement electrodes and the currents inside the head. The resistivity of the bone varied between

the references. The found resistivity values were from 1149 ohm [57] to 17760 ohm [19]. To get even more realistic model, the structure of the skull should be modelled at least with two different tissue resistivities. One tissue resistivity should be for skull compacta and one for skull spongiosa. Mentioned bone types locate in specific parts of the skull. Spongiosa is softer and more conductive tissue than compacta, and thus it affects to the potential distribution seen over the scalp. [59] Point electrodes are used in this thesis, and they are less realistic than disc electrodes. The error between mentioned two electrodes is though not so significant. When using disc electrodes there exist so called shunting current between the electrodes and the skin. Shunting current makes the amplitude smaller, but the shape of the signal remains. [39] Since the main purpose of the study is not to measure the actual potential values, but the potential distribution instead, the using of point electrodes do not affect to the results analyzed. Used model is isotropic, which is not the case in the real human body. Isotropic model most presumably brings some error as well. Although the accuracy of the model was high, the real cells in human body are still significantly smaller. Cells are the parts of the body that conduct the electric currents. Difference in the size of conductive parts between the model and real human being might bring some error as well. One significant possible error source is the presentation of the heart as a current source, using a dipole. In practice the electric activity of the heart is not just a dipole in one point. Own error comes from the fact that the structure of the model is based on the information of a different person, who is not used as a test subject in the measurements. Although the direction of the electric activity of each heart is measured, test subjects also have different kind of body structures. Body structure will affect by its own way to the results, and the influence of that is very difficult to estimate. Placing of the dipole on the AV-node, brings the current source nearer the centre of the body, than if the current source would be located in the left ventricle. Ventricles create the electric activity of the R-peak of ECG signal. If the dipole would be more on the left side of the body, there could be some difference on the potentials measured. Placing of the dipole should be taken into account in further examinations of the spreading of ECG signal.

Because of the fact that the R-peak of QRS complex only lasts some milliseconds, the average value of the peak could be better value for the comparison of modelling and measurements. There comes easily an error when taking one exact time point, especially since quite inaccurate VCG measurement is used to determine the corresponding magnitudes of that specific time point for the modelling. Along the study it also appeared that at the Department of Biomedical Engineering in Tampere University of Technology have been assumptions concerning the reliability of the modelling program itself. It is thought that there might be some error which would distort the strength of a current in some direction compared to other directions in the model. Any further studies about the assumption have not been done, and to realize the possible error the code of the program should be checked.

5 DISCUSSION

Studies in this thesis discover the heart origin potential distribution over the face and scalp varying a lot between persons. Only three test subjects were studied accurately, but the variation between them is already significant. Variation is expected due to the wide variation known to exist in normal clinical ECG measurements as well. Thesis concentrated to examine the heart vector during the R-peak of QRS complex. Average reference centred over the head was used and roughly said, the higher potential values were recorded the lower the measuring electrode located. Direction of a potential distribution seems to follow the angle of a heart vector in frontal plane. The smaller the angle in frontal plane, which means more horizontally directed heart vector, the more X-directional potential distribution is seen over the head. X-directional is in this case the direction between the ears, positive potential seen on the left side of the head. While the angle in frontal plane increases, increases also the significance of Y- and Z-directional parts of the heart vector. At least in these cases Y- and Z-directional parts of the heart vector turns the potential distribution to be more or less directed from the back of the head to the fore head. Results also suggest that the more negative angle in transverse plane, together with high frontal plane angle, could turn the potential distribution to be directed from the right side of the back of the head to the left side of the forehead. Positive potential area would then locate on the back of the head.

The angle in frontal plane can be measured with a normal 12-lead ECG measurement device, using VCG measurement. Recording to the results of this thesis, the direction of a potential distribution can be determined from the frontal plane angle. By knowing the direction of potential distribution, the location of ECG artefact with highest potential values can be determined. Information could be used to reduce the ECG artefact on the region which is desired to be examined in EEG measurement, and especially in anesthesia measurements. The location of ECG artefact with highest potential values can be also moved, by turning the head of the patient. Turning of the head turns the potential distribution and thus the location of the highest potentials of ECG artefact. Amount of test subjects in this thesis was small, and thus confident consistent conclusions about the angles and their effects to the potential distribution cannot be done. To be certain how each plane angle affects to the direction of a potential distribution, higher amount of test subjects is needed. It was also noticed that the direction of a heart vector can be determined directly from the EEG electrodes. This is based to the fact that on some time point the heart vector acts as a normal to some EEG electrode pair. Phenomenon is the same, which can be seen with a normal 12-lead ECG measurement. In the phenomenon two peaks of equal magnitudes are detected.

First peak is seen as a negative and the second peak as a positive value, or in the opposite order. Between these peaks exists a point, in where the measured potential value is zero. At that specific time point, the heart vector acts as a normal to that specific electrode pair, and the direction of the heart vector can be determined. Method would be easier to include into the current EEG measurement practice, than the VCG method, which needs extra electrodes on the thorax. Method could be implemented directly to the program used in the routine EEG measurements. It is suggested to study the accuracy of the method.

Electrodes O1 and O2 were left out from most of the measurements due to the limited amount of channels in the amplifier. Leaving O1 and O2 out was noticed to be a mistake, since in many cases the strongest ECG signal in normal 10-20 EEG electrodes would have been recorded on those electrodes. Result is though expected, since the lower the electrode locates, the nearer the heart it is. Nearer the heart, the electric field of a heart is stronger, and thus the measured voltage values higher. To be able to get more accurate results, a higher amount of electrodes is suggested to use. Potentials measured from the neck suggest that the electric field originating from the heart conducts from thorax to the head evenly from the front and back side of the neck. The potentials between the left and the right side of the neck was not examined in this thesis, and thus the answer if the potential spreads more through either of the sides can not be answered. It might be so that the potential is higher on the left side of the neck, since the heart is located more on the left side of the human body. The shorter the distance between the heart and the electrode, the stronger the electric field and the measured potential. Any kind of difference on potential magnitudes measured between left and right side of the head is not seen on the scalp.

Based on the observations on this thesis, the ECG signal can be recorded on every point of the head. The orientation of the heart and the head will then determine the points where the ECG signal is the strongest. It was possible to recognize the ECG signal from the recorded signal already after averaging the signal from the points of only 10 QRS complexes. The amount of complexes needed to be able to recognize the ECG signal is though proportional to the magnitude of the ECG signal and the amount of noise. Specific electrode montages are often used when analyzing EEG measurements and diagnosing diseases [36]. Electrode montage can be for example two specific electrodes [36]. ECG artefact appears as a strong signal also in some of these electrode pairs, while other electrode pairs do not include ECG artefact almost at all. An electrode pair in which ECG artefact exists with the greater amount varies between persons.

When examine the potential distribution during the whole heart cycle, it is seen that the direction of a potential distribution changes between P, R and T peaks. Changes in direction are expected, since it is known that the heart vector is oriented differently during different phases of QRS complex. While normal 12-lead ECG signal during an extra systole is known to differ from an ECG signal of a normal heart beat, ECG signal of an extra systole is also observed to differ by the potential distribution that it creates

over the head. Thesis included measurements only from two test subjects, who had extra systoles. Both of these test subjects showed difference on the direction of a potential distribution between an extra systole and a normal heart beat. Thus the strongest ECG artefact during an extra systole locates differently compared to a normal heart beat.

Turning of the head is clearly seen to affect to the potentials originating from the heart, and measured from the head. Turning of the head do not change the electric field, or the shape of the potential distribution over the head, but the direction of the potential distribution changes when the head is turned. Direction of the potential distribution changes, because the electric field produced by the heart does not move while the head moves. Movement of head will result to the situation that electrodes on the scalp will change their location in the electric field. Change of the locations changes the direction of the potential distribution. Change in the direction of the potential distribution is seen only, when the head is turned to the left or to the right. There is no change on the potential distribution when the head is turned backward or forward. Backward and forward turning changes the location of the EEG electrodes only in one direction, which do not change the direction of the potential distribution. Some minor differences in the potential distribution occur also when the head is turned backward and forward. Measured potentials are though changing when the head is turned what ever direction tested. Differences are both decreasing and increasing potential values, depending in what point of the electric field the electrode locates. Backward and forward turning mimic the potential changes of turning the head to the right.

Amount of difference in potential values seems to vary between persons. Reason for the varying amount of difference between persons could be the direction of the potential distribution. In some direction the amount of potential changes might be larger on each electrode, during the turning of the head. Length and thickness of the neck might as well affect to the spreading of electric activity, so that the amount of potential change differs. Discoveries will appear in EEG measurements in the way that the channel in where the ECG artefact is detected, might change during the measurement. This can happen if the person being measured moves his head. Most significant difference in the ECG potential measured between different head positions was noticed in the ME measurement. In the ME measurement the difference in the potential measured between straight and right turned head was 662%. Reveal emphasizes the fact that the orientation of the head will affect to the strength of an existing ECG artefact. Affect is especially significant in anesthesia monitoring, where the electrodes are located on fore head. Recording to this study, the highest potential values of ECG over the scalp are measured on fore head, and on back of the head. Because the highest potential values of ECG were measured from fore head, more comprehensive study of the electrode locations and the signal content used to monitor the depth of anesthesia is now suggested. During the ME measurement, potential differences between different head positions were smaller in the electrode located on left side of the fore head in every head position, compared to any head position on the electrode located on the right side of the fore head. The difference between ME electrodes on the left and right side of the

head might originate from the fact, that the ground electrode locates closer to the left side of the head. Changing the location of the monitoring electrodes for example higher on the fore head might reduce the strength of an ECG artefact in most of the patients. If the strength of the ECG artefact is reduced, the possibility of erroneous increase of BIS value is reduced. Changing the location of monitoring electrodes changes also the brain area measured, which might be a problem when trying to create the BIS value the way it is created nowadays. ME Measurement was done only to one test subject, and to get more information about the strength of the measured ECG artefact between different persons, more research should be done.

Examinations concerning the affect of physical dimensions of the neck to the ECG potential magnitudes measured over the scalp reveal expected results. The shorter and thicker the neck, the higher potential values are measured. To be able to know how much the length, and how much the thickness affects to the measured potential, larger amount of test subjects would be needed. The information got from such an examination is though not very usable in practice. Knowing the phenomenon might anyway help the hospital personnel to prepare themselves for the possible ECG artefact to exist during sleep recordings, multichannel diagnostic EEG measurement or during the ICU and OR monitoring.

Mathematical model with the parameters determined in this thesis, do not simulate the spreading of electric activity origin from the heart correctly. The correct way is thought to be the way which is seen in the results of the measurements done in this thesis. Reason for earlier might be the accuracy of segmentation, tissue resistivity values or the dipole source model used. To be able to simulate the spreading of electric activity the correct way, more accurate model is needed for the purpose. Speculations about the functioning of the modelling program are stated as well. Resolution of the model is quite high, which makes it possible the accurately model the tissues and possible conduction paths. Resolution could though be even higher. Segmentation of the tissues could be more accurate, especially when concerning the bones of the skull. In practice the skull consists at least of two different kinds of bone types [59], while the bone is now modelled using only one resistivity value for all the bones in the body. Even without new segmentation, modelling should be tried to do with different bone resistivity values. Different resistivity value of the bone might affect significantly to the solution of the model. Resistivity value of the bone varies in the literature. Resistivity is reported to be 2.7 times higher [19] or 5.8 times lower [57] than the present resistivity value used in this thesis. Dipole source in the heart could be located differently, more dipoles could be used, or the source could be changed to be potentials on the epicardial surface of the heart [5]. To line out error sources, it is recommended to run further studies so that the data used in the modelling, is from the same test subject who is measured in practice. Using the data from the same test subject means that there should be segmented image data done of that person. For this thesis, a person with image data of himself could not be found. To construct that data would have needed excessive amount of work. For the mentioned reasons it was decided to use data of another

person. As a conclusion, more research in modelling is needed to get realistic results of the spreading of electric activity originating from the heart. When having realistic results from the model, it is possible to examine the spreading of electric activity inside the body without test subjects. Examination of the electric activity deep inside the body is not possible in practical measurements using surface electrodes.

While the ECG on the area of head in EEG measurement is thought as an artefact, it can also be thought as a signal which is desired to record. Head and neck serve as an easy to approach area for measuring, since usually on this area the skin is already available for measurements. Ears have already been used to record ECG signal, which makes it possible to record the signal without chest belt or tapes [50]. If comprehensive ECG diagnosis can be done from the recordings which are measured entirely from the area of neck and head, it would ease the ECG measurement procedure and make the usage of ECG signal even more applicable. Difference in easiness to 12-lead method should though be remarkable to be able to replace the method, since 12-lead method has such an amount of previous data and the approval and knowledge of doctors all around the earth. Disadvantage on measuring the ECG from the neck and head is that the data most probably needs to be averaged. Averaging is probably needed because of high amount of noise. If the data needs to be averaged, the measurement takes a longer period of time. In addition to a longer period of time possibly needed, averaging is not a good method when details are wanted to examined. The capabilities of the measurement procedure should though be researched.

6 CONCLUSION

While EEG is a widely used method to get information about the functions of the brain, information about how and where the ECG spreads in the area of neck and head have not been studied. ECG is one of the major artefacts in the EEG measurement. The aim of this thesis was to study the spreading of ECG signal in the area of neck and head, and the factors affecting to the spreading.

Thesis succeeded to examine and illustrate the spreading of ECG signal, and studied factors that have an effect on the measured potential. Practical part of the thesis consists of clinical measurements and modelling. Results reveal that heart origin signal can be detected all around the head. Potential distribution over the head varies a lot between persons. Difference in the potential distribution originates from the fact that the direction of the heart vector varies between persons. Extra systoles are also found to produce potential distributions that are directed differently compared to a normal systole. Results suggest that angles from the VCG measurement could be used to determine the locations of the highest ECG values in the area of the head, and thus the locations of the highest possibility for ECG artefacts to exist. It was also noticed that the direction of the heart vector can also be determined directly from the EEG electrodes. Since the strength and direction of the heart vector varies, the magnitude of the measured potential varies as well. In addition, thickness and length of the neck affect to the magnitude of a measured potential.

Turning of the head was noticed to turn the potential distribution measured from the head and thus change the locations on where the highest ECG values are measured. Turning of the head had the greatest impact to the measured potential in the ME measurement. Since heart origin potential is known to bring difficulties especially in anesthesia measurements, it is now suggested to do more comprehensive research of the electrode locations and the signal content used to monitor the depth of anesthesia. It was noticed that both the VCG and the EEG electrodes can be used to determine the location of the strongest ECG signal on the scalp. The accuracy of the method should be studied. Changing the location of anesthesia monitoring electrodes higher on the forehead could decrease the possibility of ECG artefacts, but the area measured changes as well.

Mathematical model used in this thesis was not accurate enough to produce realistic spreading of heart activity, and can not be used to examine the spreading of signal inside the body. In further examinations it is suggested to model the source differently and try to segment the data including more tissues, especially concerning the bones on the skull. Different resistivity values should be tested as well, especially on the bones.

REFERENCES

[1] Access Revision [WWW]. [Accessed 17.09.2012]. Available: https://sites.google.com/site/accessrevision/biology/respiratory-and-circulatory-systems/heart-function-and-structure.

[2] Anesthesia UK, Bispectral Index (BIS). Created 16.11.2005. [Accessed 07.09.2012]. Available: http://www.frca.co.uk/article.aspx?articleid=100502.

[3] Baker, L. Principles of the impedance technique. Engineering in Medicine and Biology Magazine, IEEE, USA. 8(1989)1. pp. 11-15.

[4] Bennet, D., Hughes, J., Korein, J., Merlis, J.& Suter, C. Atlas of Electroencephalography in Coma and Cerebral Death. New York, 1976, Raven Press. 244 p.

[5] Bin, H. Modeling and Imaging of Bioelectrical Activity. New York, 2004, Kluwer Academic/Plenum Publishers. 322 p.

[6] Society of NeuroInterventional Surgery. Brain Aneurysms [WWW]. [Accessed 13.09.2012]. Available: http://www.brainaneurysm.com/.

[7] Chatrian, G. Electrodiagnosis in Clinical Neurology. New York, 1986, Raven Press. pp. 669-736.

[8] Daly, D. D.& Pedley, T. A. Current Practice of Clinical Electroencephalography. New York, 1990, Raven Press. 824 p.

[9] Draper, H., Peffer, C., Stallmann, F., Littmann, D. & Pipberger,H. The Corrected Orthogonal Electrocardiogram and Vectorcardiogram in 510 Normal Men (Frank Lead System). 30(1964). pp. 853-864.

[10] Ebersole, J. S.& Pedley, T. A. Current Practice of Clinical Electroencephalography. Philadelphia, 2003, Lippincott Williams & Wilkins. pp. 271-287. Philadelphia 2003. Lippincott Williams & Wilkins(2003) 271-287.

[11] EEGLAB - Open Source Matlab Toolbox for Electrophysiological Research [WWW]. [Accessed 19.09.2012]. Available: http://sccn.ucsd.edu/eeglab/.

[12] Eminence Medical Equipment [WWW]. [Accessed 10.09.2012]. Available: http://eminence-vcg.com/.

[13] Frank, E. An accurate, clinically practical system for spatial vectorcardiography. Circulation, 13(1956)5. pp. 737-749.

[14] Fysiotuote [WWW]. [Accessed 11.09.2012]. Available: http://www.fysituote.fi/.

[15] Gallagher, J. D. Pacer-induced artefact in the bispectral index during cardiac surgery. Anesthesiology, 90(1999)2. p. 636.

[16] Gaszynski, T. BIS in brain injury. Anesthesia & Analgesia, 100(2005)1. pp. 293-294.

[17] Geddes, L. & Baker, L. The Specific Resistance of Biological Material - Compendium of Data for the Biomedical Engineer and Physiologist. Medical & Biological Engineering, Great Britain, 5(1967)3. pp. 271-293.

[18] Goodlett, C. & Horn, K. Mechanisms of alcohol-induced damage to the developing nervous system. Alcohol research & health, 25(2001)3. pp. 175-184.

[19] Hyttinen, J., Puurtinen, H. -., Kauppinen, P., Nousiainen, J., Laarne, P. & Malmivuo, J. On the Effects of Model Errors on Forward and Inverse ECG Problems. 2(2000)2.

[20] Hyttinen, Jari. Doctor of Technology, professor, Tampere University of Technology. Tampere. Interview 10.04.2012.

[21] Kuntoväline Oy [WWW]. [Accessed 11.09.2012]. Available: http://www.kuntovaline.fi/.

[22] Law, S. Thickness and resistivity variations over the upper surface of the human skull. Brain Topography, 1993 Issue 6. pp. 99-109.

[23] Leppäluoto, J., Kettunen, R., Rintamäki, H., Vakkuri, O.& Vierimaa, H. Anatomia ja fysiologia - Rakenteesta toimintaan. Helsinki, 2008, WSOY Oppimateriaalit Oy. 520 p.

[24] Lyon, A. F. & Belletti, D. A. The Frank vectorcardiogram in normal men. Norms derived from visual and manual measurement of 300 records. British Heart Journal, 30(1968)2. pp. 172-181.

[25] Malmivuo, J.& Plonsey, R. Bioelectromagnetism - Principles and Applications of Bioelectric and Biomagnetic Fields. New York, 1995, Oxford University Press. Available online at http://www.bem.fi/book/index.htm.

[26] MedicineNet [WWW]. [Accessed 07.09.2012]. Available: http://www.medterms.com/script/main/art.asp?articlekey=11382.

[27] Mychaskiw, G., Heath, B. & Eichhorn, J. Falsely elevated bispectral index during sleep hypothermic circulatory arrest. British Journal of Anesthesia, 85(2000)5. pp. 798-800.

[28] Myles, P. & Cairo, S. Artefact in the bispectral index in a patient with severe ischemic brain injury. Anesthesia & Analgesia, 98(2004)3. pp. 706-707.

[29] Nöjd, N. Optimal electrode positions for fEMG and EOG measurements. MSc Thesis. Tampere, Finland 2007. Tampere University of Technology. 68 p. Unpublished.

[30] Noriyuki, T. Bioelectric Field Software User Manual. Tampere, Finland 2001. Tampere University of Technology. 44 p.

[31] Online Medical Dictionary [WWW]. [Accessed 10.09.2012]. Available: http://www.online-medical-dictionary.org/.

[32] Oozeer, M., Veraart, C., Legat, V. & Delbeke, J. Simulation of intra-orbital optic nerve electrical stimulation. Medical ang Biological Engineering and Computing, 43(2005)5. pp. 608-617.

[33] Partanen, J., Falck, B., Hasan, J., Jäntti, V., Salmi, T., Tolonen, U. Kliininen Neurofysiologia. Kustannus Oy Duodecim, Helsinki, 2006.

[34] Peolsson, A., Hedlund, R., Ertzgaard, S. & Öberg, B. Intra- and inter-tester reliability and range of motion of the neck. Physiotherapy Canada, 2000 Vol. 52. pp. 233-242.

[35] Plektra Trading Oy [WWW]. [Accessed 11.09.2012]. Available: http://www.plektratrading.com/.

[36] Jäntti, Ville. Doctor of Medicine, Docent, Tampere University of Technology. Seinäjoki. Interview 15.3.2012.

[37] Viik, Jari. Doctor of Technology, Professor, Tampere University of Technology. Tampere. Interview 03.05.2012.

[38] Puri, G. & Nakra, D. ECG artefact and BIS in severe brain injury. Anesthesia & Analgesia, 101(2005)5. pp. 1566-1567.

[39] Pursiainen, S., Lucka, F. & Wolters, C. Complete electrode model in EEG: relationship and differences to the point electrode model. Physics in Medicine and Biology, 57(2012)4. pp. 999-1017.

[40] Puurtinen, M. On the Effects of Interelectrode Distance and Electrode Size on Bioelectric Signal Srength. Tampere, Finland 2003. Tampere University of Technology. 68 p. Unpublished.

[41] Ramon, C., Haueisen, J. & Schimpf, P. Influence of head models on neuromagnetic fields and inverse source localizations. BioMedical Engineering OnLine, 5(2006)55. 13p. Available online at http://www.biomedical-engineering-online.com/.

[42] Ramon, C., Wang, Y., Haueisen, J., Schimpf, P., Jaruvatanadilok, S. & Ishimaru, A. Effect of myocardial anisotropy on the torso current flow patterns, potentials and magnetic fields. Physics in Medicine and Biology, 45(2000)5. pp. 1141-1150.

[43] Remond, A. Handbook of Electroencephalography and Clinical Neurophysiology. Amsterdam, 1974, Elsevier. Chapter 3C pp. 5-21.

[44] Rimpiläinen, J. Biochemical and reperfusion targeting strategies to improve brain protection during prolonged hypothermic circulatory arrest. Oulu, Finland, 2001. University of Oulu. 63 p. Available online at http://herkules.oulu.fi/isbn951425886X/.

[45] Robillard, P. & Poussart, Y. Specific-impedance measurements of brain tissues. Medical & Biological Engineering & Computing, 1977 Issue 15. pp. 438-445.

[46] Rosell, J., Colominas, J., Riu, P., Pallas-Areny, R. & Webster, J. Skin impedance from 1Hz to 1MHz. IEEE Transactions on Biomedical Engineering, 1988 Issue 35. pp. 649-651.

[47] Rosenfeld, M. Whiplash-associated disorders from a physical therapy and health-economic perspective. Göteborg, Sweden 2006. Sahlgrenska Academy at Göteborg University. 50 p.

[48] Rush, S., Abildskov, J. & McFee, R. Resistivity of body tissues at low frequencies. Circulation, 1963 Vol. 22. pp. 40-50.

[49] Schomer, D. & Lopes da Silva, F. Niedermeyer's Electroencephalography. USA 2011, Lippincott Williams & Wilkings, a Wolters Kluwer business. 1275 p.

[50] Shen, T., Hsiao, T., Liu, Y. & He, T. An ear-lead ECG based smart sensor system with voice biofeedback for daily activity monitoring. TENCON 2008 - 2008 IEEE Region 10 Conference, 19.-21.11.2008. Hualien 2008, Tzu Chi University. 6 p.

[51] Sörnmo, L.& Laguna, P. Bioelectrical Signal Processing in Cardiac and Neurological Applications. Print book, Academic Press, 688 p. Available at http://store.elsevier.com/.

[52] Sovijärvi, A., Ahonen, A., Hartiala, J., Länsimies, E., Savolainen, S., Turjanmaa, V., Vanninen, E. Kliininen Fysiologia Ja Isotooppilääketiede, Kustannys Oy Duodecim, Helsinki, 2003. 704 p.

[53] Storey, N. Electronics: A Systems Approach. Prentice Hall, 2009. 804 p.

[54] Krzyminiewski, R., Telemedical Monte Monitoring [WWW]. Faculty of Physics and the Diagnostic and Analytical Methods Centre of the AMU Foundation, Poland. [Accessed 07.09.2012]. Available: http://www.monte.net.pl/english/.

[55] Tyner, F., Knott, J., Mayer, W. Fundamentals of EEG Technology: Basic Concepts and Methods. 1983, Raven Press, New York. pp. 85-105.

[56] U.S. National Library of Medicine - Visible Human Project [WWW]. National Institutes of Health. [Accessed 11.09.2012]. Available: http://www.nlm.nih.gov/research/visible/visible_human.html.

[57] Wendel, K. The Influence of Tissue Conductivity and Head Geometry on EEG Measurement Sensitivity Distributions. Tampere, Finland 2010. Tampere University of Technology. 62 p.

[58] Wixey [WWW]. Online store. [Accessed 11.09.2012]. Available: http://www.wixey.com/anglegauge/index.html.

[59] Wolters, C., Anwander, A., Tricoche, X., Weinstein, D., Koch, M. & MacLeod, R. Influence of tissue conductivity anisotropy on EEG/MEG field and return current computation in a realistic head model: A simulation and visualization study using high resolution finite element modeling. NeuroImage, 30(2006)3. pp. 813-826.

APPENDIX A: FILTERING AND AVERAGING SIGNAL

```
%--------------------------------------------------------------------------
%------------------Electrode data processing tool----------------------
%--------------------------------------------------------------------------

% Electrode processing tool is used for processing the EEG data so
% that it is averaged at the points of ECG-peaks. This able the
% examination of the ECG signal in the EEG electrodes. One electrode
% at the time can be processed.

%--------------------------------------------------------------------------
%-------------------------Main Program-------------------------------
%--------------------------------------------------------------------------

% Window length determines the amount of samples before and after
% the ECG peak
% Threshold determines the minimum potential level for choosing
% ECG peaks to data.
% Electrode number determines the electrode data which is
% wanted to be processed.
% Filename determines the measured EEG data file for processing.
% File should be raw *.data file format without any headers.

% Main program calls the function ECG_artefact, which filters the
% signals, finds the ECG peaks and averages the data in the chosen
% electrode on those same points as ECG peaks, with a chosen
% time window. Function produces a figure of chosen ECG peaks and
% processed result as well.

window_length = 128;
threshold = 500;
electrode_number = number of the electrode in the data file;
filename = 'name of the file';
[time signal_out] = ECG_artefact(filename, window_length, threshold,
electrode_number);

% Processed data is saved to variable 'processed_data'

processed_data = signal_out;

%--------------------------------------------------------------------------
%---------------------Function ECG_artefact--------------------------
%--------------------------------------------------------------------------

function [time signal_out] = ECG_artefact(filename, windowlength,
threshold, electrode_number)

%--------------------------------------------------------------------------
% -------------FILEPATH-&-LOAD-----------------------------------------
%--------------------------------------------------------------------------

% Data is read from the file
fp='insert the path to a folder where the data is placed';
pathtofile = [fp '\' filename '.data'];
read_data = dlmread(pathtofile, '\t');

% Airflow channel has different sampling rate, and it is necessery to
% read and write the file again with zeros at empty points.
```

```
% 'dlmwrite' adds the zeros.

% New file is saved with a proper form
newfile = [filename '_fixed.data'];
dlmwrite(newfile, read_data, 'delimiter', '\t'); % Values are
separated using 'tab'

% New filepath is created and the file is loaded
newpath = [fp '\' newfile];
signal_temp = load(newpath);

% Headers are loaded and saved from a separate header file.
headerfile = [fp '\' filename '_headers.data'];
headers = textread(headerfile, '%s')';

%------------------------------------------------------------------------
%--------------FILTERING OF THE DATA-------------------------------------
%------------------------------------------------------------------------

% BANDSTOP FILTER FOR 50Hz

% All frequency values are in Hz.
Fs = 256;  % Sampling Frequency

Fpass1 = 49.6;            % First Passband Frequency
Fstop1 = 49.9;            % First Stopband Frequency
Fstop2 = 50.1;            % Second Stopband Frequency
Fpass2 = 50.4;            % Second Passband Frequency
Dpass1 = 0.057501127785;  % First Passband Ripple
Dstop  = 0.001;           % Stopband Attenuation
Dpass2 = 0.057501127785;  % Second Passband Ripple
dens   = 20;              % Density Factor

% Calculate the order from the parameters using FIRPMORD.
[N, Fo, Ao, W] = firpmord([Fpass1 Fstop1 Fstop2 Fpass2]/(Fs/2), ...
[1 0 1], [Dpass1 Dstop Dpass2]);

% Calculate the coefficients using the FIRPM function.
stop  = firpm(N, Fo, Ao, W, {dens});

% Filter is used for the data
signal_bandstop = filter(stop,1,signal_temp);

% HIGH PASS FILTER

Fs = 256;  % Sampling Frequency

Fstop = 0.5;              % Stopband Frequency
Fpass = 1.0;              % Passband Frequency
Dstop = 0.001;            % Stopband Attenuation
Dpass = 0.057501127785;   % Passband Ripple
dens  = 20;               % Density Factor

% Calculate the order from the parameters using FIRPMORD.
[N, Fo, Ao, W] = firpmord([Fstop, Fpass]/(Fs/2), [0 1], [Dstop, ...
Dpass]);

% Calculate the coefficients using the FIRPM function.
```

```
high  = firpm(N, Fo, Ao, W, {dens});

% LOW PASS FILTER

% All frequency values are in Hz.
Fs = 256;  % Sampling Frequency

Fpass = 70;              % Passband Frequency
Fstop = 75;              % Stopband Frequency
Dpass = 0.057501127785;  % Passband Ripple
Dstop = 0.0001;          % Stopband Attenuation
dens  = 20;              % Density Factor

% Calculate the order from the parameters using FIRPMORD.
[N, Fo, Ao, W] = firpmord([Fpass, Fstop]/(Fs/2), [1 0], [Dpass, ...
Dstop]);

% Calculate the coefficients using the FIRPM function.
low  = firpm(N, Fo, Ao, W, {dens});

% High and low pass filters are used for the data
signal_high = filter(high,1,signal_bandstop);
signal = filter(low,1,signal_high);

%--------------------------------------------------------------------------
%-----------------PROCESSING ORIGINAL ECG SIGNAL-----------------------
%--------------------------------------------------------------------------

% ECG signal is saved to a separate variable from the data
ECG_signal = signal(:,30);

% Peaks of the data are searched
[tmp_peaks_amp, tmp_peaks_ind] = findpeaks(ECG_signal);

% R-peaks are chosen using threshold level determined earlier
ecg_peaks_ind = tmp_peaks_ind(find(tmp_peaks_amp > threshold));
ecg_peaks_amp = tmp_peaks_amp(find(tmp_peaks_amp > threshold));

% To manually delete some ECG peak:
% indexnumber = ?
% ecg_peaks_ind(indexnumber) = [];
% ecg_peaks_amp(indexnumber) = [];

% Figure of the chosen ECG peaks is plotted with markers on the peaks.
figure(301); plot(ecg_peaks_ind, ecg_peaks_amp, '.r', ...
'MarkerSize', 15);
hold on;
axis([0 length(ECG_signal) min(ECG_signal) max(ECG_signal)])
plot(ECG_signal);
title('Chosen ECG peaks')
hold off;

%--------------------------------------------------------------------------
% Checking that ECG peak time windows do not exceed file lengths
%--------------------------------------------------------------------------

% Checking ECG file and deleting data by the length of ECG window if
necessary
```

```
last_peak_index = ecg_peaks_ind(length(ecg_peaks_ind));

if (last_peak_index + windowlength > length(ECG_signal) )

    ecg_peaks_ind = ecg_peaks_ind( 1 : length(ecg_peaks_ind)-1 );
    ecg_peaks_amp = ecg_peaks_amp( 1 : length(ecg_peaks_amp)-1 );

    Change = char('Last ECG peak deleted due to exceeding the file
length (ECG signal)')

end

first_peak_index = ecg_peaks_ind(1);

if ( first_peak_index - windowlength < 0 )

    ecg_peaks_ind = ecg_peaks_ind( 2 : length(ecg_peaks_ind) );
    ecg_peaks_amp = ecg_peaks_amp( 2 : length(ecg_peaks_amp) );

    Change = char('First ECG peak deleted due to exceeding the file
length (ECG signal)')

end

% Checking if data has been deleted and if it is, deleting data from
% the other signals in the data file as well.

last_peak_index = ecg_peaks_ind(length(ecg_peaks_ind));

if (last_peak_index + windowlength > length(signal) )

    ecg_peaks_ind = ecg_peaks_ind( 1 : length(ecg_peaks_ind)-1 );
    ecg_peaks_amp = ecg_peaks_amp( 1 : length(ecg_peaks_amp)-1 );

    Change = char('Last ECG peak deleted due to exceeding the file
length (electrode signal)')

end

%-------------------------------------------------------------------------
%----------------Averaging chosen ECG time windows--------------------
%-------------------------------------------------------------------------

% Summing the ECG electrode signal of chosen time windows
windowed_ECG_signal = 0;
for i = 1 : length(ecg_peaks_ind)

    peak_index = ecg_peaks_ind(i);

    windowed_ECG_signal = windowed_ECG_signal + ...
        ECG_signal(peak_index-windowlength : peak_index+windowlength);

end

% Averaging time window signals and producing an image of the result.
average_ECG = windowed_ECG_signal / length(ecg_peaks_ind);
```

```
figure(200); plot(average_ECG);
title('Average of all the ECG peaks with the chosen window length');

%-------------------------------------------------------------------------
%-------Averaging EEG signal at the points of chosen ECG pulses-------
%-------------------------------------------------------------------------

% Create a variable were the result is saved
windowed_electrode_x_signal = 0;
% Save the name of the electrode processed
electrode_name = headers(electrode_number);

% Summing the chosen EEG electrode signal of chosen time windows
for i = 1 : length(ecg_peaks_ind)

    peak_index = ecg_peaks_ind(i);

    windowed_electrode_x_signal = windowed_electrode_x_signal +...
        signal(peak_index - windowlength : peak_index +...
        windowlength, electrode_number);

end

% Averaging the summed signal
average_electrode_x_signal = windowed_electrode_x_signal /
length(ecg_peaks_ind);
signal_out = average_electrode_x_signal;

% Create a variable for producing the image with a real time
% in seconds. Creation must be changed appropriate
% if window length is changed.
x = ((-length(average_electrode_x_signal)+1)/2: ...
length(average_electrode_x_signal)/2)./ ...
length(average_electrode_x_signal)';
time = x;

% Producing an image of the resulting filtered and averaged signal
figure(2); plot(x, average_electrode_x_signal); hold on
title_name = (['Average of the electrode ', electrode_name{1}, ...
               ' on the same points as ECG peaks']);
title(title_name);
xlabel('Time [s]');
ylabel('Amplitude [µV]');
hold off;

end
```

APPENDIX B: MAGNITUDE AND ANGLE OF A HEART VECTOR

```
%-------------------------------------------------------------------------
%------------------PROCESSING OF VCG SIGNALS------------------------
%-------------------------------------------------------------------------

% Example code used for data which is measured from test subject one.
% After the data is filtered and ECG peaks and the length of a time
% window is chosen, the following is done:

% Manually move the baseline of the signals to be the same
signal(:,27) = signal(:,27)+85;
signal(:,16) = signal(:,16)+160;
signal(:,26) = signal(:,26)+200;
signal(:,28) = signal(:,28)+150;
signal(:,15) = signal(:,15)+80;
signal(:,30) = signal(:,30)+120;
signal(:,29) = signal(:,29)+2;

% Creating variables where the processed data is saved
windowed_frank_i = 0;
windowed_frank_e = 0;
windowed_frank_c = 0;
windowed_frank_a = 0;
windowed_frank_m = 0;
windowed_frank_f = 0;
windowed_frank_h = 0;

% Summing the VCG signal of chosen time windows for each electrode
for i = 1 : length(ecg_peaks_ind)

    peak_index = ecg_peaks_ind(i);

    windowed_frank_i = windowed_frank_i + signal(peak_index - ...
        windowlength : peak_index + windowlength, 27);
    windowed_frank_e = windowed_frank_e + signal(peak_index - ...
        windowlength : peak_index + windowlength, 16);
    windowed_frank_c = windowed_frank_c + signal(peak_index - ...
        windowlength : peak_index + windowlength, 26);
    windowed_frank_a = windowed_frank_a + signal(peak_index - ...
        windowlength : peak_index + windowlength, 28);
    windowed_frank_m = windowed_frank_m + signal(peak_index - ...
        windowlength : peak_index + windowlength, 15);
    windowed_frank_f = windowed_frank_f + signal(peak_index - ...
        windowlength : peak_index + windowlength, 30);
    windowed_frank_h = windowed_frank_h + signal(peak_index - ...
        windowlength : peak_index + windowlength, 29);

end

% Averaging summed time window signals.
average_windowed_frank_i = windowed_frank_i / length(ecg_peaks_ind);
average_windowed_frank_e = windowed_frank_e / length(ecg_peaks_ind);
average_windowed_frank_c = windowed_frank_c / length(ecg_peaks_ind);
average_windowed_frank_a = windowed_frank_a / length(ecg_peaks_ind);
average_windowed_frank_m = windowed_frank_m / length(ecg_peaks_ind);
average_windowed_frank_f = windowed_frank_f / length(ecg_peaks_ind);
average_windowed_frank_h = windowed_frank_h / length(ecg_peaks_ind);
```

```
% Calculating the X-, Y- and Z-leads of the Frank's method
frank_x_M = (0.61*average_windowed_frank_a + ...
    0.171*average_windowed_frank_c -0.781*average_windowed_frank_i);
frank_y_M = (0.655*average_windowed_frank_f + ...
    0.345*average_windowed_frank_m -1.000*average_windowed_frank_h);
frank_z_M = (0.133*average_windowed_frank_a + ...
    0.736*average_windowed_frank_m -0.264*average_windowed_frank_i ...
    - 0.374*average_windowed_frank_e -0.231*average_windowed_frank_c);

% Producing an image of the VCG loops
figure; plot(frank_x_M, frank_y_M);  hold on;
grid on;
xlabel('Axis X [uV]');
ylabel('Axis Y [uV]');
title('Presentation of a VCG measurement in Frontal plane')
hold off;

% Finding maximum value of the Y-lead, which is the point of R-peak.
[t, ix]= max(frank_y_M, [], 1);
[mx, jx] = max(t); % mx is now the maximum value of the Y-lead

%-------------------------------------------------------------------
%-----------------Magnitude and angle calculations-----------------
%-------------------------------------------------------------------

% Index of the maximum value in the point of R-peak is now (ix(jx))

% Calculating the angles of the heart vector on each plane
cathetus_right = frank_x_M(ix(jx));
cathetus_downward = mx;
angle_frontal = atan(cathetus_downward/cathetus_right)*(180/pi)

cathetus_backward = frank_z_M((ix(jx)));
cathetus_downward = mx;
angle_sagittal =
(atan(cathetus_backward/cathetus_downward)*(180/pi)+90)

cathetus_backward = frank_z_M((ix(jx)));
cathetus_right = frank_x_M((ix(jx)));
angle_transverse = -atan(cathetus_backward/cathetus_right)*(180/pi)

% Calculating dipole magnitudes
dipole_x_magnitude = frank_x_M(ix(jx))
dipole_y_magnitude = frank_y_M(ix(jx))
dipole_z_magnitude = frank_z_M(ix(jx))
```